

**SYNTHESIS AND PHYSICO – CHEMICAL STUDIES  
ON HEXACOORDINATE SILICATES OF  
2, 3 - DIHYDROXYNAPHTHALENE**

*A THESIS*

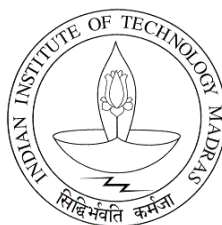
*submitted by*

**SUVITHA. A**

*for the award of the degree*

*of*

**DOCTOR OF PHILOSOPHY**



**DEPARTMENT OF CHEMISTRY  
INDIAN INSTITUTE OF TECHNOLOGY, MADRAS  
CHENNAI – 600 036**

**DECEMBER 2006**

**Dedicated to  
Almighty God**

## **THESIS CERTIFICATE**

This is to certify that the thesis entitled “**SYNTHESIS AND PHYSICO – CHEMICAL STUDIES ON HEXACOORDINATE SILICATES OF 2,3 - DIHYDROXYNAPHTHALENE**” submitted by **A. Suvitha** to the Indian Institute of Technology Madras for the award of the degree of Doctor of Philosophy is a bonafide record of research work carried out by her under my supervision. The contents of this thesis, in full or in parts, have not been submitted to any other Institute or University for the award of any degree or diploma.

Research Guide

**Dr. G. Sundararajan**

Date:

Place: Chennai – 600 036

## ACKNOWLEDGEMENTS

It is my great pleasure and esteem gratitude to thank my research guide **Prof. G. Sundararajan** for providing me an opportunity to work in his research group, for his professional guidance and support in my research. I express my sincere and gratitude to my co-guide **Prof B. Viswanathan** for his patient guidance, constant encouragement and the valuable suggestions for my research work. I would also like to thank **Prof. M. N. Sudheendra Rao** for his guidance and exposing me to this exciting field of silicon chemistry.

I sincerely thank, **Prof. B. Viswanathan, Prof. S. Vancheesan, Prof. M.N. Sudheendra Rao, Prof G. Sundararajan** the former heads and, **Prof. R. Dhamodaran** the present Head of the Department of Chemistry, IITM for guidance and support shown during my stay in the department.

I thank Indian Institute of Technology Madras for financial support and providing the necessary facilities.

My sincere thanks are to my doctoral committee members **Prof S. Sankararaman, Prof N. Balasubramanian, Prof K. Vidayasagar, Prof Indrapal Singh Aidhen, Prof D.V.S. Murthy** and **Prof T. Prasanna Kumar** for their constant encouragement, suggestions and support.

I am thankful to **Mr. A. Mohan** for his kind help in recording the HR-NMR. I thank **Mr. David** for mass spectral data, **Mr. Ramkumar** for CHN analysis and **Mr. Narayanan** for thermal analysis and surface area measurements. I also thank **Dr. M. S. Moni** (SAIF) for recording some of the NMR spectra and **Dr. Babu Varghese** for X-ray analysis and useful discussions. I would also like to thank **Prof. B.S Murthy**, department of metallurgy and material engineering, IITM for providing TEM facility.

I would like to thank **Prof. J. Subramanian**, Central Leather Research Institute, Chennai for providing EPR facility, his valuable suggestions and cooperation.

I express my deepest gratitude belongs to Dr. Vijayakrishna, Mrs. Susan Abraham, Dr. P. Sudhakar and Dr. N. S. Santhosh, who are my senior colleagues for their understanding, encouragement and advices. I would like to thank my fellow group members Everta Keren, Kiran Sagar, Karthikeyan, Dakshinamoorthy, Harikrishna, Neelima, Tanuja for their help and creating good working atmosphere. I thank Mr. Indraneel, Miss Rajeswari, Mr Sankaran, Dr. Sathish, Mr Navaliden, Mr. Magesh, Mrs. Asmita, Mrs. Kalpana, Mr. Anjee Reddi, Miss Helen, Miss Sabiah, Dr. Gnanasutha and Mr. Babu for their timely help.

I wish to thank all my research colleagues, Mr. Udayanath, Dr. Shyamala, Dr. Gayathri, Dr. Deepa, Dr. Akhila, Dr. Prabhakaran, and Dhilip for their timely help.

I thank my husband **N. S. Venkataramanan** for his constant encouragement and support. With great pleasure I express my deepest gratitude to my parents, brother and sister and my in laws for their affection, care, interest, moral support, kind cooperation and constant encouragement through out my research life.

I also thank all other family members and friends who have been supportive and shared good times with me.

I would like to thank Raja Xerox & Prints for timely printing and binding works.

Above all I would like to express my humble gratitude to **God**, The Almighty for showing me the right path throughout. I owe all my success to **God**.

**A. SUVITHA**

## ABSTRACT

**Key Words:** Hexacoordinate silicate, 2,3-dihydroxynaphthalene, microwave irradiation, X-ray structure, thermal studies, cyclic voltammetry, TGA and silica-metal oxide

Hexacoordinate silicate of 2,3-dihydroxynaphthalene has potential application in the field of reprography but synthesis and properties of this material were not studied in details so far. In this thesis work, an effective synthetic route has been formulated for tris(2,3-dihydroxynaphthalato)silicate. The structures have been analyzed. Hexacoordinate silicate of 2,3-dihydroxynaphthalene with ammonium counter cations have been synthesized under room temperature, microwave and conventional heating conditions in good yields by the reaction of tetraethoxysilane, 2,3-dihydroxynaphthalene and amines. The hexacoordinate silicates with ammonium counter cations were characterized using spectroscopic and analytical methods. Single crystal X-ray structural studies of complexes have been carried out. These studies revealed the hydrogen bonding interaction between ammonium ion and the silicates. As the bulkiness on alkyl ammonium increases, the extent of hydrogen bonding decreases. This is reflected in the variation of the solubility and solution stability behavior of the tris(2,3-dihydroxynaphthalato)silicates. The effect of counter cations on the thermal and hydrolytic stability of the tris(2,3-dihydroxynaphthalato)silicate was studied using TGA and UV-Vis spectral studies. The thermal stability of tris(2,3-dihydroxynaphthalato)silicate increases in the following order of  $3^\circ > 2^\circ > 1^\circ$  ammonium derivatives. Tris(2,3-dihydroxynaphthalato)silicates with different counter ammonium ions were used as precursor in the synthesis of mesoporous silica materials. The higher surface area silica materials were achieved under pyrolytic conditions than under hydrolytic conditions. Redox behaviour of tris(2,3-dihydroxynaphthalato)silicates with respect to counter ammonium ion has been

studied. It reveals that the stability remains the same irrespective of the counter ion. It gave three irreversible anodic peaks. The redox is a diffusion controlled process that was derived from Randles- Servick equation. The effect of the counter cations on the first oxidation potential of the silicate was examined but no meaningful structural correlation could be arrived because of the unstable nature of the intermediate 2,3-naphthoquinone. Further, 3d- transition metal complexes of ethylenediamine were synthesized using ammonium derivatives of tris(2,3-dihydroxynaphthalato)silicates to study the effect of counter anion on spectral behaviour of metal complexes. The metal complexes containing tris(2,3-dihydroxynaphthalato)silicates were used as precursors in the preparation of these metal oxide-silica doped materials.

## TABLE OF CONTENTS

<b>ACKNOWLEDGEMENTS .....</b>	<b>i</b>
<b>ABSTRACTS.....</b>	<b>iii</b>
<b>LIST OF TABLES .....</b>	<b>x</b>
<b>LIST OF FIGURES .....</b>	<b>xii</b>
<b>LIST OF SCHEMES .....</b>	<b>xv</b>
<b>ABBREVIATIONS .....</b>	<b>xvi</b>
<b>NOTATIONS.....</b>	<b>xvii</b>

### CHAPTER I INTRODUCTION

1.1	General introduction .....	1
1.2	Hypervalency .....	3
1.3	Hypervalent silicon compounds.....	6
1.3.1	Cationic Hexacoordinate Silicates .....	11
1.3.2	Anionic Hexacoordinate Silicates.....	12
1.3.3	Neutral Hexacoordinate Silicate .....	14
1.4	Chemistry of 2,3-Dihydroxynaphthalene.....	15
1.4.1	Synthesis of Pentacoordinate Silicates of 2,3-Dihydroxynaphthalene .....	16
1.4.2	Structural Characterization of Pentacoordinate Silicate of 2,3-Dihydroxynaphthalene .....	17
1.4.3	Higher Coordinate Silicate of 2,3-DHN as a Reprography Material.....	18
1.5	Methods of Synthesis of Hexacoordinate Silicates.....	19
1.5.1	Intermolecular coordination to an organosilane .....	20
1.5.2	Substitution in a tetrafunctional silane by a bidentate ligand .....	20
2.1	Synthesis of tris(Catecholato)silicate.....	21
2.1.1	Microwave methods .....	22
1.5.3.1	Thermal effect.....	22
1.5.3.2	“Hot Spots” inhomogeneities.....	23
1.6	Characterization of Hexacoordinate Silicates .....	23
1.6.1	X-ray structural characterization of hexacoordinate silicates .....	23
1.6.2	<sup>29</sup> Si NMR spectral analysis of hexacoordinate silicate .....	25
1.7	Higher Coordinate Silicates as Precursor for Silica Materials: Relevance or Biosilicification .....	27



1.7.1	Silicon Uptake Evidence of Transient Hexacoordinate Silicate .....	28
1.7.2	Studies on the decomposition of silicon complexes .....	29
1.8	Studies on Electrochemical Behaviour of Dihydroxyaryl Compounds .....	30
1.9	Metal Oxide Silica Materials - Higher Coordinate Silicate as Precursors.....	33
1.10	Objectives of the Present Study .....	33

## **CHAPTER II EXPERIMENTAL METHODOLOGY**

2.1	Purification of solvents and other reagents .....	36
2.2	Experimental techniques .....	37
2.3	Synthesis of ethylenediamine complexes of 3d-transition metals .....	38
2.4	Molybdate blue test for detect of silica formation under hydrolytic Condition.....	39
2.5	Characterization techniques .....	40
2.6	Conditions employment for measurements .....	42

## **CHAPTER III SYNTHESIS AND CHARACTERIZATION OF HEXACOORDINATE SILICATE OF 2,3- DIHYDROXYNAPHTHALENE WITH AMMONIUM COUNTER IONS**

3.1	Introduction.....	47
3.2	Experimental section.....	49
3.2.1	Synthesis of bis(ammonium)tris(2,3-dihydroxynaphthalato)silicates .....	49
3.2.1.1	Room temperature reaction.....	50
3.2.1.2	Microwave reaction .....	51
3.2.1.3	Reaction under conventional heating .....	52
3.3	Results and discussion .....	53
3.3.1	Room temperature reaction.....	54
3.3.2	Microwave reaction .....	55
3.3.5	Characterization .....	57
3.3.5.1	Infrared spectral analysis .....	58
3.3.5.2	<sup>1</sup> H – NMR spectral analysis.....	59
3.3.5.3	<sup>13</sup> C – NMR spectral analysis.....	60
3.3.5.4	<sup>29</sup> Si – NMR spectral analysis.....	61
3.3.5.5	Mass spectral analysis.....	62

3.4	Conclusions.....	63
<p style="text-align: center;"><b>CHAPTER IV SINGLE CRYSTAL X-RAY STRUCTURES OF (n</b>  <b>C<sub>4</sub>H<sub>9</sub>)<sub>3</sub>NH]<sub>2</sub>[Si(C<sub>10</sub>H<sub>6</sub>O<sub>2</sub>)<sub>3</sub>] AND [(i-</b>  <b>C<sub>4</sub>H<sub>9</sub>)<sub>2</sub>NH<sub>2</sub>]<sub>2</sub>[Si(C<sub>10</sub>H<sub>6</sub>O<sub>2</sub>)<sub>3</sub>].3CH<sub>3</sub>CN</b></p>		
4.1	Introduction.....	69
4.2	Experimental section.....	71
4.2.1	Crystallisation of bis(diisobutylammonium)tris(2,3-dihydroxynaphthalato)silicates .....	72
4.2.2	Crystallisation of bis(tri-n-butylammonium)tris(2,3-dihydroxynaphthalato)silicates .....	72
4.3	Results and Discussion .....	73
4.3.1	Structure of bis(diisobutylammonium)tris(2,3-dihydroxynaphthalato)silicates .....	74
4.3.2	Packing of bis(diisobutylammonium)tris(2,3-dihydroxynaphthalato)silicates .....	78
4.3.3	Structure of bis(tri-n-butylammonium)tris(2,3-dihydroxynaphthalato)silicates .....	79
4.3.4	Packing of bis(tri-n-butylammonium)tris(2,3-dihydroxynaphthalato)silicates .....	83
4.3.5	Effect of counter cation.....	84
4.3.5.1	Solubility.....	84
4.4	Conclusions.....	85
<p style="text-align: center;"><b>CHAPTER V PYROLYTIC AND HYDROLYTIC STABILITY OF BIS(AMMONIUM)TRIS(2,3-DIHYDROXYNAPHTHALATO) SILICATES: A STUDY WITH RELEVANCE FOR BIOSILICIFICATION</b></p>		
5.1	Introduction.....	87
5.2	Experimental section.....	89
5.2.1	Thermal stability of tris(2,3-dihydroxynaphthalato)silicates with ammonium counter cations (TGA and DTA studies) .....	89
5.2.2	Bulk Pyrolysis.....	90
5.2.3	Hydrolytic stability of tris(2,3-dihydroxynaphthalato)silicates with ammonium counter cations.....	90
5.3	Results and discussion .....	92
5.3.1	Thermal stability of tris(2,3-dihydroxynaphthalato)silicate with ammonium counter cations .....	92
5.3.2	Silica obtained by bulk pyrolysis.....	95

5.3.3	TEM studies of silica .....	96
5.3.4	SEM studies of silica .....	98
5.3.5	Hydrolytic stability .....	99
5.3.6	Colorimetric molybdate test.....	100
5.3.7	Silica obtained by hydrolysis .....	102
5.3.7.1	TEM studies of silica .....	103
5.3.7.2	SEM studies of silica .....	104
5.4	Conclusions.....	105

**CHAPTER VI CYCLIC VOLTAMMETRIC STUDIES OF  
BIS(AMMONIUM)TRIS(2,3- DIHYDROXYNAPHTHALATO)  
SILICATE**

6.1	Introduction.....	107
6.1.1	Redox behavior of 2,3-dihydroxynaphthalene.....	108
6.1.2	Redox behavior of other silicon complexes.....	109
6.2	Experimental section.....	109
6.2.1	Chemical oxidation of 2,3-dihydroxynaphthalene in tris(2,3- dihydroxynaphthalene in tris(2,3-dihydroxynaphthalato)silicate .....	112
6.3	Results and discussion .....	112
6.3.1	Cyclic voltammetric study of bis(ammonium)tris(2,3- dihydroxynaphthalato)silicates .....	113
6.3.2	Chemical oxidation of tris(2,3-dihydroxynaphthalato)silicate .....	115
6.3.3	Controlled potential electrolysis of tris(2,3-dihydroxynaphthalato)silicate .	116
6.3.4	Nature of redox process of tris(2,3-dihydroxynaphthalato)silicate .....	116
6.3.5	Stability of silicate under electrochemical condition.....	118
6.4	Conclusions.....	118

**CHAPTER VII SYNTHESIS AND THERMAL STUDIES ON TRIS(2,3-  
DIHYDROXYNAPHTHALATO)SILICATE WITH  
TRANSITION METAL COMPLEXES AS COUNTER IONS**

7.1	Introduction.....	121
7.2	Experimental section.....	122
7.2.1	Synthesis of ethylenediamine complexes of 3d-transition metals .....	122
7.2.2	Synthesis of tris(ethylenediamine)nickeltris(2,3-dihydroxynaphthalato)silicate from bis(ammonium)tris(2,3-dihydroxynaphthalato)silicates .....	123
7.2.3	Thermal analysis .....	126
7.2.4	Bulk pyrolysis .....	126

7.3	Results and discussion .....	127
7.3.1	Synthesis .....	127
7.3.2	Characterization .....	127
7.3.2.1	IR spectral analysis .....	127
7.3.2.2	Optical spectral analysis .....	128
7.3.2.3	MALDI – mass spectral analysis .....	130
7.3.2.4	Elemental analysis .....	131
7.3.2.5	EPR spectral analysis .....	132
7.3.2.6	Magnetic susceptibility analysis .....	133
7.3.2.7	Thermal studies .....	134
7.3.2.8	Bulk pyrolysis studies .....	136
7.3.2.9	Surface area measurement of pyrolysed product .....	136
7.3.2.10	Electromicrographs of silica- metal oxides .....	137
7.4	Conclusions .....	140
	<b>SUMMARY AND CONCLUSIONS .....</b>	<b>141</b>
	<b>REFERENCES.....</b>	<b>146</b>
	<b>LIST OF PAPER PUBLISHED IN PREPARATION</b>	
	<b>BASED ON THE WORK REPORTED IN THE THESIS .....</b>	<b>173</b>

## LIST OF TABLES

Table	Title	Page No.
1.1	Hexacoordinate silicates in literature.....	8
1.2	Chemical shift values of silicon sources.....	26
1.3	<sup>29</sup> Si – NMR chemical shift for hexacoordinate silicates.....	27
3.1	Experimental details for the synthesis of bis(ammonium)tris(2,3-dihydroxynaphthalato)silicate .....	51
3.2	Comparison of conventional and microwave assisted synthesis of [(XH) <sub>2</sub> ][Si(C <sub>10</sub> H <sub>6</sub> O <sub>2</sub> ) <sub>3</sub> ] derivatives.....	57
3.3	Characterizatic IR frequencies of tris(2,3-dihydroxynaphthalato)silicates .....	64
3.4	<sup>1</sup> H - Spectral data of bis(ammonium)tris(2,3-dihydroxynaphthalato)silicates ..	65
3.5	<sup>13</sup> C – NMR and <sup>29</sup> Si –NMR of bis(ammonium)tris(2,3-dihydroxynaphthalato)silicate.....	66
3.6	Analytical data of bis(ammonium)tris(2,3-dihydroxynaphthalato)silicates .....	67
4.1	Crystal data and experimental parameters for crystal structure analyses of [( <i>i</i> -C <sub>4</sub> H <sub>9</sub> ) <sub>2</sub> NH <sub>2</sub> ] <sub>2</sub> [Si(C <sub>10</sub> H <sub>6</sub> O <sub>2</sub> ) <sub>3</sub> ].3CH <sub>3</sub> CN and [( <i>n</i> -C <sub>4</sub> H <sub>9</sub> ) <sub>3</sub> NH] <sub>2</sub> [Si(C <sub>10</sub> H <sub>6</sub> O <sub>2</sub> ) <sub>3</sub> ] ....	73
4.2	Si-O bond length (Å) of SiO <sub>6</sub> core for [( <i>i</i> -C <sub>4</sub> H <sub>9</sub> ) <sub>2</sub> NH <sub>2</sub> ] <sub>2</sub> [Si(C <sub>10</sub> H <sub>6</sub> O <sub>2</sub> ) <sub>3</sub> ].3.CH <sub>3</sub> CN .....	75
4.3	Selected bond angles (°) of SiO <sub>6</sub> core for [( <i>i</i> -C <sub>4</sub> H <sub>9</sub> ) <sub>2</sub> NH <sub>2</sub> ] <sub>2</sub> [Si(C <sub>10</sub> H <sub>6</sub> O <sub>2</sub> ) <sub>3</sub> ].3.CH <sub>3</sub> CN .....	76
4.4	Hydrogen bonds for [( <i>i</i> -C <sub>4</sub> H <sub>9</sub> ) <sub>2</sub> NH <sub>2</sub> ] <sub>2</sub> [Si(C <sub>10</sub> H <sub>6</sub> O <sub>2</sub> ) <sub>3</sub> ]. 3 CH <sub>3</sub> CN [Å and °] .....	77
4.5	Si-O bond lengths (Å) of SiO <sub>6</sub> core for [( <i>n</i> -C <sub>4</sub> H <sub>9</sub> ) <sub>3</sub> NH] <sub>2</sub> [Si(C <sub>10</sub> H <sub>6</sub> O <sub>2</sub> ) <sub>3</sub> ].....	80
4.6	Selected bond angles (°) of SiO <sub>6</sub> for [( <i>n</i> -C <sub>4</sub> H <sub>9</sub> ) <sub>3</sub> NH] <sub>2</sub> [Si(C <sub>10</sub> H <sub>6</sub> O <sub>2</sub> ) <sub>3</sub> ].....	81
4.7	Hydrogen bonds for [( <i>n</i> -C <sub>4</sub> H <sub>9</sub> ) <sub>3</sub> NH] <sub>2</sub> [Si(C <sub>10</sub> H <sub>6</sub> O <sub>2</sub> ) <sub>3</sub> ] [Å and °] .....	83
5.1	Thermoanalytical data of tris(2,3-dihydroxynaphthalato)silicate with different counter ammonium ions.....	94
5.2	Surface area and pore volume of silica obtained by pyrolysis.....	98
5.3	Surface area and pore volume of silica obtained by hydrolysis.....	105
6.1	Compounds considered for the study (R <sub>3</sub> NH) <sub>2</sub> (Si(C <sub>10</sub> H <sub>6</sub> O <sub>2</sub> ) <sub>3</sub> ).....	111
6.2	Redox potential of [Si(C <sub>10</sub> H <sub>6</sub> O <sub>2</sub> ) <sub>3</sub> ] <sup>2-</sup> with different counter cation .....	114
7.1	Experimental details for the precursor-ethylenediamine complexes of 3d-transition metals.....	123
7.2	Synthesis details of transition metal containing silicates.....	124

7.3	IR and UV-Vis Spectral data of transition metal containing silicates .....	130
7.4	Analytical data of transition metal containing silicates .....	132
7.5	Thermal studies data of transition metal containing silicates .....	135
7.6	Surface area, powder XRD and Pore volume of residue of pyrolytic product	137

## LIST OF FIGURES

Figure	Title	Page No.
1.1	A partial periodic table of hypervalent non-metallic elements .....	5
1.2	Ligands used in the synthesis of cationic hexacoordinate silicon compound.	12
1.3	A variety of dianionic hexacoordinate silicates .....	13
1.4	Silicates with unsymmetric bidentate and tridentate ligands .....	14
1.5	Some of neutral hexacoordinate silicon compounds with SiO <sub>6</sub> .....	15
1.6	Pentacoordinate silicates of 2,3-dihydroxynaphthalene (2,3-DHN) .....	18
1.7	Single Crystal structures of hexacoordinate silicates .....	24
1.8	Chemical shift ranges of silicon NMR spectrum for silicon compounds .....	25
1.9	Naturally occurring naphthoquinones .....	32
3.1	Percentage yield versus time for the reaction at 110 °C (0.25 g – 2, 3- DHN; 0.11 mL-TEOS and 2 mL-amine) .....	55
3.2	Infrared spectrum of bis(diisopropylammonium) tris(2,3-dihydroxynaphthalato)silicate .....	58
3.3	<sup>1</sup> H NMR spectra of 2,3-dihydroxynaphthalene(ligand) and bis(diisopropylammonium)tris(2,3-dihydroxynaphthalato) silicate(DIPASINAP) .....	59
3.4	<sup>13</sup> C NMR spectra of 2,3-dihydroxynaphthalene(ligand) and bis(diisopropylammonium)tris(2, 3-dihydroxynaphthalato)silicate (DIPASINAP) .....	60
3.5	<sup>29</sup> Si NMR spectrum of bis(diisopropylammonium)tris(2,3- dihydroxynaphthalato)silicate .....	61
3.6	Negative mode of MALDI-MS for bis(diisopropylammonium)tris(2, 3- dihydroxynaphthalato)silicate .....	62
3.7	Postive mode of MALDI-MS for bis(diisopropylammonium)tris(2,3- dihydroxynaphthalato)silicate .....	63
4.1	Hydrogen bonding interaction between ion pairs of [( <i>i</i> - C <sub>4</sub> H <sub>9</sub> ) <sub>2</sub> NH <sub>2</sub> ] <sub>2</sub> [Si(C <sub>10</sub> H <sub>6</sub> O <sub>2</sub> ) <sub>3</sub> ]. 3 CH <sub>3</sub> CN .....	77
4.2	ORTEP diagram of [( <i>i</i> -C <sub>4</sub> H <sub>9</sub> ) <sub>2</sub> NH <sub>2</sub> ] <sub>2</sub> [Si(C <sub>10</sub> H <sub>6</sub> O <sub>2</sub> ) <sub>3</sub> ]. 3 CH <sub>3</sub> CN .....	78
4.3	Packing diagram of bis(diisobutylammonium)tris(2,3- dihydroxynaphthalato)silicate .....	79
4.4	ORTEP diagram of [( <i>n</i> -C <sub>4</sub> H <sub>9</sub> ) <sub>3</sub> NH] <sub>2</sub> [Si(C <sub>10</sub> H <sub>6</sub> O <sub>2</sub> ) <sub>3</sub> ] .....	82
4.5	Representation of hydrogen bonding interaction between ion pairs .....	82

4.6	Packing diagram of $[(n-C_4H_9)_3NH]_2[Si(C_{10}H_6O_2)_3]$ .....	84
5.1	Polymerization behavior of silica in aqueous medium A = in the presence of salts/acidic medium; B = alkaline medium (reproduced from the work of Iller) .....	89
5.2	(a) Representative TGA plot & (b) DTA plot of ammonium salt of tris(2,3-dihydroxynaphthalato)silicate .....	93
5.3	(a) IR spectra of the silica obtained from on pyrolysis (b) Powder XRD of silica obtained on pyrolysis .....	96
5.4	TEM images of silica obtained under pyrolytic condition from (a) TnBASINAP (b) DIPASINAP (c) <i>t</i> -BASINAP .....	97
5.5	(a) Diffraction pattern of the silica (b) EDAX of the silica .....	97
5.6	SEM images of silica obtained on pyrolysis of a) TnBASINAP (b) DIPASINAP (c) <i>t</i> -BASINAP .....	99
5.7	A plot of concentration of tris(2,3-dihydroxynaphthalato)silicate Vs. time .....	100
5.8	A plot concentration of silicic acid Vs time .....	102
5.9	(a) IR spectra of the silica obtained on hydrolysis (b) Powder XRD of silica .....	103
5.10	TEM images of silica obtained after 7 days in ethanol-water mixture for (a) <i>t</i> -butylammonium cation (b) diisopropylammonium cation (c) Tri- <i>n</i> -butylammonium cation containing tris(2,3-dihydroxynaphthalato)silicate .....	104
5.11	SEM images of silica obtained on hydrolysis of a) TnBASINAP (b) DIPASINAP (c) <i>t</i> -BASINAP .....	104
6.1	Cyclic Voltammogram of 2,3-dihydroxynaphthalene with TBAP in acetonitrile as supporting electrolyte .....	111
6.2	Cyclic voltammogram of bis( <i>sec</i> -butylammonium)tris(2,3-dihydroxynaphthalato)silicates .....	112
6.3	UV-Vis spectra of (a) TnBASINAP in acetone (b) TnBASINAP in aqueous KIO <sub>3</sub> .....	115
6.4	EPR spectrum of anionic radical obtained from acetone solution of TnBASINAP .....	115
6.5	Cyclic voltammogram of bis( <i>sec</i> -butylammonium)tris(2,3-dihydroxynaphthalato)silicates at different scan rates .....	117
6.6	Plot of scan rates vs anodic peak current to represent the Randles-Sevick relation .....	117
6.7	Multiple cycle voltammogram of tri- <i>n</i> -butylammonium containing tris(2,3-dihydroxynaphthalato)silicate recorded at sweep rate of 50 mV/s .....	118
7.1	IR spectrum of $[Cr(en)_3][Si(C_{10}H_6O_2)_3]$ .....	128
7.2	UV-Vis spectrum of $[Cu(en)_3][Si(C_{10}H_6O_2)_3]$ in nujol mull .....	129



7.3	EPR spectrum of $[\text{Cu}(\text{en})_3][\text{Si}(\text{C}_{10}\text{H}_6\text{O}_2)_3]$ .....	133
7.4	TGA plot of $[\text{Ni}(\text{en})_3][\text{Si}(\text{C}_{10}\text{H}_6\text{O}_2)_3]$ .....	134
7.5	SEM micrograph of (a) $\text{CuO}+\text{SiO}_2$ (b) $\text{NiO}+\text{SiO}_2$ (c) $\text{Fe}_2\text{O}_3$ (d) $\text{Co}_2\text{O}_3+\text{SiO}_2$ (e) $\text{Cr}_2\text{O}_3+\text{SiO}_2$ (f) $\text{ZnO}+\text{SiO}_2$ and (g) $\text{MnO}+\text{SiO}_2$ .....	139

## LIST OF SCHEMES

Figure No	Title	Page No
1.1	Synthesis of alkyl/arylbis(2,3-dihydroxynaphthalato)silicate .....	17
1.2	Reactivity of bis(2,3-dihydroxynaphthalato)silicate with water to form cage compounds .....	17
1.3	Synthesis of hexacoordinate silicon compound-Intermolecular coordination	20
1.4	Synthesis of hexacoordinate silicon compound- Substitution reaction .....	21
1.5	Synthesis of tris(catecholato)silicates – different routes .....	21
1.6	Oxidative cleavage of catechols to <i>cis</i> , <i>cis</i> -muconic acids .....	30
1.7	Oxidation of catecholate to quinone .....	32
3.1	Synthesis of Bis(ammonium)tris(2,3-dihydroxynaphthalato)silicate .....	50
5.1	Possible mechanism of thermolysis of different ammonium salt of tris(2,3-dihydroxynaphthalato)silicate .....	94
6.1	Energetic and structural changes in the naphthalenediol oxidation.....	109
7.1	Synthesis of ethylenediamine complexes of 3d-transition metal.....	122
7.2	Synthesis of transition metal containing tris(2,3-dihydroxynaphthalato)silicates .....	125

## ABBREVIATIONS

DTA	-	Differential thermal analysis
TGA	-	Thermogravimetric analysis
IR	-	Infrared
UV-Vis	-	Ultraviolet - visible
MALDI ionisation	-	Matrix assisted laser desorption
EPR	-	Electron paramagnetic resonance
NMR	-	Nuclear magnetic resonance
XRD	-	X-Ray diffraction
TEM	-	Transmission electron microscopy
SEM	-	Scanning electron microscopy
EDAX	-	Energy dispersive X-ray
SAD	-	Selected area diffraction
SINAP	-	Tris(2,3- dihydroxynaphthalato)silicate
TEASINAP	-	Bis(triethylammonium) Tris(2,3- dihydroxynaphthalato)silicate
mmol	.-	Millimoles
ml	-	Millilitre
DHN	-	2,3-Dihydroxynaphthalene
atm	.-	atmosphere
TEOS	-	Tetraethoxysilane

## NOTATIONS

$\text{\AA}$	-	Angstrom
$\lambda$	-	Wavelength
$\theta$	-	Bragg angle
$\alpha, \beta, \gamma$	-	Interplanar angle
$\delta$	-	Chemical shift
cc	-	Cubic centimeter
kcal	-	Kilocalories
nm	-	Nanometer
$\mu\text{m}$	-	Micrometer
K	-	Kelvin
h	-	Hour
min	-	Minute
%	-	Percentage
MB	-	Bohr magneton
$^{\circ}\text{C}$	-	Degree Celsius centigrade
mV	-	Millivolt

# **CHAPTER I**

## **INTRODUCTION**

---

## 1.1 GENERAL INTRODUCTION

Silicon (26%) is the most abundant element after oxygen (49.5%) in the earth's crust. It is found in the form of silica and silicate minerals because of the high Si–O bond strength (108 kcal / mol) (Gmelin, 1984). Silicon exists in two forms at room temperature (crystalline and amorphous). Crystalline silicon doped with boron, gallium, germanium, phosphorus or arsenic (to adjust its electrical response by controlling the number and charge of current carriers) is used in the manufacture of solid-state electronic devices such as transistors, solar cells, rectifiers and microchips (Ennis *et al*, 2002; Wronski *et al*, 1988; Kinzel, 1933; Zhou *et al*, 1996).

Naturally occurring silicates are classified based on their structural characteristics. They are nesosilicates (lone tetrahedron)  $[\text{SiO}_4]^{4-}$  *e.g.* olivine (Henry, 1998), sorosilicates (double tetrahedra)  $[\text{Si}_2\text{O}_7]^{6-}$  *e.g.* epidote, cyclosilicates (rings)  $[\text{Si}_n\text{O}_{3n}]^{2n-}$  *e.g.* tourmaline group (Winkler & Hoebbel, 1989), inosilicates (single chain)  $[\text{Si}_n\text{O}_{3n}]^{2n-}$  *e.g.* pyroxene group inosilicates (double chain) -  $[\text{Si}_{4n}\text{O}_{11n}]^{6n-}$  *e.g.* amphibole group (Henry, 1998), phyllosilicates (sheets) -  $[\text{Si}_{2n}\text{O}_{5n}]^{2n-}$  *e.g.* micas and clays (Bailey, 1984) and tectosilicates (3D framework) -  $[\text{Al}_x\text{Si}_y\text{O}_{2(x+y)}]^{x-}$  *e.g.* quartz, feldspars, zeolites.

Silicon may adopt octahedral coordination with six oxygens at high pressures, as in the dense stishovite polymorph of silica that is found in the lower mantle of the earth. This type of silicate is also formed by shock during meteorite impacts (Ringwood & Seabrook, 1963). Lack of space around the oxygen atoms makes six coordination for silicon a rare form at normal pressure, but it is known in the hexahydroxysilicate anion  $[\text{Si}(\text{OH})_6]^{2-}$  form, as found in the mineral thaumasite. The perovskite analogs

of stishovite have been reported to be  $(\text{Mg, Fe})\text{SiO}_3$ , and hollandite  $\text{CaAl}_2\text{-Si}_2\text{O}_8$  (Jacobsen *et al*, 2003).

Silicon-oxygen based cage compounds have been used for catalysis and storage systems, e.g., hydrogen storage using nanostructured silicates (microreactor, nanotubes). Silicon based materials with unique opto-electronic properties and materials for photo luminescent flat panel technology, displays, light emitting diodes, sensors, electroluminescence and non-metallic conductors have been well studied. In communication technology, silica materials have been used as glass fibres and in fabrication of quartz glass goods (Levin *et al*, 1969; 1975). Silicon forms other useful compounds such as silicon carbide that is nearly as hard as diamond and is used as an abrasive material. Sodium silicate, also known as water glass, is used in the production of soaps, adhesives and as an egg preservative. Silicon tetrachloride is used to create smoke screens. Silicone is also an important class of materials that is used for the manufacture of lubricants, polishing agents, electrical insulators and medical implants (Brook, 2000a). Organosilicon compounds in normal coordination such as trimethylchlorosilane have been used as protecting agents (Brook, 2000b). Silicon in lower coordination state such as silene, silynes and  $\text{R}_2\text{Si} = \text{E}$  ( $\text{E} = \text{N, S, O}$ ) and silicon in trivalent cationic state are under intensive examination (West *et al*, 2003). Silylenes are very reactive species that can be stabilized with bulky substituent on it. They can be trapped using methanol. Silicon can expand its valence beyond its normal valency due to inherent behaviour of higher main group elements. This is known as hypervalency.

## 1.2 HYPERVALENCY

Valence electrons of an element have relevance to the formation of molecules and molecular ions. Lewis octet theory is an important guiding factor in the rationalization of their formation. Hypervalent molecules and ions are fascinating species since they appear to violate the traditional Lewis-Langmuir theory of bonding by expanding the valence shell of a main group element. The word “HYPERVALENT” was first introduced in a classic paper by Musher in 1969 to categorize molecules and ions formed by elements in groups 14-18 of the periodic table in valence states other than their lowest stable chemical valences of 3, 2, 1 and 0 respectively. According to Musher, the species  $\text{PF}_5$ ,  $\text{PF}_6^-$ ,  $\text{SF}_6$  and even  $\text{F}_3\text{PO}$ ,  $\text{F}_2\text{SO}$  and  $(\text{CH}_3)_3\text{NO}$  are hypervalent while  $\text{SiF}_5^-$  and  $\text{SiF}_6^{2-}$  are not hypervalent though these are isoelectronic and isostructural to  $\text{PF}_5$  and  $\text{PF}_6^-$  respectively. Whether specie is hypervalent or not, depends not only on valency but also on the total valence electrons. If a molecule or an ion features an atom surrounded by more than octet of electrons, then it is said to be in hypervalent state. The definition is consistent with the word ‘Hypervalent’ since the expanded octet is the result of increased valence or bond formation (Atkins, 1990; King, 1995). **Figure 1.1** shows the partial periodic table of the hypervalent non-metallic species possessing more than an octet of electrons (Martin, 1983).

Rundles (1963a, 1963b) and Pimental (1951) have stressed the importance of the existence of hypervalent bond in molecules rather than classifying the molecule itself as hypervalent. They have invoked three center - four electron with partial electrovalency (two half bonds) for the hypervalent bond.

Hypervalency can also be defined as the ability of an element to form more number of chemical bonds than it is capable of forming on the basis of its valence shell electrons.



It is proposed that the additional chemical bonds formed are the result of the participation of energetically favorable vacant *d*-orbital of the heavier main group elements. However, based on *ab initio* theoretical study and isolated examples of hypervalent carbon species (Martin and Perozzi, 1976; Martin *et al.*, 1983) a new concept viz. negative conjugation has been proposed for understanding bonding in such molecules (Reed and Schkeyer, 1990).

Gillespie and Robinson (1995) have claimed that the hypervalency concept is redundant and the molecules such as PF<sub>5</sub> and SF<sub>6</sub> should be regarded as exceptions to the octet rule. This has been expressed as their concept to the long lasting debate on the extent of the participation of *d*-orbital in bonding of hypervalent molecules. However, they have also mentioned that more exact *ab initio* calculations require a very large set of highly modified *s*, *p* and *d* atomic orbitals.

Hypervalency is the property of main-group atoms in molecular entities to acquire coordination numbers greater than four (which would comply with the *Lewis octet rule*). Hypercoordination may be associated with hypervalency, but usually referred to peculiar atomic centers in the electron-deficient species with multicenter  $\sigma$ -bonding, in which the bonding power of a pair of electrons is spread over more than two atoms. An example of a hypercoordinated atom is the five-coordinate carbon atom in the cation methanium (CH<sub>5</sub><sup>+</sup>), where three C-H bonds may be regarded as normal two center - two electron bonds and the bonding in the remaining C-H fragment is governed by the three-center, two-electron bond (Olah *et al.*, 1987).

A description of the hypervalent bonding implies a transfer of the electrons from the central hypervalent atom to the nonbonding molecular orbital that it forms in presence of electronegative atoms, in coordination environment due to the ligands. The existence of hypervalent molecules have more than eight valence electrons at the central atom (exception from octet rule), is a topic of constant debate. Especially, for compounds with strong electron-withdrawing substituents, it seems that this concept

is not useful; e.g. recent studies proved that sulfur imides and phosphonium ylides should not be described as hypervalent species. Since there is no difference between bond in hypervalent compound and non-hypervalent compound, there is no reason to use the term hypervalency (Gillespie, 2002).

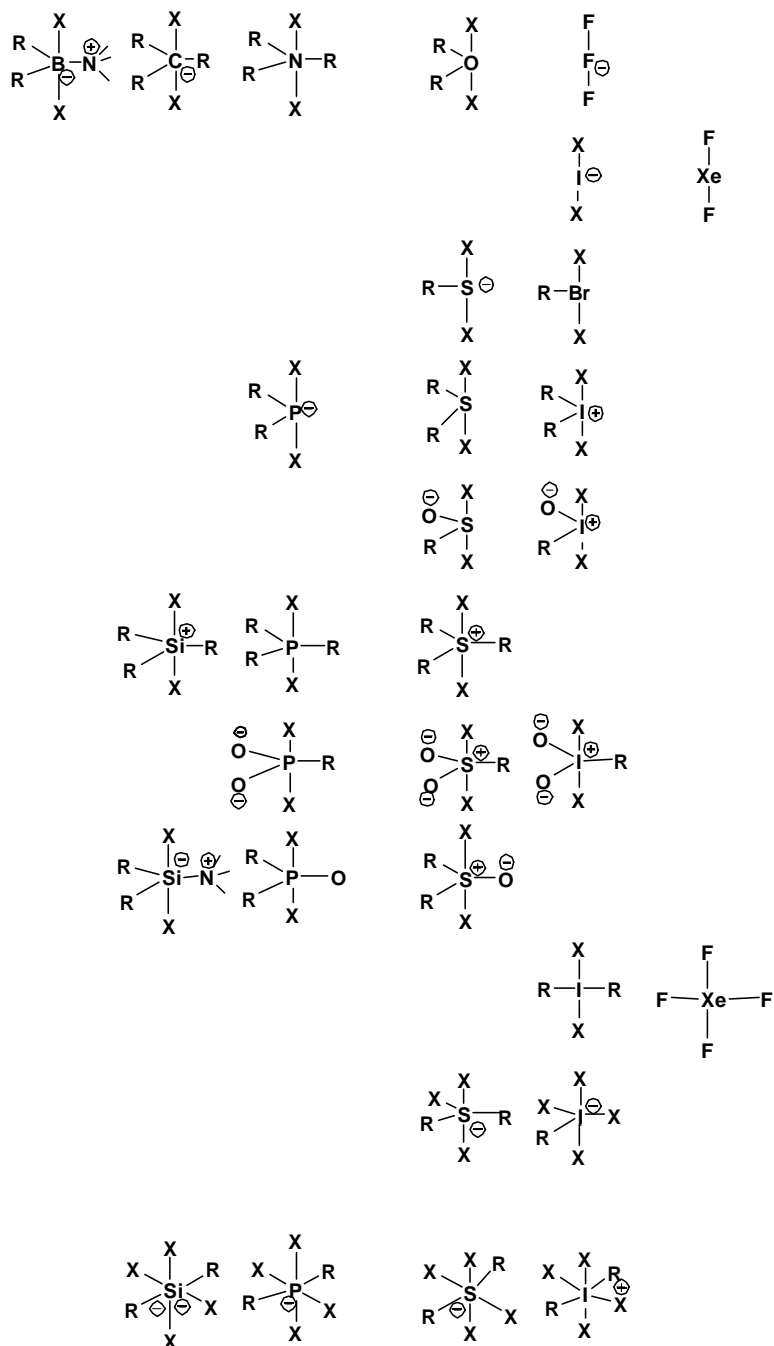


**Figure 1.1** A partial periodic table of hypervalent non-metallic elements

### 1.3 HYPERVALENT SILICON CHEMISTRY

Silicon has exhibited rich hypervalent chemistry of importance in both basic and applied nature. The developments in the study of higher coordinate silicon compounds are discussed in this section.

The first indication of the formation of a hypervalent compound by the reaction of silicon tetrachloride and ammonia was reported in early nineteenth century (Gay Lussac, 1809). Dilthey in 1903 reported a hexacoordinate cationic species of silicon  $[\text{Si}(\text{acac})_3]^+\text{HCl}_2$ . Since the pioneering work of Frye (1964; 1970), hypervalent species of silicon have received attention and have been extensively reviewed (Muller and Heinrich, 1961; Kumada *et al.*, 1982; Tandura *et al.*, 1986; Corriu and Young, 1989; Corriu, 1990; Holmes, 1990; Chuitt *et al.*, 1993; Wong and Woollins, 1994). In literature, higher-coordinate silicates comprise of penta- to octa-coordination (Holmes, 1996). The higher coordinate silicates are so far prepared by changing the environment around the silicon atom. These have been achieved by varying:

- i) **Donor atoms** like oxygen, nitrogen, sulfur, phosphorus and carbon in ligands such as aromatic and aliphatic ortho-diols, schiff base and salen, aromatic ortho-dithiol, bisphosphines (Tacke *et al.*, 2005; 2004; 2003; 2001; Wagler, 2005a; 2005b),
- ii) **Chelation-** mono to penta-dentate with ligands such as isocyanate, catechol and substituted catechol derivatives, citric acid, salen (Tacke, 2003; Verkade *et al.*, 2005; Kriegisch, 2005; Tacke, 2003; Roewer, 2005).
- iii) **Chelate ring-** size ranging from four to seven membered rings using ligands such as biphosphines, catechol, salicylic acid and phthalic acid (Caulfield *et al.*, 2001; Tacke, 2002; Singh *et al.*, 2000).

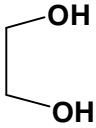
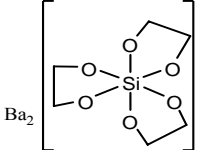
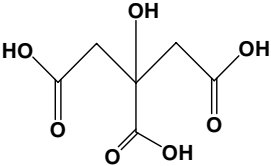
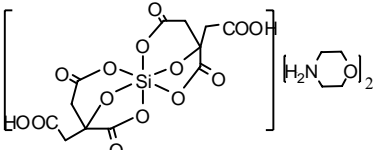
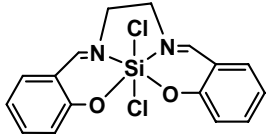
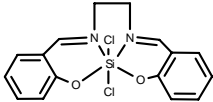
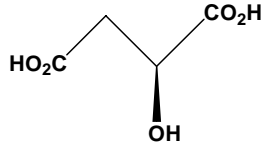
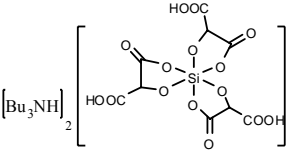
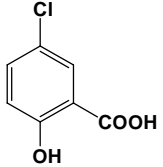
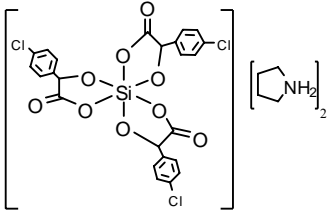
- iv) **Counter ions** like ammonium, alkali metal ion, transition metal cationic complexes,  $\text{HCl}_2^-$ ,  $\text{FeCl}_4^-$ ,  $\text{AuCl}_4^-$ ,  $(\text{TCNQ})^-$ ,  $\text{AgCl}_2^-$ ,  $\text{CF}_3\text{SO}_3^-$  (Bindu *et al*, 2003; Evans *et al*, 1990).

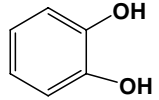
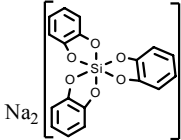
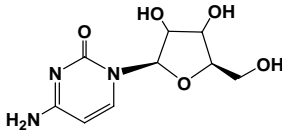
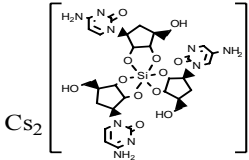
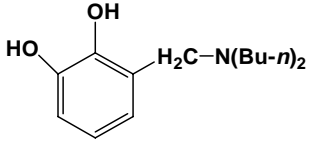
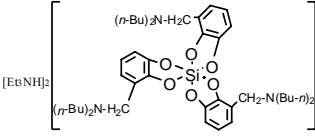
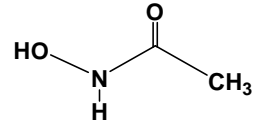
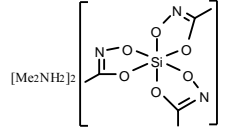
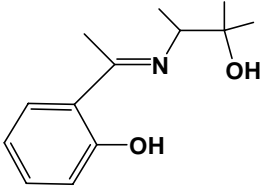
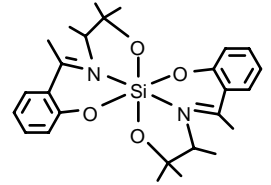
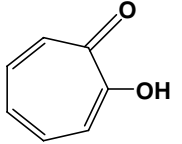
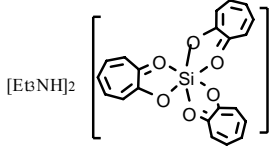
Kost and co workers have studied the stereodynamic properties of silicates containing flexible ligands and their role in stabilizing the silicates (Kost *et al*, 2004). Recent reports of hexacoordinate silicate using different ligands are given in **Table 1.1**.

The number of hypervalent silicon compounds have grown remarkably and they exhibit novel structural features, (Hosmane *et al*, 1986; Juitz *et al*, 1986; Rees *et al*, 1986; Bock *et al*, 1989), unusual chemical and biological activity and potential applications in different fields such as organic synthesis, catalysis, medicines, material science and engineering (Corey *et al*, 1963; Furin *et al*, 1988; Laine *et al*, 1991; Chuit *et al*, 1993; Herreros *et al*, 1994).

The increase of the silicon atom's coordination number to five or six by coordinating additional donors provokes an activation of all bonds around the silicon atom. Thus, hypercoordinate silicon complexes represent minima on a reaction coordinate during a substitution reaction. Both the theoretical aspects of investigating such model compounds (Bassindale *et al*, 2000) and the practical use of bond activation by hypercoordination in organic and inorganic chemistry (Denmark *et al*, 2002) are important driving forces in the development of the coordination chemistry of silicon. Referring to these basic correlations of controlled switching of the coordination number in silicon higher coordinate compound has been achieved i) by variation of solvent (Bassindale *et al*, 1999) ii) by variation of temperature (Kingston *et al*, 2001) and iii) by irradiation (Kano *et al*, 2001). Investigation of unique material of properties hypercoordinate silicon compounds as well as focused preparation of

**Table 1.1:** Hexacoordinate Silicates in the literature

S.No	Silicon source	Ligands	Reaction condition	Products	References
1	SiO <sub>2</sub>		BaO, (CH <sub>2</sub> OH) <sub>2</sub> , 12 min, MW, 200 °C		Yu, Shaoming, 2005
2	Si(OMe) <sub>4</sub>		MeOH, Morpholine, THF, 20°C, 20 d		Tacke, 2004
3	SiCl <sub>4</sub>		THF, Et <sub>3</sub> N		Rower, 2005
4	Si(OMe) <sub>4</sub>		1.) Bu <sub>3</sub> N, THF, 20 °C, 48 h 2.) CH <sub>3</sub> CN, reflux		Tacke, 2003
5	Si(OMe) <sub>4</sub>		Pyrrolidine, THF, 20 °C, 30 d		Tacke, 2002

6	Rice husk		NaOH, MeOH		Chandrasekhar, 1998
7	SiO <sub>2</sub>		CsOH, H <sub>2</sub> O, Ultrasound		Kinrade, 2003
8	Si(OEt) <sub>4</sub>		EtOH, Et <sub>3</sub> N		Caulfield, 2001
9	Si(OMe) <sub>4</sub>		Me <sub>2</sub> NH, MeCN		Tacke, 2002
10	Ph <sub>2</sub> SiCl <sub>2</sub>		THF, Et <sub>3</sub> N (excess)		Kira, 1996
11	CMe <sub>2</sub> CHCH <sub>2</sub> Si(OMe) <sub>3</sub>		Et <sub>3</sub> N, PhMe		Caulfield, 1998

hypercoordinate silicon compounds for certain applications, e.g., rhodenticides or anti-cancer drugs (Kalka *et al*, 2000), are prospering branches of silicon coordination chemistry. Chiral hypercoordinate silicon compounds are involved in the chirality transfer from silicon to carbon, which is another emerging field in this line of research (Oestreich, 2006).

Higher coordinate silicates are found to play a major role in organic syntheses as catalysts and intermediates. The arylbis(catecholato)silicates are used in the C-C coupling reactions, a substitute to organoborane and organostannane reagents (Seganish *et al*, 2004). Recently, citrate containing hexacoordinate silicates have found their use in dietary supplement and in cosmetics (Tacke *et al*, 2003). Since dianionic hexacoordinate silicates have relevance to biosilicification, such systems have been synthesized and structurally characterized (Sahai *et al*, 2002). Higher coordinate silicates have been classified based on the coordination number as penta-, hexa-, hepta- and octa-coordinate silicates.

Pentacoordinate silicates chemistry well established and they were classified based on the ligand(cyclic, acyclic and zwitterionic). Acyclic pentacoordinate silicates are used as starting material for the synthesis of cyclic and zwitterionic silicates. Pentacoordinate silicates are used as alkylating, hydrogenating agents(Holmes *et al*, 1996)

As the present study involves the synthesis of higher coordinated silicon complexes with different counter ions a brief introduction on the higher coordinated silicates of anionic, cationic and neutral species that have been reported so far is presented in the following sections.

### 1.3.1 Cationic Hexacoordinate Silicates

Cationic pentacoordinate silicon complexes with  $\text{SiO}_5$  skeletons have not yet been investigated, whereas the chemistry of cationic hexacoordinate silicon species with  $\text{SiO}_6$  skeletons is well established. In 1964, the syntheses of the cationic tris[1-oxopyridin-2-olato(-1)]silicon(IV) complexes with a variety of counter anions have been reported by Weiss *et al.* These systems have been characterized by elemental analysis and ESCA analysis (Meyer *et al.*, 1974).

Kummer *et al.* have prepared  $\text{MeHSi}[\text{bpy}]_2]^{2+}\text{I}_2$  in 1977. Bassindale *et al.* in 1984 have prepared 1:2 complex of  $\text{Me}_2\text{SiHX}$  with N-methylimidazole and 4-methylaminopyridine. Hensen and coworkers have studied the structural aspect of these silicon complexes (2000).

Muetterties in 1969 and Dilethy in 1985 have reported the cationic hexacoordinate silicon complexes with tropolone and diketone as ligand. But these cationic silicon complexes of tropolone and diketone have been structurally established by Kira *et al.* and Ueyama *et al.*, respectively (1995; 1984). Evans *et al.* have reported the preparation of similar water-soluble hexaaxosilicon complexes using the ligands that are listed in **Figure 1.2**, in which the overall charge is positive (1990). They have used silicon tetrachloride and tetraethoxysilane as silicon sources to obtain these cationic silicon complexes.



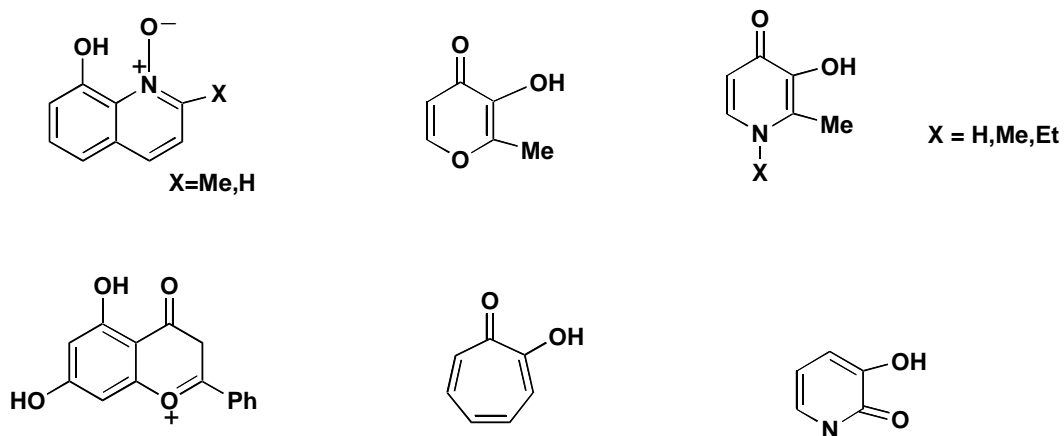


**Figure 1.2** Ligands used in the synthesis of cationic hexacoordinate silicon compound

Evans *et al* have employed counter ions like  $\text{HCl}_2^-$ ,  $\text{FeCl}_4^-$ ,  $\text{AuCl}_4^-$ ,  $(\text{TCNQ})^-$ ,  $\text{AgCl}_2^-$ ,  $\text{CF}_3\text{SO}_3^-$  and have studied their effect on the stability of hexacoordinate silicon species (1990). Pal *et al* have reported on the electrochemically active tris(9-oxophenalenone)silicon(IV)tetrakis[3,5-bis(trifluoromethyl)phenyl]borate ( $8+\text{TFPB}^-$ ) using silicon tetrachloride as silicon source (2006).

### 1.3.2 Anionic Hexacoordinate Silicates

The dianion  $[\text{Si}(\text{OH})_6]^{2-}$  can be regarded as the parent system for dianionic silicon species with  $\text{SiO}_6$  skeleton. Unlike  $[\text{SiF}_6]^{2-}$  the  $[\text{Si}(\text{OH})_6]^{2-}$  dianion has not yet been isolated and characterized. An example of a naturally occurring hypervalent silicate is stishovite. The formation of stishovite takes place at high temperatures and pressures (250-1300 °C at 35000 - 120000 atm (Herreros *et al*, 1994). However the synthesis of the first derivative tris[catecholato]silicate dianion has been reported (Resonheim *et al*, 1920). The tris[catecholato]silicate has been obtained as the pyridinium salt, the identity of which has been unequivocally established five decades later by single crystal structure

determination (Flynn and Boer, 1969). In the mean time many derivatives of tris[catecholato]silicate dianion with different cations and or substituted catechol have been synthesized and various aspects of their chemistry have been studied (Bindu *et al*, 2000; 2003; 2004; Evans *et al*, 1990; Caufield *et al*, 2001).

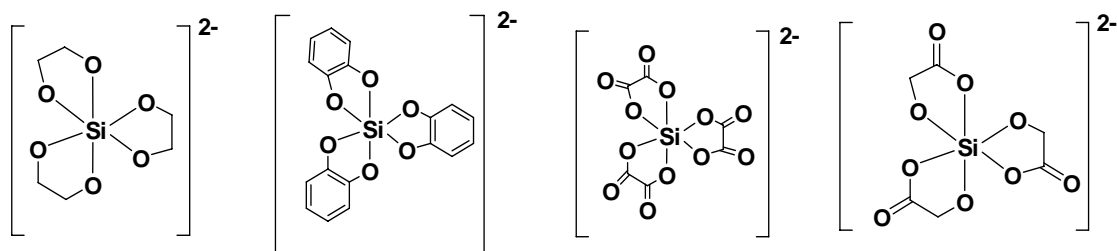


**Figure 1.3** A variety of dianionic hexacoordinate silicates

In contrast to the well established chemistry of the tris[catecholato]silicate dianion, the tris[ethan-1,2-diolato]silicate dianion has not been well studied (Hoppe *et al*, 1993). In 1969 first example of tris[oxalato]silicate dianion has been reported (Dean *et al*,) and nineteen years later the structure has been studied (Balkus *et al*, 1995; Seilver *et al*, 2002). Reactivity aspects of tris(catecholato)silicate have also been studied (Boudin *et al*, 1986; Carre *et al*, 1992).

Tacke *et al*,(2002) have developed synthetic strategy for silicates with unsymmetric bidentate ligand that are derived from aceto- or benzohydroxamic acid, glycolic acid, benzillic acid and hydroxycarboxylic acid like salicylic acid (**Figure 1.5**). Their stereochemical features such as fac/mer isomers have been well established (Tacke *et al*, 2004)

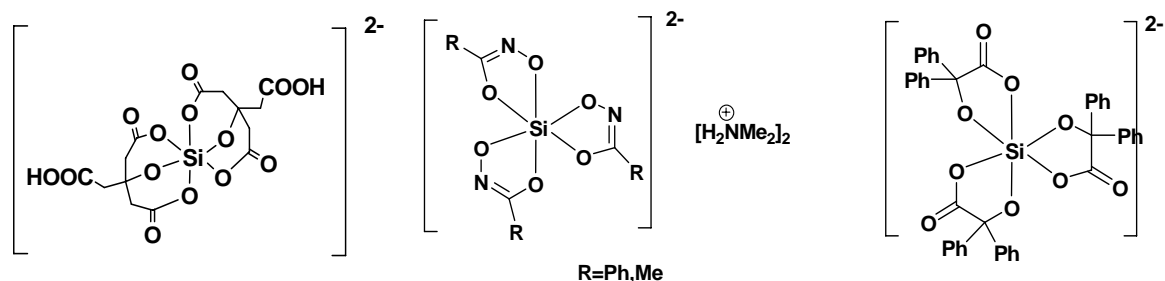


**Figure 1.4** Silicates with unsymmetric bidentate and tridentate ligands

Apart from bidentate ligands tridentate ligands have also been reported. For this chelate like citric acid, has been employed. These systems have been synthesized and their structures have been investigated (Tacke *et al*, 2003). Tris(catecholato)silicates with different counter cations were studied in literature (Kingston and Verkade, 2005).

### 1.3.3 Neutral Hexacoordinate Silicate

The chemistry of anionic and cationic hexacoordinate silicon complexes have been well established compared to neutral hexacoordinate silicon species (Juitz, 2003). The neutral hexacoordinate silicon complexes that are shown in **Figure 1.5** have been synthesized and characterized (Pike *et al*, 1965; Yamaguchi *et al*, 1998; Kira, 1995; Tacke *et al*, 2004; Xu *et al*, 2004)

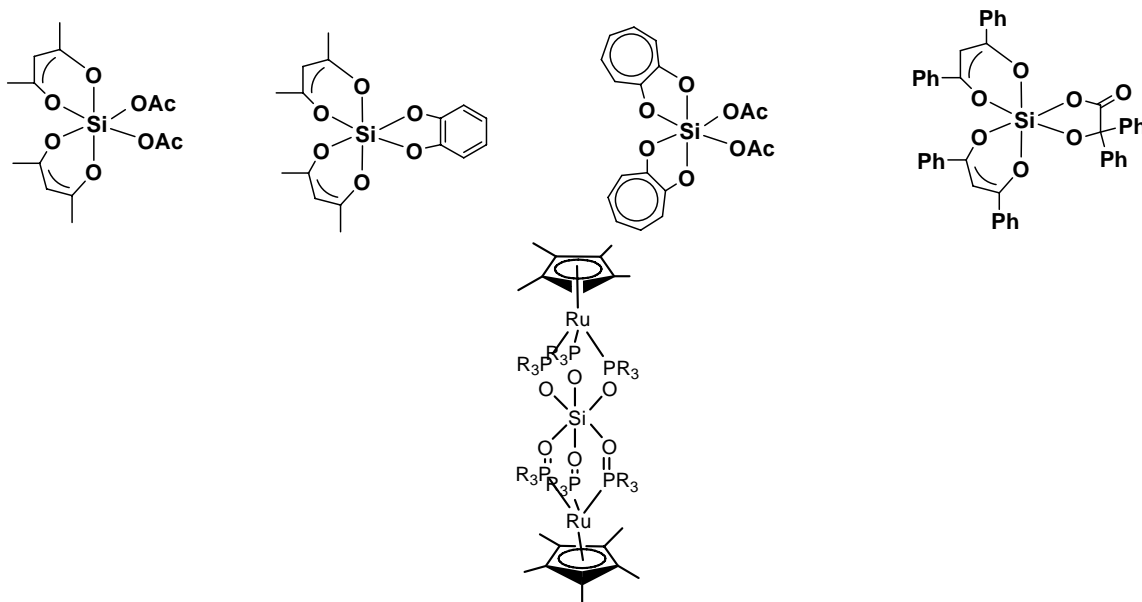


**Figure 1.5** Some of neutral hexacoordinate silicon compounds with  $\text{SiO}_6$

Tacke *et al*, in 2004 have carried out the structural characterization of the first heteroleptic neutral hexacoordinate silicon compound by XRD.

In literature, so far in the synthesis of dianionic hexacoordinate silicates, several ligands have been used and in the case of aromatic diols, catechol and substituted catechol derivatives have been well studied unlike the ortho-diolato naphthalene derivatives. The catechol silicon complexes of ammonium derivatives are not stable in the solid state for longer period. However it has interesting applications in the synthesis of organic reagents. This triggered us to synthesize analogue naphthalato derivatives.

#### 1.4 CHEMISTRY OF 2,3-DIHYDROXYNAPHTHALENE

Aromatic hydroxyl compounds are weak acids. 2,3-dihydroxynaphthalene has a  $\text{pK}_a$  value of 13.9 and at low pH it is a poor ligand. Apart from that, 2,3-dihydroxynaphthalene is well known for its biological activity as catecholase inhibitor.

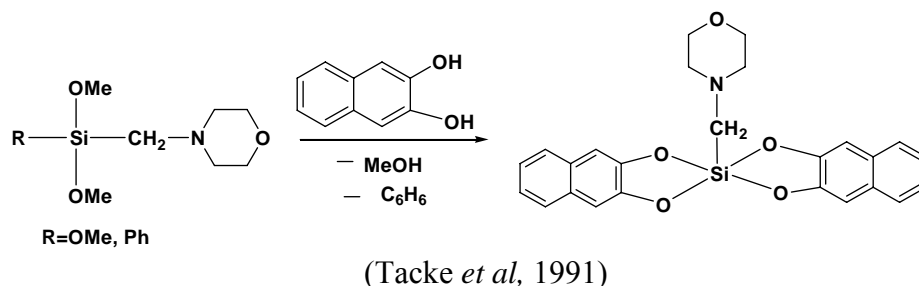
2, 3-dihydroxynaphthalene acts as an electron donor and complexing agent for a variety of metals (Joshi *et al*, 2002; Tarafder *et al*, 1994; El-Hendawy *et.al*; 1989; Comotti *et al*, 1998; Larkins *et al*, 1963; Readio *et al*, 1981; Yang *et al*, 1997)

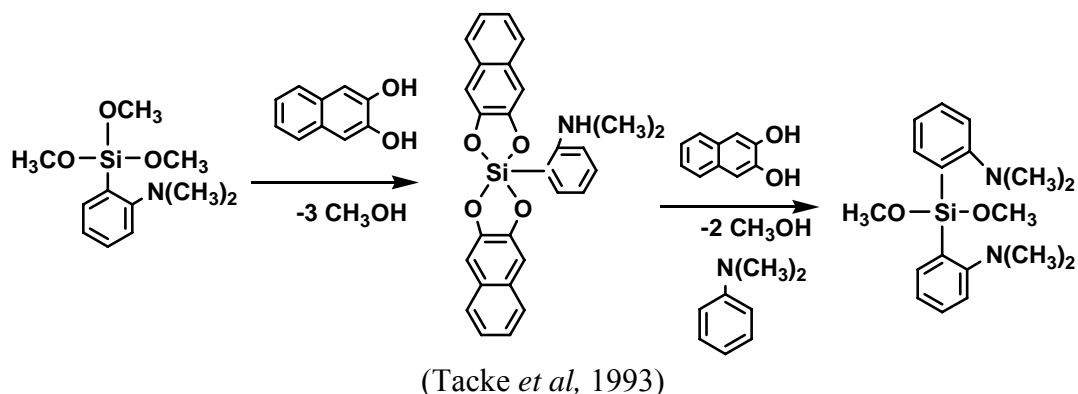
Prominently, only bis(2,3-dihydroxynaphthalato)silicates, have been mentioned in literature. Some of the bis(2,3-dihydroxynaphthalato)silicates containing phenyl/allyl/alkylamine as fifth substituent on silicon have been synthesized and structurally characterized. Tacke *et al* have prepared pentacoordinate silicates by the reaction of  $\text{RSiX}_3$  with 2,3-dihydroxynaphthalene in presence of a base (Tacke, 1991; Holmes *et al*, 1999; Tacke *et al*, 1993).

Regarding tris(2,3-dihydroxynaphthalato)silicates only scanty report is available. Meyer and co-workers have described synthetic procedure for tris(catecholato)silicates using silicon tetrachloride and they mentioned that this method is applicable for 2,3-dihydroxynaphthalene ligand (Meyer *et al*, 1969).

#### 1.4.1 Synthesis Of Pentacoordinate Silicates of 2,3-Dihydroxynaphthalene

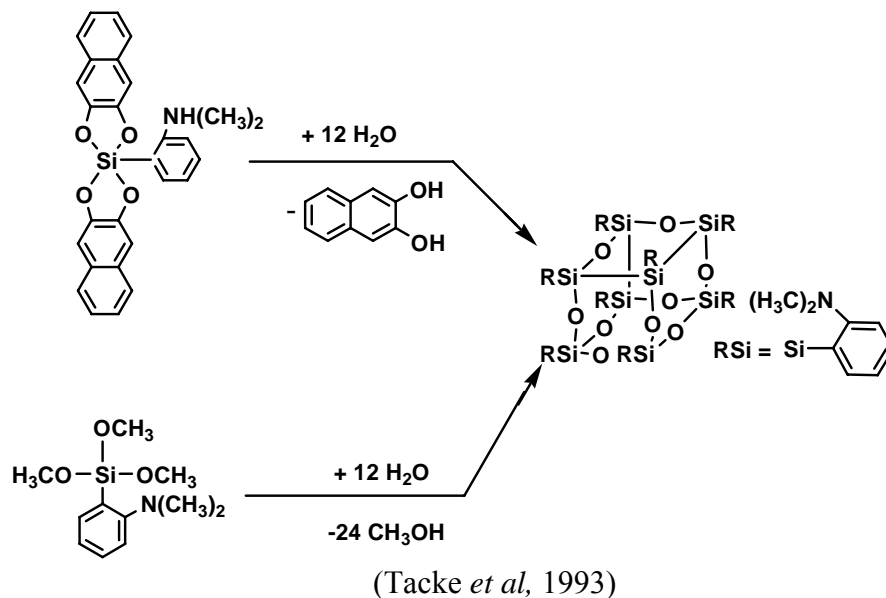
Some of the synthetic routes reported in the literature are outlined in the **Scheme 1.1**





**Scheme 1.1** Synthesis of alkyl/arylbis(2,3-dihydroxynaphthalato)silicate

Arylbis(2,3-dihydroxynaphthalato)silicate used as a precursor for cage compounds is shown in **Scheme 1.2**.



**Scheme 1.2:** Reactivity of bis(2,3-dihydroxynaphthalato)silicate with water to form cage compounds

#### 1.4.2 Structural Characterization of Pentacoordinate Silicate of 2,3-Dihydroxynaphthalene

Pentacoordinate silicate of 2,3-dihydroxynaphthalene adopts trigonal bipyramidal geometry. This geometry is preferred over the square pyramidal due to steric bulkiness of

the ligand and the interaction with the ligand on fifth position as shown in the **Figure 1.6**. Si-O bond length lies in the range of 1.699-1.79 Å and Si-C bond length lies in the range of 1.885-1.92 Å, where Si-C bond length is shorter than the normal Si-C bond. There has been an intramolecular hydrogen bonding seen in the case of zwitterionic species (Tacke *et al*, 1993; 1991; Holmes, 1999).

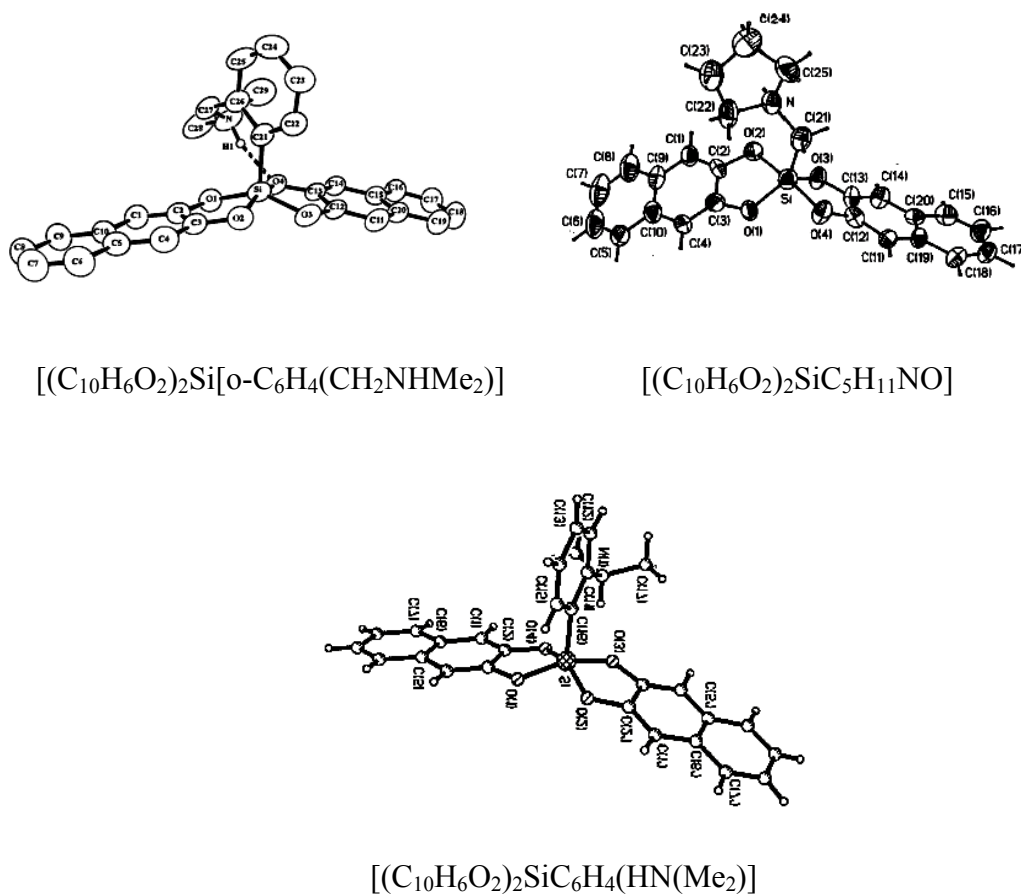


**Figure 1.6:** Pentacoordinate silicates of 2,3-dihydroxynaphthalene (2,3-DHN)

### 1.4.3 Higher Coordinate Silicate of 2,3-DHN as a Reprography Material

Reprography is a general term for the reproduction of documents or images especially those that are virtually indistinguishable from the original. Reprography can be by

mechanical, electronic, or photographic means such as photocopying or xerography, scanning, digital printing, and photography. Toners contain catechol derivative of silicon and these are used in a monocomponent image developing process. The toners show a good friction-charging property and provide good images (Tanaka *et al*, 1995). The charge-controlling agent contains a silicon complex with catechol and 2,3-dihydroxynaphthalene, polycyclic aromatic diols and hydroxycarboxylic acid as ligands (Sugata *et al*, 1992; Ishii, 1991). Thermal recording materials comprise of compounds selected from phenylurethane and silicon or phosphorus derivatives of phenols which forms phenols by pyrolysis; organic iron compounds and microcapsules containing hydrophobic bases (Shioi *et al*, 1988). Reprography materials comprise of a sensitive layer containing a chromogenic compound e.g. a diazo compound and a silicon or phosphorus derivative of 2,3-dihydroxynaphthalene that decomposes on heating or on contact with a fluid, e.g. NH<sub>3</sub>, to liberate a silicon derivative of 2,3-dihydroxynaphthalene which in turn reacts with the chromogenic compound to give a colored image (Ceintrey, 1979).

### **1.5. METHODS OF SYNTHESIS OF HEXACOORDINATE SILICATES**

Synthesis of dianionic hexacoordinate silicates has been achieved at room temperature as well as in reflux reaction conditions other than ultrasonication that has been used for synthesis of tris(catecholato)silicate using silica as starting material (Chandrasekhar *et al*, 1998; Chuit *et al*, 1989)

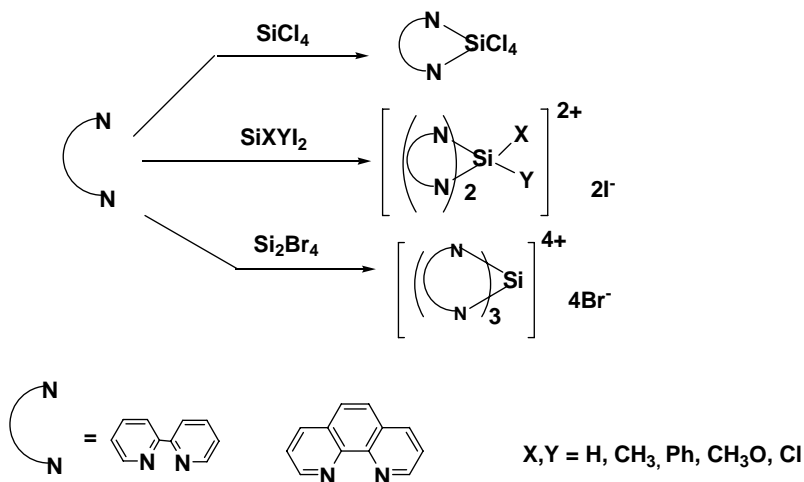
By varying silicon sources such as rice husk, colloidal silica, tetramethoxysilane, tetraethoxysilane, silicon tetrachloride and tetraisothiocyanatosilane, hexacoordinate silicon compounds have been obtained (Holmes *et al*, 1996).



The various types of reactions that are involved in the synthesis of hexacoordinate silicate are as follows:

### 1.5.1 Intermolecular coordination to an organosilane

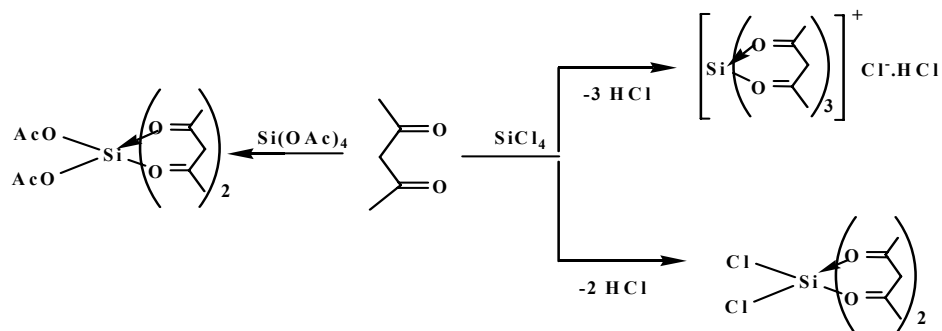
Silicon tetrahalides when reacted with bipyridyl or 1,10-phenanthroline by intermolecular coordination form hexacoordinate silicon compounds is given in **Scheme 1.3** (Holmes, 1996).



**Scheme 1.3:** Synthesis of hexacoordinate silicon compound-Intermolecular coordination

### 1.5.2 Substitution in a tetrafunctional silane by a bidentate ligand

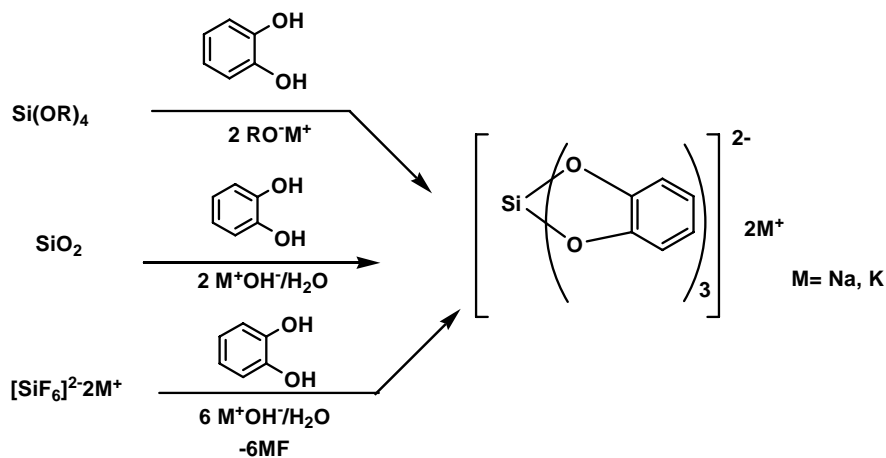
Tetrafunctional silane is substituted by bidentate ligand due to chelation effect. A representative reaction of acetylacetonato with silicon tetrafunctional is given in **Scheme 1.4**. It is an effective route for both aliphatic and aromatic bidentate ligands (Holmes *et al*, 1996)



**Scheme 1.4** Synthesis of hexacoordinate silicon compound- Substitution reaction

### 1.5.2.1 Synthesis of tris(Catecholato)silicate

Tris(catecholato)silicates have been synthesized by varying the silicon source and also the base as shown in **Scheme 1.5**. By varying conditions such as ultrasonication, reflux and even at room temperature these derivatives are obtained in good yield. The chelation effect of bidentate ligand is the driving force for complexation (Rosehman *et al*, 1931; Laine *et al*, 1991; Berzelius *et al*, 1924).



**Scheme 1.5** Synthesis of tris(catecholato)silicates – different routes

The importance of microwave irradiation and the versatile pharmacological activity of organosilicon compounds prompted Singh *et al* to report for the first time a microwave assisted method for the synthesis of some new biologically potent organosilicon complexes (2005; Manju *et al*, 2006).

### **1.5.3 Microwave methods**

Microwave energy generates rapid intense heating of polar substances resulting in significant reduction of reaction times, high selectivity and in many cases, higher yields. The main advantage of microwave heating has been the instantaneous ‘in-core’ heating of materials in a homogeneous system. This implies a considerable saving of energy. Organometallic and coordination compounds have received surprisingly little attention in the microwave-assisted synthesis relative to the other areas of study (Michael *et al*, 2002; Ravi *et al*, 1998). The acceleration in reaction rate can be attributed to thermal and hot spot effects under microwave irradiation (Antonio *et al*, 2005).

#### **1.5.3.1 Thermal effect**

The thermal effects observed under microwave irradiation conditions, may be a consequence of the inverted heat transfer, the inhomogeneities of the microwave field within the sample and the selective absorption of the radiation by polar compounds. These effects can be used efficiently to improve processes, modify selectivities or even to perform reactions that do not occur under conventional reaction conditions.

### 1.5.3.2 “Hot Spots” inhomogeneities

This is a non-thermal effect or special effect that arises as a consequence of the inhomogeneity of the applied field, resulting in the temperature in certain zones within the sample being greater than the macroscopic temperature. The higher conversion under microwave irradiation has been attributed to the presence of hot spots. Zhang *et al* estimated the temperature in the hot spots to be about 300 – 400 K higher than the bulk temperature (1999; 2001).

## 1.6 CHARACTERIZATION OF HEXACOORDINATE SILICATES

In higher coordinate silicon complexes the interaction between silicate and counter ions can be established by single crystal X-ray structures.  $^{29}\text{Si}$  NMR helps to understand the coordination number and ligand environment around silicon.

### 1.6.1 X-ray structural characterization of hexacoordinate silicates

A structural study of higher coordinate silicates helps in explaining their unusual chemical and biological behaviour. A large number of X-ray structures have been reported (Kingston and Verkade, 2005; Tacke *et al*, 2004; Seilver *et al*, 2002, 2004; Rower *et al*, 2006; Bindu *et al*, 2003, Pak *et al*, 2002). The structures of a few examples representing different types of ligand environment in silicon complexes are given in the **Figure 1.7**. The extent of variation in bond length and bond angles was found to be influenced by i) the nature and choice of the ligand ii) the degree of hypervalency attained by the silicon centre and iii) the neutral or ionic nature of the hypervalent silicon

system. Structural study has been carried out to explain the reactivity of hypervalent silicon compounds.

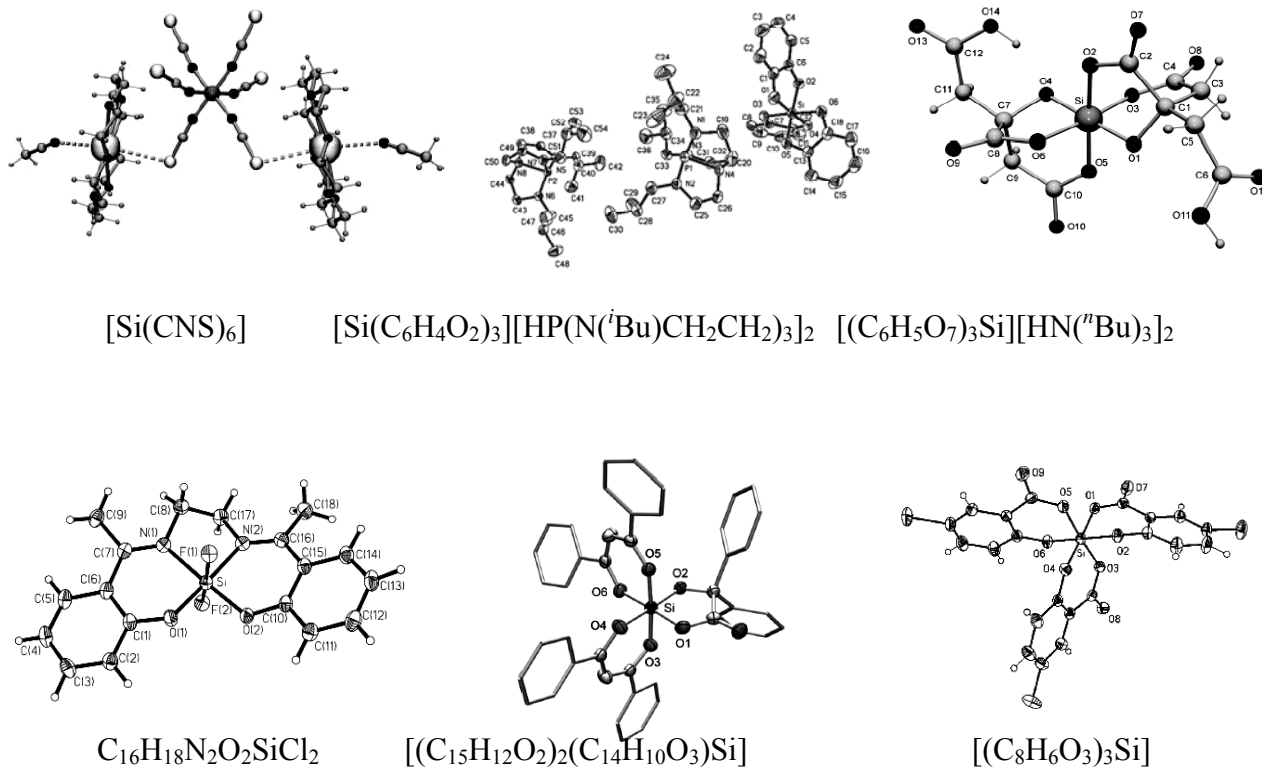


**Figure 1.7:** Single Crystal structures of hexacoordinate silicates

In hexacoordinate silicon complexes irrespective of the dentation of ligand and chelate ring size, silicon is in distorted octahedral geometry. Si-O bond lengths lie in the range of 1.69-1.820 Å but the variation may be due to the type and the extent of hydrogen bond that is involved with their counter ion. In most of the cases there has been an extended hydrogen-bonding network depending on the nature of counter ion. In the case of hydroxyalkylammonium counter cation containing silicate bifurcate type of hydrogen bonding is observed. The facial- meridional isomers arising due to substituent on the ligand were also structurally studied (Tacke *et al*, 2003).

### 1.6.2. $^{29}\text{Si}$ NMR spectral analysis of hexacoordinate silicate

$^{29}\text{Si}$  is a low sensitivity nucleus that has spin  $\frac{1}{2}$  with natural abundance of 4.6832%. Dilute TMS in  $\text{CDCl}_3$  is generally used as reference. Reference line width is 0.15 Hz and T1 of reference is 5s. The spectrum always contains a broad background signal at -110 ppm due to quartz present in the NMR tube material. The chemical shift ranges of the silicon compounds are depicted in the **Figure 1.8**.

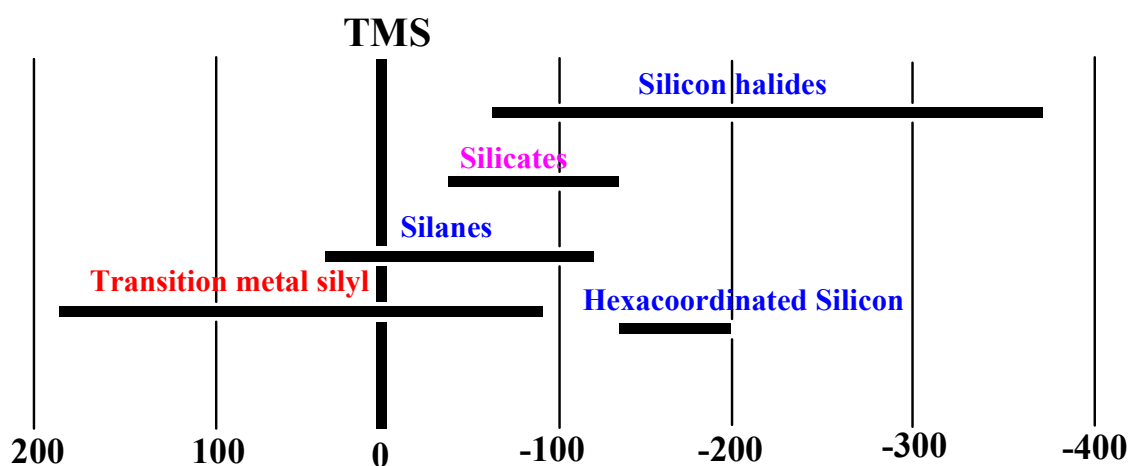


**Figure 1.8:** Chemical shift ranges of silicon NMR spectrum for silicon compounds

A number of reviews covering all aspects of  $^{29}\text{Si}$ -NMR are available (Williams and Cargioli, 1979; Schramb *et al*, 1976; Marsmann, 1981). Analysis of the data reveal i) high field shift of the silicon signal as the coordination number increases from four, ii) donor-acceptor interaction that leads to neutral complexes, which causes only smaller changes in chemical shift value, and iii) in the case of hexacoordinated silicon species as long as the nature of the substituent and bond type are the same, the chemical shift does not seem to depend on the neutral or ionic nature of the compound (Cella *et al*, 1980)

Silicon complexes of aromatic ligand have lower  $\delta$  value compared to aliphatic ligands due to the delocalization of electron in the aromatic ring. Silicon complex of citric acid, the higher  $\delta$  value is due to aliphatic nature of the ligand. Whereas, in the case of monodentate ligand  $\text{Si}(\text{NCS})_6$  the highest value, may be due to accumulation of charge on silicon. There has been no significant variation in  $\delta$  values when counter ion was varied. Six-coordinate silicon complexes are found to have variation in  $\delta$  value with change in the chelate ring size. When the chelate ring size is five then  $\delta$  value lies in the range of -130 to -150 ppm whereas, when it is six the range is -190 to -200 ppm, which have been identified by Wongs and coworkers (1994).

The commonly used silicon sources and the observed chemical shift values are listed in **Table 1.2**. Chemical shift values of a variety of silicates with varying dentation of the ligand are given in the **Table 1.3**.

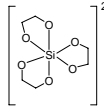
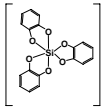
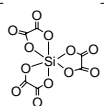
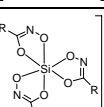
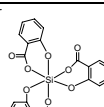
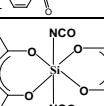
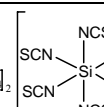
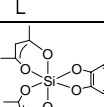
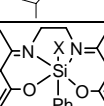
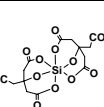
**Table 1.2:** Chemical shift values of silicon sources

<b>Compounds</b>	<b>Chemical shift (ppm)</b>	<b>Reference.</b>
$\text{Si}(\text{OEt})_4$	-83.5	Meyer, 1979
$\text{Si}(\text{OMe})_4$	-78.29	Cella, 1980
@ $\text{SiCl}_4$	-45.00	Cella, 1980
* $\text{SiO}_2$	-80 to -120	Meyer, 1979

\* - Recorded in solid state

@- using TMS as solvent

**Table 1.3:**  $^{29}\text{Si}$  Chemical Shift for Hexacoordinate Silicates

S.No.	Compounds	$\delta$ , ppm	Reference
1		-145.5	Palavai, 1995
2		-139.3	Kingston, 2005
3		-173.2	Tacke, 2002
4		-138.1	Tacke, 2002
5		-188.5	Tacke, 2004
6		-206.6	Tacke, 2002
7		-256.5	Tacke, 2002
8		-176.1	Tacke, 2004
11		-181.5	Rower, 2005
12		-166.4	Tacke, 2004

## 1.7 HIGHER COORDINATE SILICATES AS PRECURSOR FOR SILICA MATERIALS: RELEVANCE FOR BIOSILICIFICATION

Silicon in the form of silica plays a role in biological systems, where it serves as an important trace element in microorganism, plants and higher organisms (Van Soest,



2006). The remarkable level of structure control exhibited by the organism over biomineralisation of silica has inspired the attempts of biologists and material scientists to define and mimic this ability (Patwardhan *et al*, 2005).

### **1.7.1 Silicon Uptake Evidence of Transient Hexacoordinate Silicate**

Despite being located just below carbon in the periodic table, silicon has been found to have very little involvement in life processes. Silicon is a trace element present in plants and animals whose uptake is of interest. Considerable progress has been made in understanding proteins that control the biological production of silica nanostructures. Kinrade *et al* have reported on the aqueous silicate being complexed with sugar. This may play a role in silicon uptake (1999). Later, they observed that diatom species studied under enriched silicon environment gave a peak at  $-131$  ppm that is characteristic of higher coordinated organosilicate (Kinrade, 2002). They have studied the extract of xylem exudate from wheat (Casey *et al*, 2004).  $^{29}\text{Si}$  NMR spectra indicated the existence of two silicon containing species in the xylem exudate, mono and disilicic acid ( $\text{H}_4\text{SiO}_4$  and  $(\text{HO})_3\text{Si}(\mu\text{-O})\text{Si}(\text{OH})_3$ ) in a ratio of approximately 7:1. Significantly, there was no evidence of organosilicate complexes (Kinrade, 2004). This is in contradiction to earlier results. They have found that aqueous silicate solutions react with straight-chain polyhydroxy compounds (glycitol such as xylitol, threitol, and sorbitol) to form hexacoordinate silicon species (2003). The evidence provided by Kinrade *et al* was based entirely on  $^{13}\text{C}$  and  $^{29}\text{Si}$  NMR experiments. In strongly basic solutions, they found  $^{29}\text{Si}$  signals that are due to the formation of penta- and hexa- coordination species and they are prominent (2003). They have observed several peaks, indicating that several higher coordinate silicon species formed by sugar presumably via oxygen chelates

(Kinrade *et al*, 2001a). Klufers and co-workers suggested that the connection between the glycitols and silicic acid takes the form of a five-membered diolato ring (2005). Silica material is generally synthesized by sol-gel process (Suhukara, 2005) and structured silica was obtained using template directed synthesis (Isyama *et al*, 2005). Such a study triggered the interest in synthesis of bioinspired materials.

### **1.7.2 Studies on the decomposition of silicon complexes**

The kinetic studies on the decomposition of silicon complexes have relevance in biosilicification. Kinrade *et al* have reported that transient species in the process of biosilicification in some low organism is found to be hexacoordinate silicon species based on silicon NMR observation. The study on the formation and stability of silicon complexes in aqueous medium near neutral conditions has been carried out as structural mimicking model (1999; 1988).

Catechol is a basic skeleton of the ferritin kind of natural complexing agent and tris(catecholato)silicates are soluble in water. Perry *et al*, studied the effect of counter cations on the decomposition of tris(catecholato)silicates. It was reported that small cations with high charges such as  $\text{Fe}^{3+}$  and  $\text{Mg}^{2+}$  stabilize the silica oligomerisation strongly compared to uncharged ions, such as  $\text{Na}^+$ .

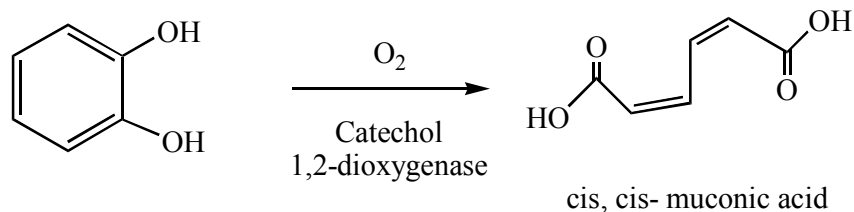
The decomposition of tris(catecholato)silicate is pH dependent. For example, at pH 4.0, when silicic acid molecules are not ionized, metal ions have no effect on silica polymerization kinetics. For silicate system at high pH, the majority of ions are ionized (1992). Kinrade and Pole in 1992 have shown that there are three distinct ways in which alkali metal cations can influence aqueous silicate equilibria. These include 1)

electrostrictive water structuring by small cations, notably lithium that increases the overall level of polymerization, 2) Silicate-M<sup>+</sup> ion pairing that enables the formation of siloxane bonds. The repulsive forces between anions is reduced (the effect is most pronounced for Cs<sup>+</sup> where the ion-pair formation constant is the lowest and the extent of polymerization is the least and 3) cations of ion pair stabilize specific oligomers by immobilizing labile appendages and large ring structures (Harrison *et al*, 1995).

In the presence of cellulose the particle are physically distinct from one another when the silicon complexes were hydrolysed. Cellulose plays a major role in determining spatial availability for particle growth and spatial organization. So in nature cellulose plays a role in silica precipitation process leading to structured silica (Perry *et al*, 1992).

## 1.8 STUDIES ON ELECTROCHEMICAL BEHAVIOUR OF DIHYDROXYARYL COMPOUNDS

The oxidative cleavage of catechol and other dihydroxy aromatic compounds is a key step in the biodegradation of naturally occurring aromatic molecules and many aromatic pollutants in the environment. Catechol-1,2-dioxygenase (CTD) and Protocatechuate-3,4-dioxygenase (PCD) are bacterial non-heme iron enzymes, which catalyze the oxidative cleavage of catechols to *cis, cis*-muconic acids with the incorporation of molecular oxygen via a mechanism involving a high-spin ferric center (Yukikazu *et al*, 1980) (Scheme 1.6).



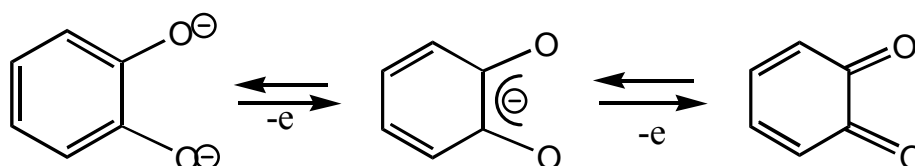
**Scheme 1.6:** Oxidative cleavage of catechols to *cis, cis*-muconic acids

The catalytic role of metal cations in enzymatic redox reactions has merited recent attention. Redox enzymes have demonstrated the involvement of metal cations at their active sites. Since most redox coenzymes contain a lone pair of heteroatoms, the interaction of the redox coenzyme with metal cations result in enhancement of the redox activity of the enzyme (Okamoto *et al*, 2002). Metal cations and ammonium ions have been shown to influence the reactivity of quinone in the amine oxidation reaction and in electron transfer from the reduced quinone cofactor to amicyanin (Bishop *et al*, 1997). In case of quinone, hydrogen bond formation between the quinone cofactor and ammonium ion play an important role in controlling the electron transfer reactions (Frontana *et al*, 2005).

Naturally occurring quinones have a hydroxyl function (represented as Q–OH) in their structure. The presence of this type of hydroxyl functionality seems to be related to the biological activity of this kind of compound and the position of this functional group can alter the typical redox behaviour of the quinoid moiety. This has relevance to most of the biological activity of quinonoid systems in relating their capacity to carry out free radical generation via redox reactions (Ossowski *et al*, 2004).

Quinones, naphthoquinones and their derivatives possess potent photodynamic action (Diwu *et al*, 1993). Molecules derived from quinones are highly redox active and can undergo redox cycle with their semiquinone radicals, leading to the formation of superoxide, H<sub>2</sub>O<sub>2</sub> and ultimately to the hydroxyl radicals (Sihna *et al*, 1990). Naturally occurring naphthoquinones and binaphthoquinones are known for their cytotoxic action against human breast cancer MCF-7 cell (Motilall *et al*, 2005).

Merhdad *et al* in 1999 have studied redox behaviour of catechol and its analogues *o*-hydroxyamino, *o*-hydroxythiol aromatic compounds. Metal complexes of catechol and substituted catechol were studied as a function model of catechol dioxygenase. The oxidation of catechol to quinone is shown in the **Scheme 1.7**.



**Scheme 1.7:** Oxidation of catecholate to quinone

Among naphthoquinone compounds, redox behaviour of 1,2 and 1,4 - dihydroxynaphthalene are well studied. Since the quinone of these compounds are stable. 2,3-dihydroxynaphthalene compounds have been studied under electrochemical conditions but there is no structural inference on account of their instability (Horak *et al*, 1981). Chemically oxidized product of 2,3-dihydroxynaphthalene has been studied by trapping naphthoquinone-using cyclopentadiene. Wanzlick *et al* have reported 1,1'-dimer as chemically oxidized product in absence of cyclopentadiene (1957). The naturally occurring naphthoquinone are given in the **Figure 1.9** (Weissenberg *et al*, 1997).

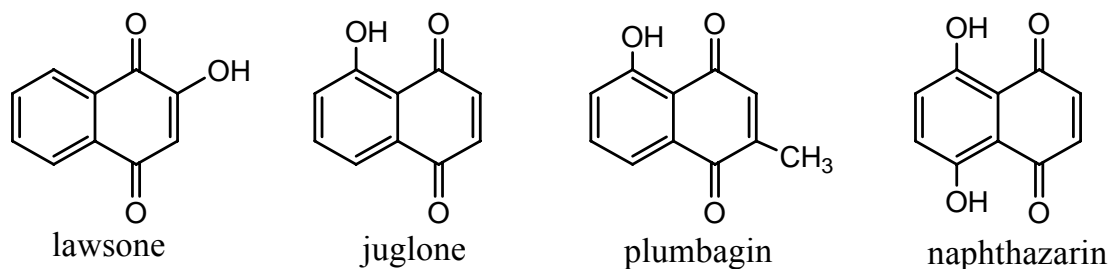


**Figure 1.9:** Naturally occurring naphthoquinones

## 1.9 METAL OXIDE SILICA MATERIALS - HIGHER COORDINATE SILICATE AS PRECURSORS

ZnO-silica material was synthesized in four-stage via sol-gel route (Moleski *et al*, 2006). The synthesis of CuO/SiO<sub>2</sub> and NiO/SiO<sub>2</sub> with bimodal pore structure was achieved by sol-gel method. Tetramethoxysilane, metal nitrate in the presence of poly(ethylene oxide) and the catalyst (acetic acid) were used for synthesis of CuO/SiO<sub>2</sub> and NiO/SiO<sub>2</sub> (Zheng *et al*, 2006). Incipient wetness impregnation method has been used to prepare silica supported manganese oxide catalyst that was used for oxidation of acetone (Reed *et al*, 2005). Silica-metal oxide composites have application in various fields such as magnetic, optics, electronics and catalysis (Scott *et al*, 2001). Pyrolysis is a single step method to synthesize structured silica (Boryseko *et al*, 2004). Metal chalcogenides were also synthesised by one pot pyrolytic route (Vittal, 2006). Recently, Guo *et al* in 2006 have synthesized ZnO from ethylenediamine complex of zinc in presence of air at lower temperature. Like catechol, 2, 3-dihydroxynaphthalene has also been used as a template for preparation of structured tubular silicates (Isayama *et al*, 2005).

$[M(en)_3]^{2+}$  (M = 3d-transition metal; en = ethylenediamine) derivative of tris(catecholato)silicates on pyrolysis leads to the formation of transition metal orthosilicate/metaloxide-silica mixture with good catalytic activity (Bindu *et al* in 2004).

### 1.10 OBJECTIVES OF THE PRESENT STUDY

The synthesis of tris(2,3-dihydroxynaphthalato)silicates was undertaken with the following objectives

- ✓ To develop an optimized synthetic strategy for hexacoordinate silicates incorporating 2,3-dihydroxynaphthalene ligands with various ammonium or transition metal containing counter cations.
- ✓ To investigate structure of tris(2,3-dihydroxynaphthalato)silicate and also their stability in presence of different counter ions under thermal and hydrolytic conditions.
- ✓ To study the redox behaviour of 2,3-dihydroxynaphthalene ligand in hexacoordinate silicon coordination environment.
- ✓ To utilize these silicates for the synthesis of catalytic materials such as micro-, meso-porous silica and metal silicates.

## **CHAPTER II**

### **EXPERIMENTAL METHODOLOGY**

---



This chapter provides an account on the purification of solvents and other reagents and general description of the experimental techniques employed in this study. The preparation, purification and characterization of some of the starting materials will also be covered in this chapter.

## 2.1 PURIFICATION OF SOLVENTS AND OTHER REAGENTS

The standard procedures were employed to purify the following solvents and reagents (Vogel, 1975; Perrin *et al.*, 1980; Dean, 1987).

### i) Acetonitrile

Acetonitrile (LR) was distilled twice over  $P_4O_{10}$  (5 g/L) and  $CaH_2$  (1 g/L). The constant boiling fraction (81 °C) was collected and stored over Linde type molecular sieves (4 Å).

### (ii) Diethyl ether

Diethyl ether (commercial grade) was washed with freshly prepared  $FeSO_4$  solution (to remove any peroxide impurities), dried over anhydrous  $CaCl_2$  (1 day), refluxed over sodium for 2 h and distilled. Then it was refluxed over sodium-benzophenone for 4 h and distilled slowly to obtain the constant boiling fraction (35 °C) and stored over sodium wire in a dark and cool place.

### (iii) Amines

Tri-*n*-butylamine (216 °C), triethylamine (89 °C) (Ranbaxy), diisopropylamine (84 °C), diisobutylamine (140 °C), morpholine (129 °C), N-methylpiperazine (138 °C), piperidine (106 °C), pyrrolidine (87 °C), *sec*-butylamine (63 °C), *t*-butylamine (46 °C), 2-

aminopyridine (58 °C), aniline (184 °C) and ethylenediamine (118 °C) (S. D. Fine Chem.) were kept overnight over KOH pellets, decanted, distilled over sodium wire to collect the constant boiling fraction and the distillates were stored over fresh sodium wire.

Piperazine (m.pt. 108-110 °C) (E Merck) was recrystallized from benzene-hexane (2:1) mixture before use.

#### (iv) **Silicon reagents**

Tetraethoxysilane (TEOS)  $\text{Si}(\text{OEt})_4$  was 99.9 % pure (Metkem Silicons, Mettur). It was used as received (b.pt. 168°C) and handled under  $\text{N}_2/\text{Ar}$  atmosphere.

#### (v) **2,3-dihydroxynaphthalene**

2,3-dihydroxynaphthalene was 99.8 % pure (Acros Organics). It was used as received (m.pt. 160 °C).

## **2.2. EXPERIMENTAL TECHNIQUES**

On account of air and moisture sensitive nature of many of the starting materials *viz.* tetraethoxysilane and tetrachlorosilane their storage and handling was done by the use of suitable glassware (side-arm flasks, filtering frits, pressure equalized dropping funnel, schlenck tubes and techniques like inert atmosphere manipulations, vacuum line operations, solvent still, Schlenck line technique (Shriver and Drezdson, 1986). Oxygen free, dry nitrogen/argon were obtained by passing the commercially available gas (Indian oxygen Ltd.) through a series of towers containing i) vanadyl solution (prepared by

reducing ammonium metavanadate solution in conc. H<sub>2</sub>SO<sub>4</sub> with zinc amalgam) ii) conc. H<sub>2</sub>SO<sub>4</sub> iii) KOH pellets iv) P<sub>4</sub>O<sub>10</sub> and v) silica gel blue.

All the distilled solvents were handled under inert atmosphere. Generally, pure products were isolated from various reaction mixtures by making use of solvent extraction.

### **2.3 SYNTHESIS OF ETHYLENEDIAMINE COMPLEXES OF 3D-TRANSITION METALS**

The synthesis procedure reported in Vogel *et al*, in 1975 has been adopted in this work. To a stirred methanol solution of the MX<sub>y</sub>.nH<sub>2</sub>O, (where y = 2 for M = Mn, Fe, Ni, Cu, Zn & 3 for M = Cr and Co and X = Cl, Br, SO<sub>4</sub><sup>2-</sup>) ethylenediamine was added dropwise for 15 minutes in 1:3 molar ratio at 273 K. Since dissolution of ethylenediamine is exothermic in nature, a slow addition of ethylenediamine was done by maintaining the bath temperature at 273 K. From the reaction mixture, the ethylenediamine metal complexes start precipitating out immediately. The precipitate was filtered from the reaction mixture and the precipitate was washed with methanol (2x10 mL) to remove the unreacted metal salts. The precipitate was dried under vacuum and was characterized by IR.

In the case of CrCl<sub>3</sub>.6H<sub>2</sub>O, the methanol solution of CrCl<sub>3</sub>.6H<sub>2</sub>O salt was taken in a round bottom flask and ethylenediamine was added in 1:3 molar ratio. Since CrCl<sub>3</sub> is inert zinc dust was added to the reaction mixture to reduce the CrCl<sub>3</sub>. The reaction mixture was allowed to reflux for 3h. The mixture was cooled, to room temperature, filtered and washed with methanol (2x5 mL) to get the pure (Cr(en)<sub>3</sub>)Cl<sub>3</sub> complex. The precipitate was dried under vacuum.

## 2.4. MOLYBDATE BLUE TEST

Experiments to study the oligomerization reactions were carried out at room temperature (293 K). Solutions ( $0.14 \text{ mmol}^{-1}$ ) of complexes were made up with double distilled water and ethanol mixture of 4:1 in a plastic container. The resulting complex in solution undergoes decomposition to give orthosilicic acid and oligomerisation of the newly formed silicic acid was measured as a function of orthosilicic acid concentration by a modified molybdenum blue colorimetric method described by Iller. One mL aliquot of solution was removed and 32 mL of distilled water was added. 3 mL of an acidic solution containing ammonium molybdate was added immediately and the resulting solution was allowed to stand for 10 min thereby allowing any dimers present to decompose to monomers that could be detected by the colorimetric method. 15 mL of a reducing solution containing metol was then added and the absorbance of the blue silicomolybdate complex was measured at 810 nm using UV - Vis spectrometer. Calibration of this method showed a linear relationship between the concentration and absorbance over the concentration range of 0.1 mmol to 50 mmol. The experimental error in the measurement was  $\pm 1.0$ .

Orthosilicic acid concentrations were measured at regular intervals between 0 and 240 min. It was also recorded in regular intervals for 7 days. Experiments on all the three silicate derivatives (TnBASINAP, DIPASINAP and *t*-BASINAP) were carried out on the same day in order to validate the experimental observations.

## **2.5. CHARACTERIZATION TECHNIQUES**

The details of various physical, analytical, spectral and diffraction techniques employed for identification and structural characterization of compounds are briefly given below.

### **1. Melting point**

Melting point apparatus (Toshnival, India) provided with electrically controlled heating of aluminum block having a temperature range from 40-280 °C was used.

### **2. Infrared spectra**

Infrared spectra were recorded on Perkin Elmer 1430 and Shimadzu model IR-470 spectrophotometers using KBr pellets.

### **3. UV - Vis spectra**

Shimadzu UV-240 and Shimadzu NIR 3100 spectrophotometers were used.

### **4. NMR spectra**

Multinuclear NMR spectra ( $^1\text{H}$ -(400MHz),  $^{13}\text{C}$ -(100 MHz),  $^{29}\text{Si}$ -(59.6 MHz)) were recorded on Bruker AVANCE 400 spectrometer.  $^{13}\text{C}$  NMR spectra were recorded in the proton decoupled mode.

### **5. Mass spectra**

Matrix-Assisted Laser Desorption Ionization (MALDI), Applied Biosystems Voyager DE PRO time-of-flight mass spectrometer was employed for this study.

## **6. EPR spectra**

Varian E112 EPR spectrometer was used.

## **7. Magnetic measurement**

George Associates model 300 Lewis coil force magnetometer was used.

## **8. Elemental analysis**

Perkin Elmer CHN rapid micro analyzer was used.

## **9. Thermal analysis**

A Stanton Redcraft thermobalance (STA-710) operating both in TG (with an accuracy of 0.1mg) and DT mode was employed.

## **10. Electrochemical studies**

Cyclic voltammetric study was carried out using CH Instrument 660 Electrochemical work Station.

## **11. Powder XRD data**

The powder X-ray diffraction patterns were obtained on a Rigaku miniflex table top model and Philips XPERT MPD XRD system.

## **12. Single crystal X-ray diffraction**

Enraf-Nonius CAD-4 diffractometer was employed.

### **13. Transmission Electron Microscopy**

Particle size of the silica material was obtained using Philips CM12 transmission electron microscope & Energy Dispersive Spectroscopy (EDS) detector for micro-analysis.

### **14. Scanning Electron Microscopy**

Morphology of the silica material was studied using FEI Scanning electron microscope.

### **15. Surface area measurements**

Surface area and pore size distribution were studied using CE Instruments model Sorptomatic 1990.

## **2.6. Conditions Employed for Measurements**

- ✓ Infrared spectra were recorded using KBr pellet ( $4000\text{-}600\text{ cm}^{-1}$ ).
- ✓ UV - Visible spectra (190-800 nm) were recorded as solution ( $\text{CH}_3\text{CN}$  and  $\text{C}_2\text{H}_5\text{OH-H}_2\text{O}$  mixture) in quartz cells or as nujol mull smeared on the filter paper.
- ✓  $^1\text{H}$  and  $^{13}\text{C}$ - NMR spectra were recorded in  $\text{CDCl}_3/\text{CD}_3\text{CN-CD}_3\text{OD}$  solvent using tetramethylsilane as an internal standard. The chemical shifts ( $\delta$ ) are quoted in ppm.
- ✓ The solid-state  $^{29}\text{Si}$  Cross Polarization Magic Angle Spinning (CPMAS) spectra were obtained on a Bruker ADVANCE 400 FT-NMR (59.62 MHz) spectrometer. The Hartmann Hahn cross polarization was established using a spinning sample of silica gel and the spinning was kept at around 2.3 kHz. The FIDs were accumulated in a 23.8 kHz spectral window using a proton  $\pi/2$  pulses of 5.7  $\mu\text{sec}$

- and contact time of 5 msec. Typically 500 accumulations were done before Fourier Transformation. An exponential line broadening of 10 Hz was used before Fourier Transformation. The chemical shifts ( $\delta$ ) are referred to TMS (external).
- ✓ Mass spectra were recorded under MALDI TOF condition operating with electron power and the matrix used is  $\alpha$ -cyano-4-hydroxycinnamic acid. Since the compounds have both cationic and anionic species, the spectra were recorded in both negative and positive modes.
  - ✓ The thermogravimetric (TG) and differential thermal (DT) analysis data were obtained by heating the sample from room temperature to 973 K in static air atmosphere with  $\alpha$ -Al<sub>2</sub>O<sub>3</sub> as reference.
  - ✓ X-ray crystallographic analysis: A suitable crystal of the sample was glued at the sharpest point on to a glass fiber. The X-ray data were collected with MoK $\alpha$  as the source ( $\lambda=0.71073$  Å). The cell constants were obtained by least square refinement employing 25 carefully chosen reflections in the range  $8^\circ < \theta < 12^\circ$ . The data were collected at 293 K and were corrected for Lorentz and polarization effects. The reflections were measured using the  $\omega$ -2 $\theta$  scan technique. Numerical absorption corrections were made using in-built software in the diffractometer.
  - ✓ The structure was solved by direct method using the SHELXS-86 program (Sheldrick, 1985) and refined by full-matrix least square method using the



- program SHELX-93 (Sheldrick, 1993). All the hydrogen atoms could be located from the difference Fourier electron density maps during the refinement. All the non-hydrogen atoms are isotropically fixed.
- ✓ EPR spectra were recorded by taking 5-10 mg of the sample at room temperature and at liquid nitrogen temperature using DPPH as the standards in the X-band (100 GHz).
  - ✓ The samples were dispersed in chloroform and the samples was coated on copper coated carbon grid and dried. The electron micrographs were recorded using Philips CM12 transmission electron microscope at 200 keV.
  - ✓ The samples were dispersed onto double sided sticky tape and mounted on aluminium stubs with edges of the tape being painted with quick drying silver paint to prevent charging of the sample. All loose aggregates were removed by tapping the stub before the silica samples were coated with a layer of gold using sputter coater.
  - ✓ The surface area of silica material that obtained by pyrolytic and hydrolytic method was determined using sorption system via the Braunaure-Emmett-Teller method (Brunauer *et al*, 1938). A gaseous mixture of nitrogen and helium was allowed to flow through the analyzer at constant rate of 30 cc/min. Nitrogen was used to calibrate the analyzer and was also used as the adsorbate at liquid nitrogen temperature. Each sample was degassed at 403 K for 16 h before analysis. The surface area obtained from a five-point isotherm at  $P/P_0$  ratio less than 0.3. The

results were computed based on the desorption branch and the dried weight of the sample after analysis.

- ✓ Pore size distributions were calculated by the application of the BJH theory to the adsorption data. However, the materials under investigation show a variety of adsorption/desorption hysteresis loops and so for consistency adsorption data were used for the calculations. This is mainly due to the fact that the adsorption data are not affected by the varied shape of the pores to the extent as that of desorption process (Barrett *et al*, 1951).

**CHAPTER III**

**SYNTHESIS AND CHARACTERIZATION OF HEXACOORDINATE  
SILICATES OF 2,3-DIHYDROXYNAPHTHALENE WITH  
AMMONIUM  
COUNTER IONS**

---

### 3.1 INTRODUCTION

Aromatic polyols, abundant micronutrients in our diet, act as antioxidants and play an active role in the prevention of degenerative diseases such as cancer and cardiovascular diseases (Middleton *et al*, 2000). Among the aromatic polyols, metal complexes of catechol and its derivatives have been most studied due to their ability to act as functional models for the catechol dioxygenases (Hardemare *et al*, 2006). In addition, catechol forms stable complexes with transition metals and it is nature's choice as the functional group in siderophores such as enterobactin (Matzanke *et al*, 1989; Winkelmann *et al*, 1991). The synthesis, physical and structural study of tris(catecholato)titanate has been done by Raymond *et al* (1984). Parr *et al*, have reported the synthesis of tris(catecholato)germanium with potassium as counter ion. Its crystal structure has revealed extended hydrogen bonding network (1994). The synthesis and crystal structure of tris(catecholato)tin complex and its physical studies has been reported (Denekamp *et al*, 1992). In the later years, hexacoordinated complexes of gallium, chromium, vanadium and iron with catecholato ligand have also been reported (Raymond *et al*, 1976; Sofen *et al*, 1979; Cooper *et al*, 1989).

Synthesis of several tris(catecholato)silicates with different ammonium counter ions and the effect of counter ion on the thermal stability were reported by Kingston *et al* (2000). Bindu *et al* have reported that the ammonium ions of bis(ammonium) tris(catecholato)silicates can be replaced with cationic transition metal complexes by ion exchange reaction (2003). Recently the use of super bases in the isolation of tris(catecholato)silicates in high yields has been demonstrated (Kingston and Verkade,

2005). The tris(catecholato)silicates were used in the high yield synthesis of organophosphorus reagent by Kingston *et al*, (1997). But these tris(catecholato)silicates are unstable in the solid state other precursors have been examined. For example, silica gels, colloidal silica, tetraethoxysilane, tetraethoxysilane and tetracholorsilane (Resenheim *et al*, 1931; Denxnis *et al*, 1972; Weiss *et al*, 1969; Tacke *et al*, 2000, Kingston *et al*, 2000) have been used for the synthesis of hexacoordinate silicates such as tris(catecholato)silicates.

Reports indicate that 2, 3-naphthalenediol, acts as an inhibitor of catechol oxidase (Keilin and Mann, 1940). 2, 3-dihydroxynaphthalene was known in the literature only for the synthesis of pentacoordinated silicon derivatives (Tacke *et al*, 1991; 1992). Interestingly, such highercoordinate silicates of 2, 3-dihydroxynaphthalene have been exploited in reprography materials as a charge-controlling agent in patent literature (Yoshiyuk *et al*, 1992; Tanaka *et al*, 1995). Lim *et al*, have reported the synthesis and application of boron complexes of 2, 3-dihydroxynaphthalene and 2, 3-dihydroxyquinoxaline in organic electroluminescent devices (2003). Prompted by these observations and also because of the continued interest in the synthesis of higher coordinate silicates, several tris(2, 3-dihydroxynaphthalato)silicates have been prepared by the synthetic strategy developed by Kingston *et al*, (2000). Singh *et al* have reported the microwave-assisted synthesis of neutral highercoordinate silicates and their antibacterial and antifungal activities (2005). The potential of microwave irradiation towards the synthesis of six coordinate silicates of 2, 3-dihydroxynaphthalene is described in this chapter.

Therefore, the synthesis of bis(ammonium)tris(2, 3-dihydroxynaphthalato)silicates and its structure have been studied to examine the stability of the silicates when catechol is modified with its higher homologue naphthalene. In addition, with the exception of patent literature and a scanty report, no other reports are available to date on synthesis of hexacoordinate silicon of 2, 3-dihydroxynaphthalene (Meyer *et al*, 1968).

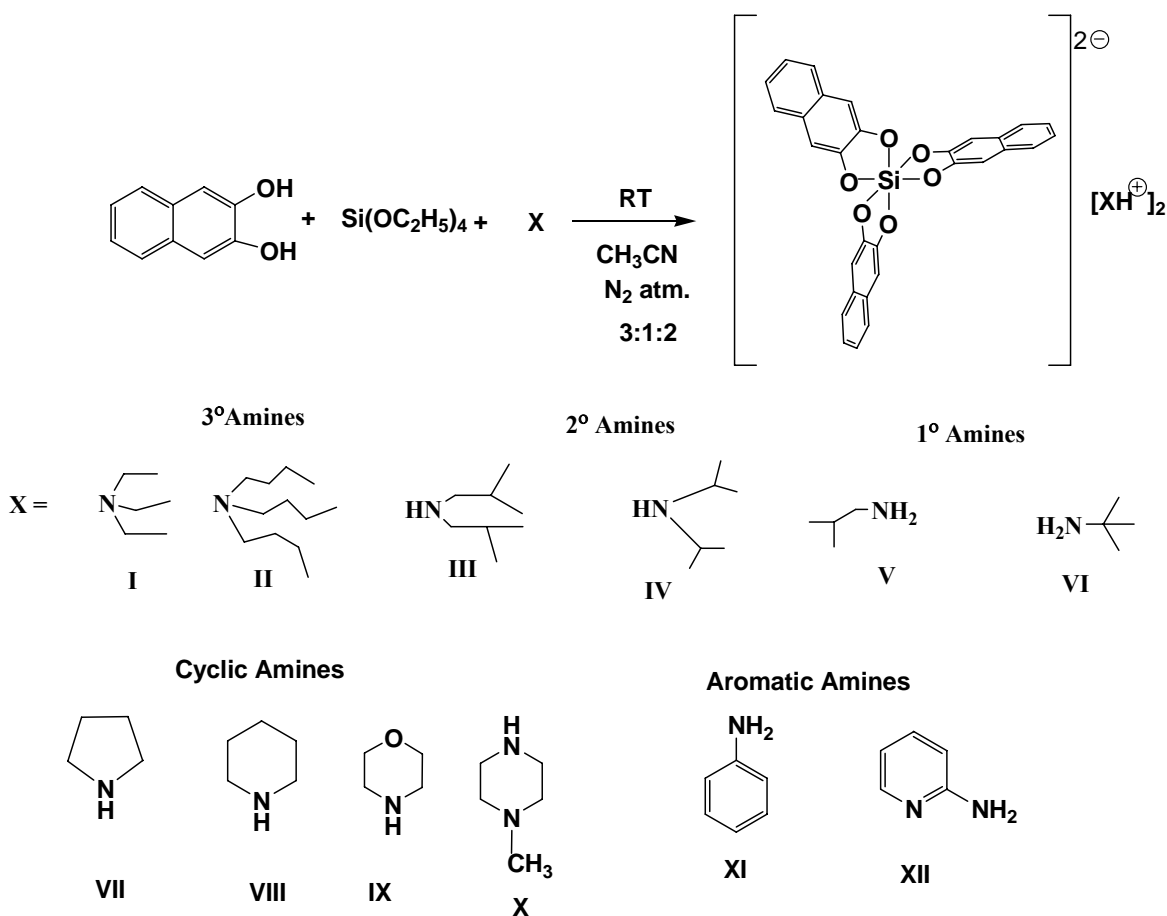
## **3.2. EXPERIMENTAL**

### **3.2.1. Synthesis of Bis(tri-*n*-butylammonium)tris(2, 3-dihydroxynaphthalato)silicate**

#### **3.2.1.1 Room temperature reaction**

To the stirred solution of 2,3-dihydroxynaphthalene (0.45 g, 2.85 mmol) in acetonitrile (15 mL) and tri-*n*-butylamine (0.32 mL, 1.88 mmol) was added under nitrogen atmosphere followed by dropwise addition of a neat liquid of tetraethoxysilane (0.2 mL, 0.94 mmol) at room temperature. The resulting mixture was stirred for 5 h. The precipitate obtained was filtered and washed with diethylether to remove unreacted ligand. The compound **II** was obtained (**Table 3.1**) as a white powder (*ca.*70%). Some portion of the product was dissolved in acetonitrile which was recovered by cooling the concentrated acetonitrile filtrate to 0°C for a day (for compound **II** & **III** only). The isolated yield of compound **II** was 92% (0.75 g).

The derivatives (**I**, **III-XIII**) were obtained by repeating the procedure using corresponding amine as shown in **Scheme 3.1**.



**Scheme 3.1:** Synthesis of Bis(ammonium)tris(2,3-dihydroxynaphthalato)silicate

Experimental, spectral and analytical data of the prepared bis(ammonium)tris(2, 3-dihydroxynaphthalato)silicate are given in **Tables 3.1 to 3.6**. Microwave assisted synthesis was carried out for compounds **I to VI**.

### 3.2.1.2. Microwave reaction

The 2, 3- dihydroxynaphthalene (0.25g, 1.56 mmol), tetraethoxysilane (0.1 mL, 0.52 mmol) and triethylamine (2 mL) were taken in a pressure tube under nitrogen atmosphere. The pressure tube was closed with teflon lid and inserted in a beaker containing silica gel. This was then kept in an unmodified domestic microwave oven (Panasonic, 1100 W) at a

minimum power for 7 min. The contents were then washed with small amounts of diethyl ether and dried in vacuum to obtain compound **I** (0.45g, 95%). Similarly compounds **II to VI** were synthesized by repeating the procedure. Spectral and analytical data of the products obtained are observed to be the same as that of the products obtained in the reaction at room temperature. To validate that the microwave reaction is not due to thermal effect, the reaction was carried out by conventional oil bath heating.

### **3.2.1.3. Conventional Heating**

The 2, 3-dihydroxynaphthalene (0.25 g, 1.56 mmol), tetraethoxysilane (0.1 mL, 0.52 mmol) and triethylamine (2 mL) were taken in a pressure tube under nitrogen atmosphere. The pressure tube was closed with teflon lid and kept in the oil bath at 383 K. The reaction mixture was allowed to reflux for 1h. The resultant white precipitate was washed thoroughly using diethylether (4 x10mL) to remove the unreacted ligand and finally the product was vaccum dried. The isolated yield of compound **I** was 90% .

Compound **II to VI** were prepared by adopting the same procedure. The spectral and analytical data are similar to the compounds that obtained for the reaction at room temperature.



**Table 3.1.** Experimental details for the synthesis of Bis(ammonium)tris(2, 3-dihydroxynaphthalato)silicates (SINAP)

Amines ( pK <sub>a</sub> )	Amount of amines g (mmol) <sup>#</sup>	Isolated Yield (%)	Reaction time (h)	Products
Triethylamine (10.75)	0.25 (2.5)	96	4	TEASINAP <b>(I)</b>
Tri- <i>n</i> -butylamine (11.95)	0.45 (2.4)	92	5	T <i>n</i> BASINAP <b>(II)</b>
Diisopropylamine (12.78)	0.25 (2.5)	60	4	DIBASINAP <b>(III)</b>
Diisobutylamine (11.72)	0.35 (2.7)	93	6	DIPASINAP <b>(IV)</b>
<i>Sec</i> Butylamine (10.56)	0.25 (3.4)	75	5	<i>Sec</i> -BASINAP <b>V</b>
<i>t</i> -butylamine (10.68)	0.25 (3.4)	65	4	<i>t</i> -BASINAP <b>(VI)</b>
Pyrrolidine (12.0)	0.23 (3.2)	60	6	PydSINAP <b>(VII)</b>
Piperidine (10.70)	0.26 (3.1)	72	7	PidaSINAP <b>(VIII)</b>
Morpholine (8.36)	0.26 (3.0)	68	4	MopSINAP <b>(IX)</b>
N-Methylpiperazine (4.75)	0.28 (2.8)	75	3	NMPSINAP <b>(X)</b>
2.Aminopyridine (6.82)	0.27 (2.9)	70	4	2- <i>Am</i> SINAP <b>(XI)</b>
Aniline (30.6)	0.27 (2.9)	45	12	AniliniumSINAP <b>(XII)</b>

# All the reactions were carried out with 0.45g of 2, 3-dihydroxynaphthalene and 0.21g of tetraethoxysilane in acetonitrile (15 mL) medium.

### 3.3 RESULTS AND DISCUSSION

In the literature, the synthesis of tris(catecholato)silicates under basic conditions, conceivably both depolymerisation of silica to simple and discrete silicate ion and deprotonation of catechol takes place which facilitate the formation of tris(catecholato)silicates (Rosenheim *et al*, 1931, Laine *et al*, 1991). M<sub>2</sub>[SiF<sub>6</sub>] was used as silicon source to obtain tris(catecholato)silicate, though Si-F bond is a strong which got cleaved possibly due to chelate effect of catechol (Berzelius, 1924). The role of the base in the synthesis of the tris(catecholato)silicate using silicon tetrachloride was also

justified as it promotes the formation of tris(catecholato)silicate ion by i) deprotonation of catechol and ii) removal of HCl, the byproduct of the reaction.

The reaction of catechol, tetraethoxysilane and organic amines yielded tris(catecholato)silicate. Organic amine was used to deprotonate the catechol. Ethanol was obtained as byproduct. The merit of this route is the use of relatively safe, convenient and inexpensive silicon source under homogenous conditions. Thus the process falls under the class of green chemistry. Based on the arguments, in the present study, tetraethoxysilane and organic amines were employed. The  $pK_a$  of 2, 3-dihydroxynaphthalene is 13.7 (Bordwell *et al*, 1988). The  $pK_a$  for the amines considered in the study are listed in **Table 3.1**.

### **3.3.1. Room temperature reactions**

The reaction of 2, 3-dihydroxynaphthalene, tetraethoxysilane and amine were taken in (3:1:2) molar equivalence in acetonitrile. It proceeds smoothly at room temperature to afford the corresponding bis(ammonium)tris(2,3-dihydroxynaphthalato)silicate as shown in the **Scheme 3.1**. In this reaction, pink coloured acetonitrile solution of 2, 3-dihydroxynaphthalene, gives a white precipitate on addition of amine under nitrogen atmosphere possibly due to the formation of ammonium naphthalate. Further addition of tetraethoxysilane leads to a clear solution and the product starts precipitating out after 30 min. The isolated yield of DIBASINAP (III) is very low even after repetitive crystallization from the reaction mixture. Reaction duration (3-12h) dependence on the amines used, unlike in the case of tris(catecholato)silicate(**Table 3.1**). This variation can be attributed to the difference in the bulkiness and  $pK_a$  of the ligands. The products seem to undergo

decomposition in acetonitrile medium even with trace amount of water. To avoid such product deterioration, the reaction was carried out in neat condition under conventional oil bath heating and microwave route.

### **3.3.2 Microwave reaction**

Reaction between 2,3-dihydroxynaphthalene and tetraethoxysilane in 3:1 molar equivalence in the presence of excess amine proceeds under microwave conditions to afford the corresponding bis(ammonium)tris(2, 3-dihydroxynaphthalato)silicates in a shorter reaction time. The formation of white precipitate after addition of amine to the ligand was observed even in heterogeneous conditions. The reaction mixture was washed repeatedly using diethyl ether to remove unreacted ligand. The time required for the completion of the reaction under microwave condition lies in the range of 4-7 min unlike room temperature reaction which was in the range of 3-12 h, **Table 3.1**. This apparent acceleration of reaction may be due to non-thermal effect. To prove this aspect, the reaction was carried out under similar conditions using conventional oil bath heating at the same temperature as reached under microwave conditions. The temperature of the reaction mixture under microwave condition was monitored by the thermocouple setup under identical conditions and the temperature was found to be 383 K.

### **3.3.2. Reaction under conventional heating**

The reaction was repeated using neat mixture of tetraethoxysilane, 2,3-dihydroxynaphthalene in 1:3 molar equivalence with excess amine by maintaining oil bath at a temperature of 383 K which was observed under microwave conditions, (determined using thermocouple setup) at different reaction times (7 min, 15 min, 30 min,

60 min). Similar workup procedure was employed. The trend of time versus percentage yield under microwave and conventional oil bath heating conditions is shown in **Figure 3.1**.

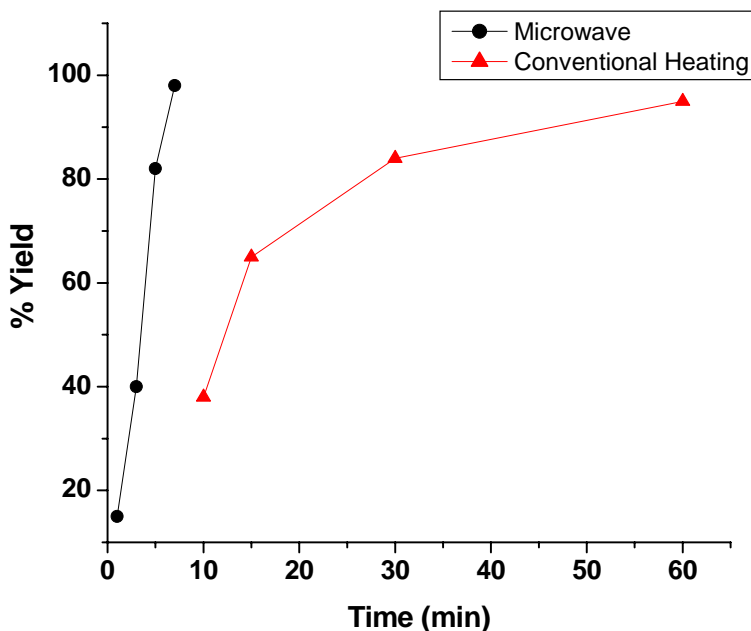


**Figure 3.1.** Percentage yield versus time for the reaction at 110 °C (0.25 g -2, 3- DHN; 0.11 mL-TEOS and 2 mL-amine)

The plot would suggest that the reaction does not reach completion even after 1 h while under microwave irradiation the reaction is complete within 7 min. This might suggest the influence of non-thermal effects in the acceleration process.

### 3.3.4 Microwave radiation – a route to effective synthesis of silicates

Tris(2,3-dihydroxynaphthalato)silicate has been synthesized under three different conditions i.e. room temperature, microwave and conventional oil bath heating. The acceleration in the reaction rate under microwave condition compared to the conventional heating may be due to non-thermal effects.

Macroscopically, the temperature of the reaction mixture under microwave conditions could have been similar to what has been employed by conventional oil bath heating procedure. However, the temperature of the mixture may not have been similar at microscopic level. In fact, Zhong *et al* (1999) have shown that the temperature of reaction mixture can differ from probe temperature by 300 - 400 K in dielectric solids like alumina. If this observation were to be true, then the acceleration found in this study could have been due to hot spot or selective microscopic heating effect. So the rapid reaction under microwave conditions can be attributed to special effects such as selective heating or hot spot effect that are common in the case of heterogeneous reaction under microwave irradiation.

The yield of the products obtained in the synthesis of tris(2,3-dihydroxynaphthalato)silicate under different reaction conditions like, room temperature, microwave irradiation and conventional heating are given in **Table 3.2**. Microwave assisted synthesis is advantageous over the other two methods in terms of the shortening of the reaction duration. In addition, microwave technique does not require the presence of a solvent and hence can be termed as a green process.

**Table 3.2.** Comparison of conventional and microwave assisted synthesis of  $[(XH)_2][Si(C_{10}H_6O_2)_3]$  derivatives

Compounds	Reaction condition and yield					
	RT		Microwave <sup>#</sup>		Conventional Heating	
	Time (h)	Yield (%)	Time (min)	Yield (%)	Time (h)	Yield (%)
T <i>n</i> BASINA P	5	92	6	98	1	90
TEASINAP	4	96	7	95	1	92
DIPASINAP	4	60	7	88	1	75
D <i>n</i> BASINA P	6	93	5	94	1	90
MOPSINAP	4	60	7	90	1	88
<i>t</i> -BASINAP	4	65	5	90	1	87

# Acetonitrile was used as solvent.

### 3.3.5. Characterization

Bis(ammonium)tris(2,3-dihydroxynaphthalato)silicates obtained under room temperature, microwave and conventional heating conditions were relatively more stable in solid state compared to the corresponding tris(catecholato)silicate derivatives. Differences in the solubility of silicates in organic polar solvents were observed with the change in the ammonium counter ion. For example,  $[((C_2H_5)_3NH)_2(Si(C_{10}H_6O_2)_3)]$  is sparingly soluble in acetonitrile while  $[((n-C_4H_9)_3NH)_2][Si(C_{10}H_6O_2)_3]$  is highly soluble in acetonitrile. This may be due to H-bonding variation with respect to the counter cations. The colour of products obtained ranges from pale yellow to pale pink powders. All these silicates were high melting solids where melting point was higher than 525 K. The

bis(ammonium)tris(2, 3-dihydroxynaphthalato)silicates were characterized by IR, NMR ( $^1\text{H}$ ,  $^{13}\text{C}$  and  $^{29}\text{Si}$ ) and MALDI-MS techniques.

### 3.3.5.1 Infrared spectra

Infrared spectra of all the derivatives (**I-XII**) show characteristic vibrational stretching frequencies of bis(ammonium)tris(2, 3-dihydroxynaphthalato)silicate at around 1585, 1470, 1260, 1165, 870, 850, 750, 640, 590, and  $420\text{cm}^{-1}$ . Strong peaks, attributable to Si-O bond stretching frequency of the silicate ion appear in the range of  $1247$  to  $1275\text{cm}^{-1}$  (**Table 3.3**) which seems to suggest that there is interaction of counter cations with the tris(2, 3-dihydroxynaphthalato)silicates. Similar observation was recorded in the case of tris(catecholato)silicates (Kingston *et al* 2000). The N-H stretches of amines are in the region  $3500$ - $3030$  (s, br)  $\text{cm}^{-1}$ . The ammonium cations show the red shift of N-H stretching frequencies for primary and secondary ammonium ions. The representative spectrum of tris(2, 3-dihydroxynaphthalato)silicate is given in **Figure 3.2**.

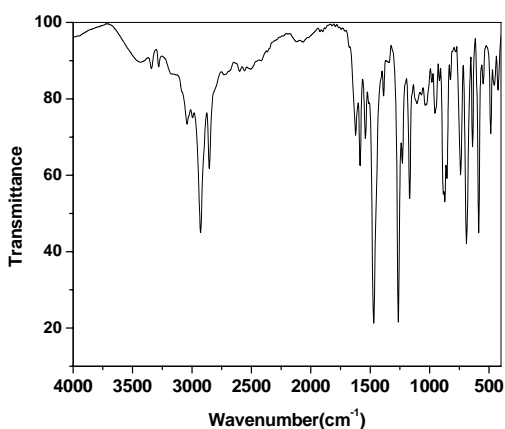


**Figure 3.2:** Infrared spectrum of bis(diisopropylammonium)tris(2, 3-dihydroxynaphthalato)silicate

### 3.3.5.2 $^1\text{H}$ - NMR analysis

In all the cases (**I-XII**), the  $^1\text{H}$ -NMR spectrum shows a characteristic multiplet pattern for naphthalato ring proton centered at around  $\delta$  7.4 and 7.1 ppm and a singlet at 6.7 ppm (**Table 3.4**). The similar splitting patterns for naphthalate ring hydrogens have been observed for pentacoordinate silicates indicating the ligands are in identical environments (Tacke *et al* 1991). The presence of alkyl ammonium counter cations of the silicate ion is also indicated by their characteristic proton signals (**Figure 3.3**). For example, the N-CH(CH<sub>3</sub>)<sub>2</sub> proton appeared as a septet at 3.35 ppm and the expected doublet due to its NCH(CH<sub>3</sub>)<sub>2</sub> proton appears at 1.40 ppm. Interestingly, N-H protons of the ammonium ions are not observed in the expected range of 5-6 ppm unlike as observed in tris(catecholato)silicate derivatives.

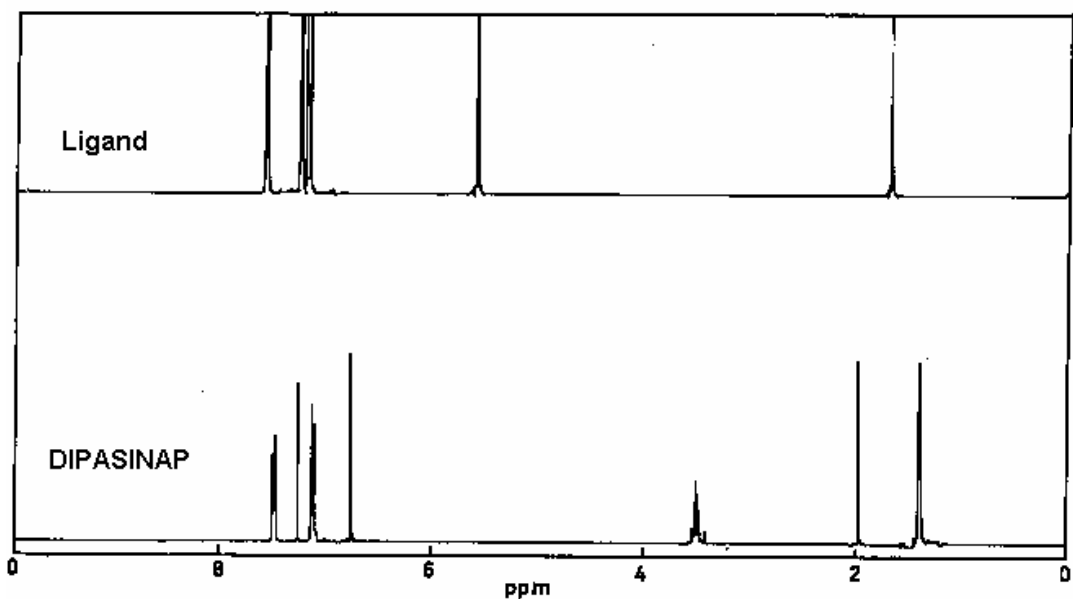


**Figure 3.3.**  $^1\text{H}$  NMR spectra of 2, 3-dihydroxynaphthalene (ligand) and bis(diisopropylammonium)tris(2, 3 - dihydroxynaphthalato)silicate (DIPASINAP)



### 3.3.5.3 $^{13}\text{C}$ - NMR analysis

$^{13}\text{C}$  - NMR spectra of (I-XII) revealed corroborative evidence towards their structure identification. In all the cases, the characteristic peak of naphthalate moiety appears in aromatic region at around 153, 130, 126, 122, 104 ppm (**Table 3.5**). Due to the decrease in the electron density on carbon of C - O that involve in complexation, an upfield shift is observed for C-O of ligand peak at 110 ppm to 104 ppm as shown in **Figure 3.4**. Tacke *et al*, have reported such an observation in the pentacoordinate silicon complexes of 2, 3-dihydroxynaphthalene (Tacke *et al*, 1991). In the aliphatic region the peaks are observed in the range of 4-70 ppm correspond to the alkyl group in the respective ammonium counter cations of the tris(2, 3-dihydroxynaphthalato)silicates.

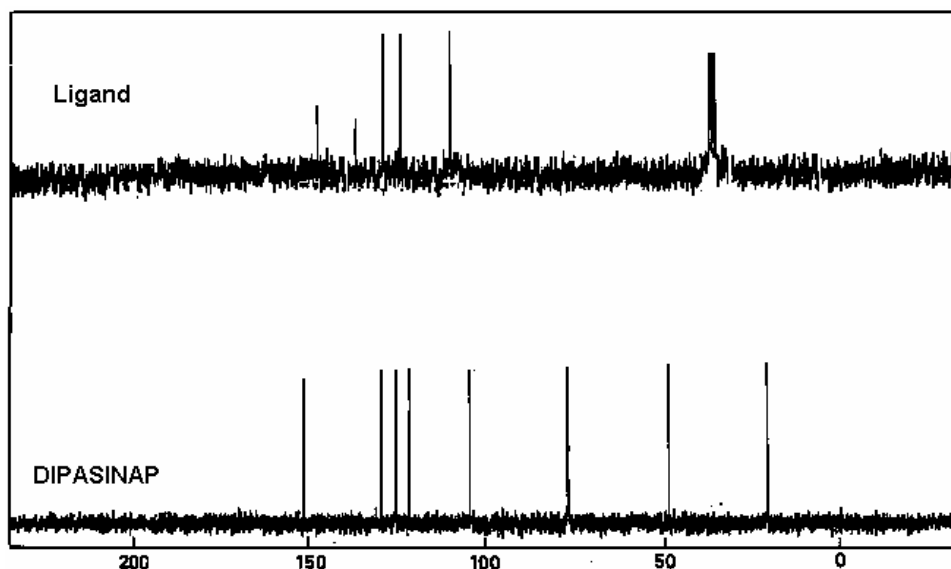


**Figure 3.4.**  $^{13}\text{C}$  NMR spectra of 2, 3-dihydroxynaphthalene (ligand) and bis(diisopropylammonium)tris(2, 3-dihydroxynaphthalato)silicate (DIPASINAP)

### 3.3.5.4 Silicon-29 NMR analysis

Silicon NMR spectroscopy is a widely used technique for the characterization of silicon compounds (Williams and Gargioli 1970; Schramb *et al* 1976; Marsmann *et al*, 1981). Nature of the substituents and the coordination number around silicon influences the  $^{29}\text{Si}$  NMR chemical shift. In general the chemical shift of higher coordinate silicates where silicon is hexacoordinated with six oxygen atoms of diolato ligand appears in the highly shielded region. In the  $^{29}\text{Si}$  NMR spectra of the bis(ammonium)tris(2,3-dihydroxynaphthalato)silicate, a sharp peak at around -140 ppm is observed (**Table 3.5**). This observation confirms hexacoordination around the silicon atom (**Figure 3.5**). Woolins and co workers have reported that hexacoordinated silicon with five membered chelated rings give a singlet peak of  $\delta$  value lying in the range of -130 to -150 ppm. The four coordinate tetraethoxysilane (starting material) gives a sharp peak at -83.5ppm.

Due to poor solubility of compound I and V,  $^{13}\text{C}$  and  $^{29}\text{Si}$  CP-MAS NMR spectra were recorded in the solid state.

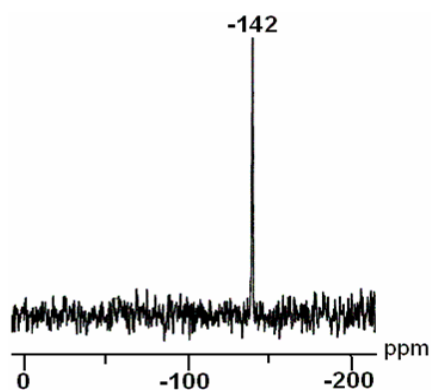


**Figure 3.5:**  $^{29}\text{Si}$  NMR spectrum of bis(diisopropylammonium)tris(2,3-dihydroxynaphthalato)silicate

### 3.3.5.5 Mass spectral analysis

MALDI-TOF mass spectra were obtained in both positive and negative ion modes for all the cases to identify ammonium ion and  $[\text{Si}(\text{C}_{10}\text{H}_6\text{O}_2)_3]^{2-}$  ion.

#### 3.3.5.5.1 Negative Mode

$[\text{Si}(\text{C}_{10}\text{H}_6\text{O}_2)_3]^{2-}$  ion gives a M+1 peak at  $m/z = 503$  (100%) that may be due to  $\text{H}[\text{Si}(\text{C}_{10}\text{H}_6\text{O}_2)_3]^-$  species. These silicate moiety undergoes further stepwise fragmentation to give other transient species such as  $[\text{Si}(\text{C}_{10}\text{H}_6\text{O}_2)_2\text{H}]^-$  and  $[\text{Si}(\text{C}_{10}\text{H}_6\text{O}_2)\text{H}_2]^-$  which can be proposed based on the possible fragmentation for  $m/z = 345$  and 188 respectively (**Figure 3.6**).

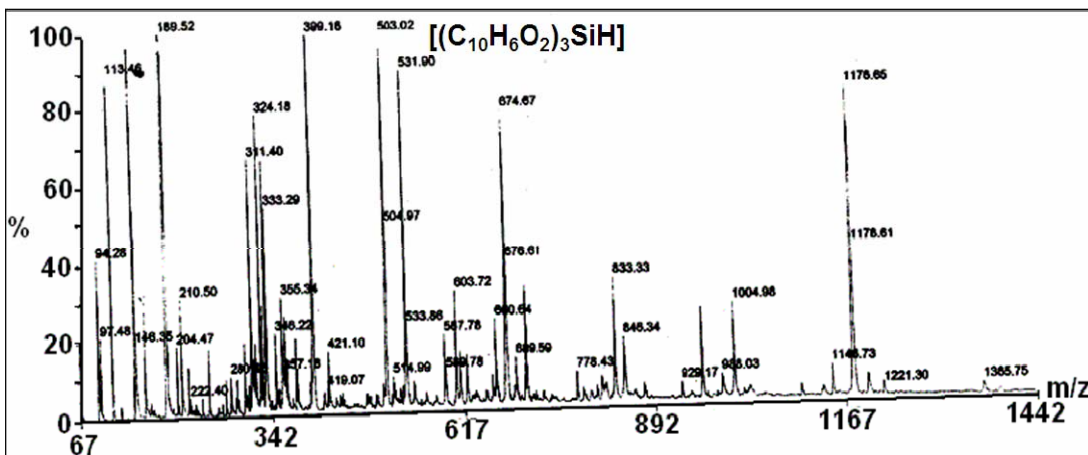


**Figure 3.6.** Negative mode of MALDI-MS for bis(diisoprylammonium)tris(2, 3-dihydroxynaphthalato)silicate

#### 3.3.5.5.2 Positive Mode

The 100 % (M+1) peak observed in the positive mode, possibly due to the ammonium counter cation, the most stable ion. For example, in the spectrum shown in **Figure 3.7**

the peak at  $m/z=102$  corresponds to diisopropylammonium ion which is the counter cation in bis(diisopropylammonium)tris(2,3-dihydroxynaphthalato)silicate. The values of  $m/z$  for all the ammonium derivatives of tris(2, 3-dihydroxynaphthalato)silicate are tabulated in **Table 3.6**.

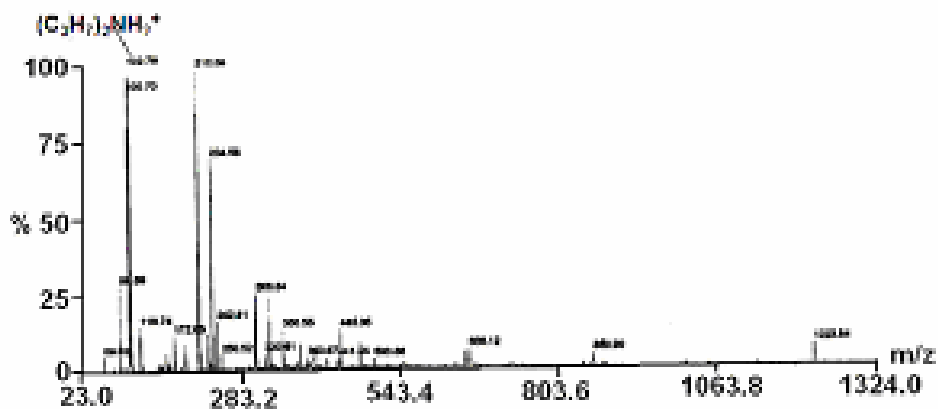


**Figure 3.7:** Postive mode of MALDI-MS for bis(diisopropylammonium)tris(2,3-dihydroxynaphthalato)silicate

### 3.4 CONCLUSION

- ✓ Synthesis of hexacoordinate silicon complexes with 2,3-dihydroxynaphthalene as ligand using tetraethoxysilane has been demonstrated. Silicates with various ammonium counter ions have been synthesized, by the three different (room temperature, microwave and conventional heating) conditions.
- ✓ Microwave assisted synthesis was found to be an effective route to achieve bis(ammonium)tris(2, 3-dihydroxynaphthalato)silicates in terms of shorter reaction time.
- ✓ Microwave technique has been used and its efficiency has been studied to achieve bis(ammonium)tris(2,3-dihydroxynaphthalato)silicates in a green process, without using solvent and with ethanol as by product.

**Table 3.3:** Characteristic Infrared frequencies of tris(2, 3-dihydroxynaphthalato)silicates

Compound	IR Frequencies (cm <sup>-1</sup> )
2, 3-DHN	1590 (m, sh), 1490 (s, sh), 1268 (m, sh), 1166 (s, sh), 871(s, br), 846 (s, sh), 742 (w), 692 (w, sh), 640 (s), 583 (w, sh), 484 (w, br), 420(w)
TEASINAP	3020(s, br), 1586 (m, sh), 1478 (s, sh), 1266 (m, sh), 1166 (s, sh), 871(s, br), 846 (s, sh), 742 (w), 692 (w, sh), 640 (s), 583 (w, sh), 484 (w, br), 420 (w)
TnBASINAP	3039 (s, br), 2960 (w, br), 2872 (s, br), 1586 (m, sh), 1477 (s, sh), 1381 (m, sh), 1263(m, sh), 1166 (s, sh), 871 (s, br), 850 (s, sh), 738 (w), 688 (w, sh), 639 (s), 589 (w, sh), 485 (w, br), 420 (w)
DIPASINAP	3030 (s, br), 2986 (s, br), 1587 (m, sh), 1477 (s, sh), 1265 (m, sh), 1167(s, sh), 871(s, br), 850(s, sh), 744 (w), 686 (w, sh), 644 (s), 591 (w, sh), 485 (w, br), 420 (w)
DIBASINAP	2962(s, br), 2931(s, br), 2868(s, br), 1587(m, sh), 1472(s, sh), 1261(m, sh), 1167(s, sh), 1108(s, sh), 871(s, br), 739(w), 693(w, sh), 638(s), 586(w, sh), 485(w, br)
MOPSINAP	3030 (s, br), 2937(s, br), 2857 (s, br), 1586(m, sh), 1474(s, sh), 1275(m, sh), 1166 (s, sh), 868 (s, br), 839 (s, sh), 743 (w), 696 (w, sh), 585 (w, sh), 484 (w, br), 419(w)
NMPSINAP	3020 (s, br), 1586 (m, sh), 1478 (s, sh), 1266 (m, sh), 1166(s, sh), 871 (s, br), 846(s, sh), 742 (w), 692 (w, sh), 640 (s), 583 (w, sh), 484 (w, br), 420(w)
PIDASINAP	3050 (s, br), 2986 (m, sh), 1587 (m, sh), 1477(s, sh), 1254(m, sh), 1167(s, sh), 871(s, br), 846(s, sh), 744(w), 686(w, sh), 640 (s), 591(w, sh), 485(w, br), 420(w)
PYDASINAP	3030 (s, br), 2986(s, br), 1587(m, sh), 1477(s, sh), 1265(m, sh), 1167 (s, sh), 871(s, br), 846(s, sh), 744 (w), 686(w, sh), 640(s), 591(w, sh), 485(w, br), 420(w)
<i>sec</i> -BASINAP	3020(s, br), 1586(m, sh), 1478(s, sh), 1257(m, sh), 1166(s, sh), 871(s, br), 846(s, sh), 742(w), 692(w, sh), 640(s), 583(w, sh), 484(w, br), 420(w)
<i>t</i> -BASINAP	3026(s, br), 2958(s, br), 1587(m, sh), 1473(s, sh), 1259(m, sh), 1166(s, sh), 868(s, br), 845(s, sh), 748(w), 698(w, sh), 638(s), 595(w, sh), 487(w, br), 421(w)
2- <i>Am</i> PYSINAP	3035(s, br), 2958(s, br), 1587(m, br), 1473(s, sh), 1247(m, sh), 1166(s, sh), 868(s, br), 845(s, sh), 748(w), 698(w, sh), 638(s), 595(w, sh), 487(w, br), 421(w)
AniliniumSINAP	3041(s, br), 1586(m, sh), 1478(s, sh), 1266(m, sh), 1166(s, sh), 871(s, br), 846(s, sh), 742(w), 692(w, sh), 640(s), 583(w, sh), 484(w, br), 420(w)

- s- short; br-broad; sh=sharp; w=weak

**Table 3.4:**  $^1\text{H-NMR}$  Spectral data of bis(ammonium)tris(2,3-dihydroxynaphthalato) silicates

Compd No.	Compounds	$^1\text{H NMR}$ ( $\delta$ , ppm)	
		Aliphatic region (counter cation)	Aromatic region(Naphthalene ring of silicate)
1	2, 3-DHN	-----	7.63(m, 2H), 7.31(m, 2H), 7.22(s, 2H)
2	TEASINAP	3.07(q, 12H), 1.18(t, 18H)	7.40(m, 6H), 7.01(m, 6H), 6.68(s, 6H)
3	TnBASINAP	3.27(m, 6H), 1.71(m, 6H), 1.25(m, 6H), 0.74(t, 9H)	7.43(m, 6H), 7.08(m, 6H), 6.69(s, 6H)
4	DIPASINAP	3.50(sep, 24H), 0.40(d, 4H)	7.48(m, 6H), 7.11(m, 6H), 6.76(s, 6H)
5	DIBASINAP	0.90(d, 18H) 2.13(sep, 3H), 2.98(d, 18H),	6.75(s, 6H), 7.05(m, 6H), 7.44(m, 6H)
6	MOPSINAP	3.91 (m, 8H), 3.35 (b, 4H), 3.32 (m, 8H)	7.46(m, 6H), 7.06 (m, 6H), 6.79(s, 6H)
7	NMPSINAP	2.30 (s, 6H) , 3.00 (t, 8H), 3.3 (t, 8H)	7.46(m, 6H), 7.06 (m, 6H), 6.79 (s, 6H)
8	PIDASINAP	3.27 (m, 6H), 1.71 (m, 6H), 1.25 (m, 6H), 0.74 (t, 9H)	7.45(m, 6H), 7.05(m, 6H), 6.68(s, 6H)
9	PYDASINAP	3.27(m, 6H), 1.71(m, 8H), 1.25(m, 8H)	7.33(m, 6H), 7.18(m, 6H), 6.70(s, 6H)
10	<i>Sec</i> -BASINAP	3.27(m, 4H), 1.71(m, 12H), 1.25(m, 2H)	7.43(m, 6H), 7.08(m, 6H), 6.77(s, 6H)
11	<i>t</i> -BASINAP	1.04(s, 18H)	7.45(m, 6H), 7.14(m, 6H), 6.93(s, 6H)
12	2- <i>Am</i> PYSINAP	-----	7.43(m, 6H), 7.08(m, 6H), 6.69(s, 6H) 6.7(m, 4H), 7.48(m, 4H), 8.11(m, 2H)
13	AniliniumSINAP	-----	7.43(m, 6H), 7.08(m, 6H), 6.69(s, 6H) 6.27(m, 6H), 7.01(m, 4H),

**Table 3.5**  $^{13}\text{C}$  &  $^{29}\text{Si}$ -NMR Spectral data of bis(ammonium)tris(2,3-dihydroxynaphthalato)silicates

Compd No.	Compounds	$^{13}\text{C}$ NMR ( $\delta$ , ppm)#	$^{29}\text{Si}$ NMR ( $\delta$ , ppm)
1	TEASINAP	<b>153.4(C)</b> , <b>130.2(C)</b> , <b>125.1(CH)</b> , <b>122.1(CH)</b> , <b>103.4(CH)</b> , 46.1(CH <sub>2</sub> ), 7.6(CH <sub>3</sub> )	-139.0
2	TnBASINAP	<b>152.3(C)</b> , <b>129.6(C)</b> , <b>125.2(CH)</b> , <b>121.1(CH)</b> , <b>104.1(CH)</b> , 52.8(CH <sub>2</sub> N), 25.2(CH <sub>2</sub> ), 11.0(CH <sub>2</sub> ), 13.4(CH <sub>3</sub> )	-141.3
3	DIPASINAP	<b>153.8(C)</b> , <b>130.5(C)</b> , <b>126.2(CH)</b> , <b>122.0(CH)</b> , <b>104.4(CH)</b> , 49.2(CH <sub>2</sub> ), 19.4(CH <sub>3</sub> )	-140.9
4	DIBASINAP	<b>104.7(CH)</b> , <b>122.3(CH)</b> , <b>126.3(CH)</b> , <b>130.6(C)</b> , <b>153.5(C)</b> , 20.3(CH <sub>3</sub> ), 26.1(CH), 56.2(CH <sub>2</sub> N),	-143.9
5	MOPSINAP	<b>153.5(C)</b> , <b>131(C)</b> , <b>126.7(CH)</b> , <b>122.6(CH)</b> , <b>105.2(CH)</b> , 65.2(CH <sub>2</sub> O), 45(CH <sub>2</sub> NH)	-142.8
6	NMPSINAP*	<b>153.5(C)</b> , <b>131(C)</b> , <b>126.6(CH)</b> , <b>122.6(CH)</b> , <b>105.2(CH)</b> , 46(CH <sub>2</sub> ), 57.4(CH <sub>2</sub> ), 43.1(CH <sub>3</sub> )	-142.1
7	PIDASINAP*	<b>152.3(C)</b> , <b>129.6(C)</b> , <b>125.2(CH)</b> , <b>121.1(CH)</b> , <b>104.2(CH)</b> , 48.3(CH <sub>2</sub> ), 28.1(CH <sub>2</sub> ), 25.6(CH <sub>2</sub> )	-140.9
8	PYDASINAP*	<b>153.5(C)</b> , <b>131(C)</b> , <b>126.7(CH)</b> , <b>122.6(CH)</b> , <b>105.2(CH)</b> , 48.7(CH <sub>2</sub> ), 28.1(CH <sub>2</sub> )	-141.2
9	<i>sec</i> -BASINAP	<b>152.3(C)</b> , <b>129.7(C)</b> , <b>125.2(CH)</b> , <b>121.1(CH)</b> , <b>104(CH)</b> , 50(CH <sub>2</sub> N), 31.4(CH), 20.3(CH <sub>3</sub> )	-142.8
10	<i>t</i> -BASINAP*	<b>153.5(C)</b> , <b>130.6(C)</b> , <b>126.3(CH)</b> , <b>122.2(CH)</b> , <b>104.8(CH)</b> , 28(CH <sub>3</sub> ), 26(C)	-140.6
11	2- <i>Am</i> PYSINAP*	<b>153.8(C)</b> , <b>130.6(C)</b> , <b>126.2(CH)</b> , <b>122.1(CH)</b> , <b>104.4(CH)</b> , 148(C <sub>py</sub> ), 159(C <sub>py</sub> ), 109(CH <sub>py</sub> ), 113(CH <sub>py</sub> ), 138(CH <sub>py</sub> )	-142.9
12	AniliniumSINAP*	<b>153.3(C)</b> , <b>131.0(C)</b> , <b>126.7(CH)</b> , <b>122.6(CH)</b> , <b>105.2(CH)</b> , 148(C <sub>an</sub> ), 122(CH <sub>an</sub> ), 130(CH <sub>an</sub> )	-143.2

\*-  $^{29}\text{Si}$  NMR is recorded in solid state CP-MAS (due to poor solubility)

# - Bolded data are aromatic carbon of dihydroxynaphthalato moiety

**Table 3.6:** Analytical data of Bis(ammonium)tris(2,3 -dihydroxynaphthalato)silicate

Com pd No.	Compounds	Elemental analysis			MALDI-MS	
		C (%)	H (%)	N (%)	Positive Mode	Negative Mode
1	TEASINAP	71.09 (71.39)	6.96 (7.08)	4.10 (3.97)	102.18	94.2, 144.5, 159.5, 189.5, 346.2, <b>503.0</b> , 531.9
2	TnBASINAP	73.83 (74.14)	8.55 (8.47)	3.19 (3.20)	186.12	96.5, 145.8, 162.8, 189.9, 346.7, <b>503.7</b> , 530.9
3	DIPASINAP	70.71 (71.39)	7.03 (7.08)	4.33 (3.97)	102.00	94.4, 144.8, 163.8, 178.9, 346.7, <b>503.5</b> , 535.4
4	DIBASINAP	72.4 (73.94)	7.71 (7.61)	3.33 (3.67)	130.15	94.2, 144.5, 159.5, 189.5, 346.2, <b>503.0</b> , 531.9
5	MOPSINAP	74.93 (74.83)	7.73 (7.62)	3.28 (3.23)	88.32	96.5, 147.8, 160.8, 185.9, 346.7, <b>503.7</b> , 530.9
6	NMPSINAP	67.89 (68.04)	4.61 (4.51)	4.07 (4.17)	101.23	94.4, 144.8, 159.8, 188.9, 346.7, <b>503.5</b> , 535.4
7	PIDASINAP	68.28 (68.14)	6.58 (6.29)	7.75 (7.95)	86.15	94.2, 144.5, 159.5, 189.5, 346.2, <b>503.0</b> , 531.9
8	PYDASINAP	70.66 (70.56)	5.87 (5.92)	4.55 (4.33)	72.15	96.5, 147.8, 160.8, 186.9, 346.7, <b>503.7</b> , 530.9
9	<i>sec</i> -BASINAP	70.20 (70.12)	6.4 (6.52)	4.42 (4.31)	74.16	94.4, 146.8, 169.8, 188.9, 346.7, <b>503.5</b> , 535.4
10	<i>t</i> -BASINAP	70.30 (70.12)	6.8 (6.52)	4.32 (4.31)	74.54	94.4, 144.8, 164.8, 185.9, 346.7, <b>503.5</b> , 535.4
11	2- <i>Am</i> PYSINAP	73.18 (73.07)	4.20 (4.09)	7.39 (7.19)	95.16	96.5, 147.8, 160.8, 189.9, 346.7, <b>503.7</b> , 530.9
12	AniliniumSINAP	72.3 (72.48)	4.87 (4.56)	4.12 (4.22)	94.42	94.4, 144.8, 157.8, 187.9, 346.7, <b>503.5</b> , 535.4



## CHAPTER IV

### SINGLE CRYSTAL X-RAY STRUCTURES OF

$[(n\text{-C}_4\text{H}_9)_3\text{NH}]_2[\text{Si}(\text{C}_{10}\text{H}_6\text{O}_2)_3]$  AND

$[(i\text{-C}_4\text{H}_9)_2\text{NH}_2]_2[\text{Si}(\text{C}_{10}\text{H}_6\text{O}_2)_3].3\text{CH}_3\text{CN}$

---

## 4.1 INTRODUCTION

Silicates exist as extended network in naturally occurring materials, such as pyroxene or feldspar. The network in these silicates was formed due to the strong covalent bonding between O-Si-O units (Gmelin, 1984). On the other hand, in organosilicates the network was formed because of the existence of hydrogen bonding between silicate anions, solvent molecules and the counter cations (Tacke *et al*, 2003). Tetra- and penta-coordinated silicon compounds are structurally well studied (Tacke *et al*, 1999). Single crystal X-Ray structural study of hexacoordinate complexes reveals the nature of interactions between ion pairs with respect to various factors such as change in chelate ring size. For example, in the case of titanium complexes of catechol, salicylic acid and biphenols that was reported to have difference in nature of interaction such as van der Waals interaction, hydrogen bonding and polar interactions respectively (Gigant *et al*, 2001). Raymond *et al* reported that by keeping the ligand environment the same and varying the central atom the, isomerisation behavior has been well understood by structural study. For example, in the case of modified catechol complexes of titanium, gallium and germanium effect of metal on isomerisation were studied. Titanium(IV) tris catecholate complexes undergo faster intramolecular isomerization (*fac/mer*) than gallium and germanium that could be understood based on structural study. The facile isomerization of the Ti(IV) complexes is attributed to the availability of the empty d orbitals of Ti(IV) for participation in metal-ligand bonds. This bonding results in a reduced ligand bite that decreases steric repulsion in the inner coordination sphere (Davis *et al*, 2006).

Tris(catecholato) complexes of other metals such as chromium, vanadium, titanium, germanium, gallium were also structurally studied as a biological functional model (Yamahara *et al*, 2002 and Davis *et al*, 2006). The existence of tris(catecholato)silicate was confirmed by the single crystal XRD data which was earlier deduced to be in pentacoordinate silicate based on spectral observation (Flynn *et al*, 1969). The interactions between the counter cations such as alkali metal ions, ammonium ions, and cationic transition metal complexes with the tris(catecholato)silicate anions have been studied by several groups (Ekkehardt *et al*, 1995; Kingston *et al*, 2000 and Sackerer *et al*, 1977).

Flynn *et al* have shown that the interaction between tris(catecholato)silicates and its pyridinium counter cations was due to the  $\pi - \pi$  stacking between the aromatic rings of catechol and pyridinium ring (Flynn *et al*, 1969). Based on the single crystal X-ray structural data of tris(catecholato)silicate with diisobutyl and diisopropylammonium counter cations were reported by Kingston *et al*, and Bindu *et al*, in which the tris(catecholato)silicate with 2<sup>o</sup> ammonium ions allows the crystal lattice to accommodate the solvent moiety and the counter ammonium ion forming the extended silicate network through the hydrogen bonding (2000; 2003). In the case of  $[\text{OH}(\text{CH}_2)_n\text{NH}_3^+]$ , the network was supported by both hydroxyl and ammonium groups due to inter and intra molecular bifurcated hydrogen bonding with silicate anion (Tacke *et al*, 2000). Verkade and Kingston have stated that the formation of hydrogen bonding between the ion pairs has not favoured in the case of  $[\text{Si}(\text{C}_6\text{H}_5\text{O}_2)_3][\text{HP}(\text{N}^i\text{Bu})\text{CH}_2\text{CH}_2)_3]_2$  that was due to their orientation and steric crowding of bulkier counter cations  $[\text{HP}(\text{N}^i\text{Bu})\text{CH}_2\text{CH}_2)_3]$  (2005).

In view of these observations reported in literature, it has been considered worthwhile to investigate the nature of interaction between new higher coordinate silicates.

In the case of silicon complexes of 2,3-dihydroxynaphthalene only pentacoordinate species was reported in literature with elaborate structural discussion (Tacke *et al*, 1991 & 1993 and Holmes *et al*, 1985). The structural details for the tris(2,3-dihydroxynaphthalato)silicates with diisobutyl and tri-*n*-butyl ammonium counter cations have been reported for the first time. This study reveals the nature of interactions between silicate and ammonium counter cations.

## 4.2 EXPERIMENTAL SECTION

The crystal was mounted on an Enraf Nonius CAD4 diffractometer equipped with graphite monochromator. The MoK $\alpha$  ( $\lambda=0.71073$  Å) radiation was employed for diffraction studies. The unit cell parameters were obtained by the method of short vectors followed by least square refinement of 25 reflections collected through search routine. The intensity data were gathered using  $\omega$ -2 $\theta$  scan mode. Systematic absences confirmed the space group to be P4<sub>1</sub>2<sub>1</sub>2 for the crystal system [(*n*-C<sub>4</sub>H<sub>9</sub>)<sub>3</sub>NH]<sub>2</sub>[Si(C<sub>10</sub>H<sub>6</sub>O<sub>2</sub>)<sub>3</sub>]. The structure was solved by direct methods [SIR 92, WINGX] (Sheldrick *et al*, 1985 and 1993) and the non-hydrogen atoms were refined anisotropically by using full-matrix least squares on F<sup>2</sup> with all unique reflections (SHELXL -97) (Sheldrick *et al*, 1985). Hydrogen atoms were refined using riding model. One such crystal (0.3 x 0.2 x 0.2 mm) was chosen and tested with polarizing microscope (Lexica DML SP) for single crystallinity.

#### 4.2.1 Crystallization of Bis(diisobutylammonium)tris(2,3-dihydroxynaphthalato)silicate $[(i\text{-C}_4\text{H}_9)_2\text{NH}_2]_2[\text{Si}(\text{C}_{10}\text{H}_6\text{O}_2)_3]\cdot 3\text{CH}_3\text{CN}$

Diffraction quality crystals were obtained by cooling a concentrated acetonitrile solution of bis(diisobutylammonium)tris(2,3-dihydroxynaphthalato)silicate at 0 °C for a period of seven days. The crystal of appropriate size was chosen and mounted with mother liquor in a Lindemann capillary tube as the crystal loses its crystallinity, when removed from the mother liquor.

#### 4.2.2 Crystallization of bis(tri-*n*-butylammonium)tris(2,3-dihydroxynaphthalato)silicate $[(n\text{-C}_4\text{H}_9)_3\text{NH}]_2[\text{Si}(\text{C}_{10}\text{H}_6\text{O}_2)_3]$

Suitable crystals of bis(tri-*n*-butylammonium)tris(2,3-dihydroxynaphthalato)silicate were obtained by cooling a concentrated acetonitrile solution of bis(tri-*n*-butylammonium)tris(2,3-dihydroxynaphthalato)silicate in the refrigerator over a period of 10 days. The crystal was mounted in a glass fiber unlike  $[(i\text{-C}_4\text{H}_9)_2\text{NH}_2]_2[\text{Si}(\text{C}_{10}\text{H}_6\text{O}_2)_3]\cdot 3\text{CH}_3\text{CN}$  since it was stable.

The experimental crystal data, collection conditions and structure refinement parameters for compounds **II** and **IV** are given in **Table 4.1**.

**Table 4.1** Crystal data and experimental parameters for crystal structure analyses of compounds  $[(i\text{-C}_4\text{H}_9)_2\text{NH}_2]_2[\text{Si}(\text{C}_{10}\text{H}_6\text{O}_2)_3] \cdot 3\text{CH}_3\text{CN}$  and  $[(n\text{-C}_4\text{H}_9)_3\text{NH}]_2[\text{Si}(\text{C}_{10}\text{H}_6\text{O}_2)_3]$

Parameters	Compound IV	Compound II
Empirical formula	C <sub>54</sub> H <sub>74</sub> N <sub>2</sub> O <sub>6</sub> Si	C <sub>52</sub> H <sub>67</sub> N <sub>5</sub> O <sub>6</sub> Si
Formula weight	875.24	886.20
Temperature	293(2) K	293(2) K
Wavelength	0.71069 Å	1.54180 Å
Crystal system, space group	Tetragonal, P <sub>4</sub> <sub>1</sub> 2 <sub>1</sub> 2	Triclinic, P-1
Unit cell dimensions	a = 14.928(4) Å c = 23.208(2) Å α = 90° β = 90° γ = 90°	a = 9.919(4) Å α = 104(6)° b = 12.701(9) Å β = 94.24(4)° c = 21.568(14) Å γ = 99(5)°
Volume	5173(2) Å <sup>3</sup>	2572(3) Å <sup>3</sup>
Z, Calculated density	4, 1.124 Mg/m <sup>3</sup>	2, 1.144 Mg/m <sup>3</sup>
Absorption coefficient	0.094 mm <sup>-1</sup>	0.807 mm <sup>-1</sup>
F(000)	1896	952
Crystal size	0.3 x 0.2 x 0.2 mm	0.3 x 0.2 x 0.2 mm
θ range for data collection	2.12 ° to 24.95 °	2.13 ° to 68.04 °
Limiting indices	0 ≤ h ≤ 17, 0 ≤ k ≤ 17, 0 ≤ l ≤ 27	0 ≤ h ≤ 11, -15 ≤ k ≤ 15, -25 ≤ l ≤ 25
Reflections collected / unique	5014 / 4539 [R(int) = 0.0568]	9945 / 9358 [R(int) = 0.0680]
Completeness to θ = 24.95 °	99.9 %	99.9 %
Absorption correction	Psi-scan	Psi-scan
Max. and min. transmission	0.9986 and 0.9744	0.9959 and 0.9656
Refinement method	Full-matrix least-squares on F <sup>2</sup>	Full-matrix least-squares on F <sup>2</sup>
Data / restraints / parameters	4539 / 0 / 286	9358 / 1 / 578
Goodness-of-fit on F <sup>2</sup>	0.843	1.046
R indices	R1 = 0.2154, wR2 = 0.2071	R1 = 0.0942, wR2 = 0.1858
Absolute structure parameter	0.1 (4)	-

### 4.3 RESULTS AND DISCUSSION

The silicate minerals that make up most of Earth's crust nearly always contain silicon in four-coordination with oxygen. Si–O bonds on Si (IV) are rather short with an average

bond distance R ( $^{IV}\text{Si-O}$ ) of about 1.626 Å for natural silicate minerals (Pauling 1980; Gibbs 1982). At pressures above 10 GPa, silicon atoms can achieve six-coordination with oxygen atoms resulting in the  $(\text{SiO}_6)^{8-}$  octahedron, having longer Si-O bonds with R ( $^{IV}\text{Si-O}$ ) of about 1.794 Å. In 1969 first single crystal X - ray structure of dianionic hexacoordinate silicate of catecholato was studied and subsequently, the structural studies were reported of silicates with variety of aliphatic and aromatic bidentate and tridentate ligands (glycolic acid, hydroximic acid, ethyleneglycol, catechol and citric acid). Tris(catecholato)silicates having different counter cations like alkali metals, aromatic and aliphatic ammonium ions and super bases have been structurally examined. The aromatic bidentate ligands are essentially only based on catechol and substituted catechols. Hence, we have employed 2,3-dihydroxynaphthalene as the ligand, in place of catechol, and examined its effect on structural features such as nature of hydrogen bonding, geometry around silicon and  $\pi$ -  $\pi$  interactions between the silicate moiety.

#### **4.3.1 Structure of Bis(diisobutylammonium)tris(2,3-dihydroxynaphthalato)silicate [(i-C<sub>4</sub>H<sub>9</sub>)<sub>2</sub>NH<sub>2</sub>]<sub>2</sub>[Si(C<sub>10</sub>H<sub>6</sub>O<sub>2</sub>)<sub>3</sub>].3CH<sub>3</sub>CN**

Bis(diisobutylammonium)tris(2,3-dihydroxynaphthalato) silicate crystallizes with three acetonitrile molecules in the lattice. The crystal loses its crystallinity once it has been removed from the mother liquor. This may be due to the weak interaction of solvent moiety that gets disturbed with change in environment. Bis(diisobutylammonium)tris(2,3- dihydroxynaphthalato) silicate crystallizes in triclinic crystal system with space group of P-1. Whereas, the tris(catecholato)silicate with same ammonium counter cation but with one water molecule crystallizes in trigonal crystal system.

The asymmetric unit consists of a tris(2,3-dihydroxynaphthalato)silicate anion and two diisobutylammonium cations with three molecules of acetonitrile in the lattice. Two of acetonitrile molecules present in the crystal lattice by van der Waals interaction unlike other solvent moiety that involved in hydrogen bonding with counter cations. The oxygen coordination around silicon is in slightly distorted octahedral geometry, with ligand bite angles O1—Si1—O2 = 87.93 (10) Å, O3—Si1—O4 = 87.79 (9) Å and O5—Si1—O6 = 88.83 (10) Å. Compared to tris(catecholato)silicate which was reported in literature shown that one of the ligand bite angle is almost the same in both the cases whereas the other angles varies about 10° may be due to difference in steric crowding of the naphthalate and catecholate (Bindu et al, 2003). Si-O bond lengths were in the range of for tris(2,3-dihydroxynaphthalato)silicate that was similar to the reported tris(catecholato)silicates. Pentacoordinate silicate of 2,3-dihydroxynaphthalene has been reported to have Si-O bond lengths in range of 1.690-1.802Å (Tacke *et al*, 1991) similar to that of hexacoordinate silicate systems. The data are given in **Table 4.2** and **Table 4.3**.

Table 4.2 Si-O bond length (Å) of SiO<sub>6</sub> core for [((i-C<sub>4</sub>H<sub>9</sub>)<sub>2</sub>NH<sub>2</sub>)<sub>2</sub>][Si(C<sub>10</sub>H<sub>6</sub>O<sub>2</sub>)<sub>3</sub>]. 3.CH<sub>3</sub>CN

Bonds	Bond length (Å)
O (1)-Si (1)	1.79(19)
O (2)-Si (1)	1.79(2)
O (3)-Si (1)	1.79(2)
O (4)-Si (1)	1.78(19)
O (5)-S i(1)	1.77(2)
O (6)-Si (1)	1.76(2)



**Table 4.3:** Selected bond angles ( $^{\circ}$ ) of SiO<sub>6</sub> core for [((*i*-C<sub>4</sub>H<sub>9</sub>)<sub>2</sub>NH<sub>2</sub>)<sub>2</sub>][Si(C<sub>10</sub>H<sub>6</sub>O<sub>2</sub>)<sub>3</sub>].  
3.CH<sub>3</sub>CN

Bonds	Bond Angles ( $^{\circ}$ )
C(1)-O(1)-Si(1)	113(14)
C(8)-O(2)-Si(1)	113(14)
C(11)-O(3)-Si(1)	113(14)
C(18)-O(4)-Si(1)	113(14)
C(21)-O(5)-Si(1)	113(15)
C(28)-O(6)-Si(1)	113(15)
O(6)-Si(1)-O(5)	89(9)
O(6)-Si(1)-O(4)	94(10)
O(5)-Si(1)-O(4)	91(9)
O(6)-Si(1)-O(1)	91(9)
O(5)-Si(1)-O(1)	94(9)
O(4)-Si(1)-O(1)	173(8)
O(6)-Si(1)-O(2)	176(8)
O(5)-Si(1)-O(2)	88(9)
O(4)-Si(1)-O(2)	88(9)
O(1)-Si(1)-O(2)	88(9)
O(6)-Si(1)-O(3)	90(10)
O(5)-Si(1)-O(3)	178(9)
O(4)-Si(1)-O(3)	88(9)
O(1)-Si(1)-O(3)	87(9)
O(2)-Si(1)-O(3)	93(9)

The two of the N(1,2)-H in counter diisobutylammonium cations form N—H...O hydrogen bonds with two of oxygen (O(2) and O(3)) atoms of the different naphthalate moiety in silicate anion [N(1)-H(1B)...O(3)= 1.90 and N(2)-H(2A)...O(2)#1 = 1.97] as shown in **Figure 4.1** .

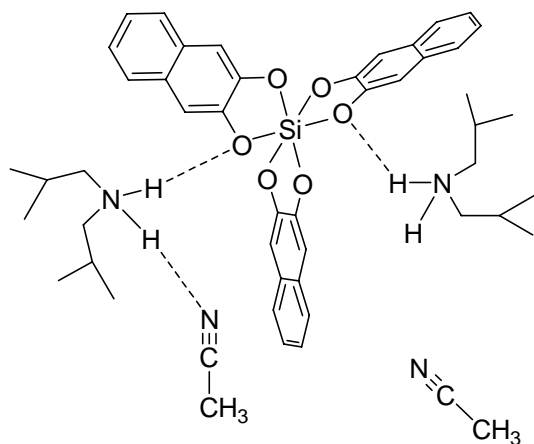


**Figure 4.1:** Hydrogen bonding interaction between ion pairs of  $[(i\text{-C}_4\text{H}_9)_2\text{NH}_2]_2[\text{Si}(\text{C}_{10}\text{H}_6\text{O}_2)_3] \cdot 3 \text{CH}_3\text{CN}$

One of the solvent acetonitrile molecule forms an N—H...N hydrogen bonding with the diisobutylammonium cations ( N(2)-H (2B)...N(3)#1 = 2.18) as shown in the ORTEP diagram (**Figure 4.2**). For comparison the hydrogen bonding details are given in **Table 4.4**.

**Table 4.4.** Hydrogen bonds for  $[(i\text{-C}_4\text{H}_9)_2\text{NH}_2]_2[\text{Si}(\text{C}_{10}\text{H}_6\text{O}_2)_3] \cdot 3 \text{CH}_3\text{CN}$  [ $\text{\AA}$  and  $^\circ$ ].

D-H...A	d(D-H)	d(H...A)	d(D...A)	<(DHA)
N(1)-H(1B)...O(3)	0.90	1.90	2.78(3)	165.2
N(2)-H(2A)...O(2)#1	0.90	1.97	2.86(3)	171.3
N(2)-H(2B)...N(3)#1	0.90	2.18	3.05(5)	163.3

Symmetry transformations used to generate equivalent atoms: #1 x-1, y, z

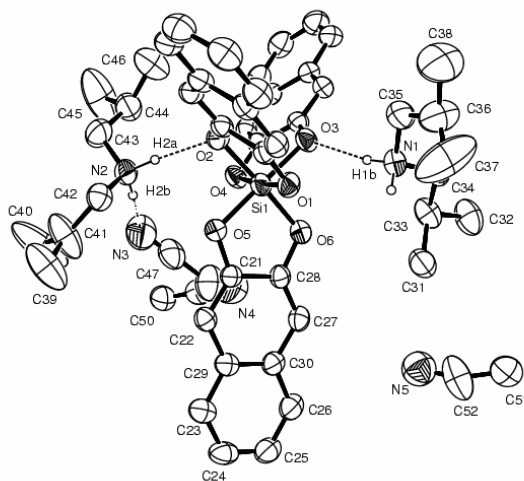


Figure 4.2: **ORTEP diagram** of  $[(i\text{-C}_4\text{H}_9)_2\text{NH}_2]_2[\text{Si}(\text{C}_{10}\text{H}_6\text{O}_2)_3] \cdot 3 \text{CH}_3\text{CN}$

Unlike the tris(catecholato)silicates that form extended network, through hydrogen bonding, the tris(2,3-dihydroxynaphthalato)silicate forms no extended network of silicates may be due to crowding of the naphthalate and so the orientation of the silicate might not has favoured for the extended network.

In the case of tris(catecholato)silicates the two oxygens that are involved in the hydrogen bonding are from the same catechol moiety whereas, in naphthalato silicate two oxygens of two different naphthalato moieties are involved. This observation possibly has relevance to the thermal decomposition pattern. In the case of tris(catecholato)silicate there was spirosilane formation irrespective of the counter cations whereas in tris(2,3-dihydroxynaphthalato)silicates the spirosilane formation is not observed.

#### 4.3.2 Packing of bis(diisobutylammonium) tris(2,3-dihydroxynaphthalato)silicate

The packing arrangement of bis(diisobutylammonium)tris(2,3-dihydroxynaphthalato)silicate in the unit cell is shown in Figure 4.3. There is a crystallographic  $C_2$  axis

symmetry seen in the unit cell. Though naphthalate moiety has aromatic nucleus, the steric hindrance of the three naphthalene groups did not allow  $\pi$ - $\pi$  interaction between two silicate units. Among the three solvent moieties found in the crystal lattice, only one is involved in discrete hydrogen bonding. The other two solvent moieties are held in the lattice by van der Waals interaction.

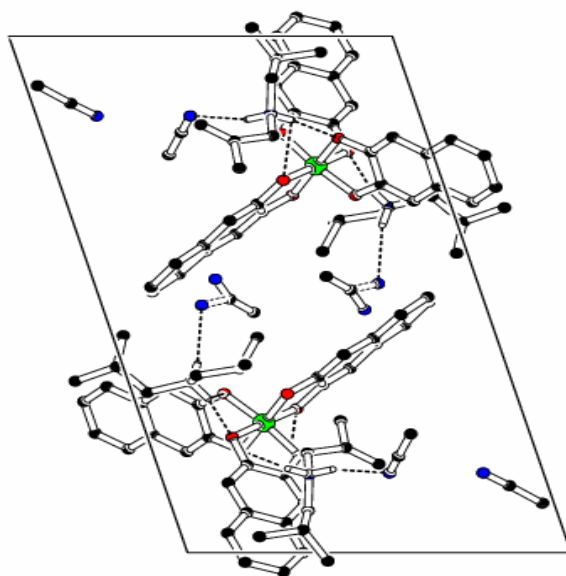


Figure 4.3: **Packing diagram of bis(diisobutylammonium)tris(2,3-dihydroxynaphthalato)silicate**

#### **4.3.3 Bis(tri-*n*-butylammonium)tris(2,3-dihydroxynaphthalato) silicate**

Bis(tri-*n*-butylammonium)tris(2,3-dihydroxynaphthalato)silicate has crystallizes without any solvent molecules unlike the tris(catecholato)silicate with triethylammonium counter cations. Crystals of this compound remain unaffected even when removed from the mother liquor.

Bis(tri-*n*-butylammonium)tris(2,3-dihydroxynaphthalato)silicate crystallizes in the tetragonal crystal system with space group P4<sub>1</sub>2<sub>1</sub>2 similar to that of the naturally occurring six coordinate silicate “Stishovite” (Sclar *et al*, 1964). Crystallographically, half the molecule was contained in the asymmetric unit. The two-fold axis at ¼ of *c* and parallel to the diagonal of *ab*-plane bisects the molecule. The 8 equivalent positions of the space group generate four molecules in the unit cell. The structure reveals hexacoordinate silicon with slightly distorted octahedral geometry. This can be clearly seen in ORTEP plot is given in **Figure 4.4**. Si-O bond length was found to be 1.775Å for stishovite as reported by Sclar *et al*. Si – O bond lengths of tris(2,3-dihydroxynaphthalato)silicate are listed in the **Table 4.5** matches with literature values that lies in the range of 1.76-1.81Å. Varying ligand environment from catechol to 2,3-dihydroxynaphthalene has no effect on Si-O bond length when compared with literature values of tris(catecholato)silicate (Bindu *et al*, 2003).

**Table 4.5** Si-O bond lengths (Å) of SiO<sub>6</sub> core for [((*n*-C<sub>4</sub>H<sub>9</sub>)<sub>3</sub>NH)<sub>2</sub>][Si(C<sub>10</sub>H<sub>6</sub>O<sub>2</sub>)<sub>3</sub>].

Bonds	Bond length (Å)
Si(1)-O(2)#1	1.76(4)
Si(1)-O(3)#1	1.79(4)
Si(1)-O(1)#1	1.81(4)

Symmetry transformations used to generate equivalent atoms: #1 -y+1,-x+1,-z+1/2

Distorted Octahedral geometry is due to slight distortion of O-Si-O bond angles from ideal angles 90° and 180° (ref. **Table 4.6**). Dihedral angles among the three SiO<sub>2</sub>C<sub>2</sub> rings (83.23° and 85.59°) have been restrained to be close to 90° to satisfy the near octahedral

coordination. The hydrogen bonding interaction between ammonium counter cations and silicate is as depicted in the **Figure 4.5**.

**Table 4.6** Selected bond angles ( $^{\circ}$ ) of  $\text{SiO}_6$  for  $[(n\text{-C}_4\text{H}_9)_3\text{NH}]_2[\text{Si}(\text{C}_{10}\text{H}_6\text{O}_2)_3]$

Bonds	Bond Angles ( $^{\circ}$ )
C(8)-O(1)-Si(1)	112(3)
C(1)-O(2)-Si(1)	116(3)
C(11)-O(3)-Si(1)	114(4)
O(2)-Si(1)-O(2)#1	173(3)
O(2)-Si(1)-O(3)	90(18)
O(2)#1-Si(1)-O(3)	95(19)
O(2)-Si(1)-O(3)#1	95(19)
O(2)#1-Si(1)-O(3)#1	90(18)
O(3)-Si(1)-O(3)#1	87(3)
O(2)-Si(1)-O(1)	88(17)
O(2)#1-Si(1)-O(1)	87(18)
O(3)-Si(1)-O(1)	176(19)
O(3)#1-Si(1)-O(1)	90(17)
O(2)-Si(1)-O(1)#1	87(18)
O(2)#1-Si(1)-O(1)#1	88(17)
O(3)-Si(1)-O(1)#1	90(17)
O(3)#1-Si(1)-O(1)#1	176(19)
O(1)-Si(1)-O(1)#1	93(2)

Symmetry transformations used to generate equivalent atoms: #1  $-y+1, -x+1, -z+1/2$

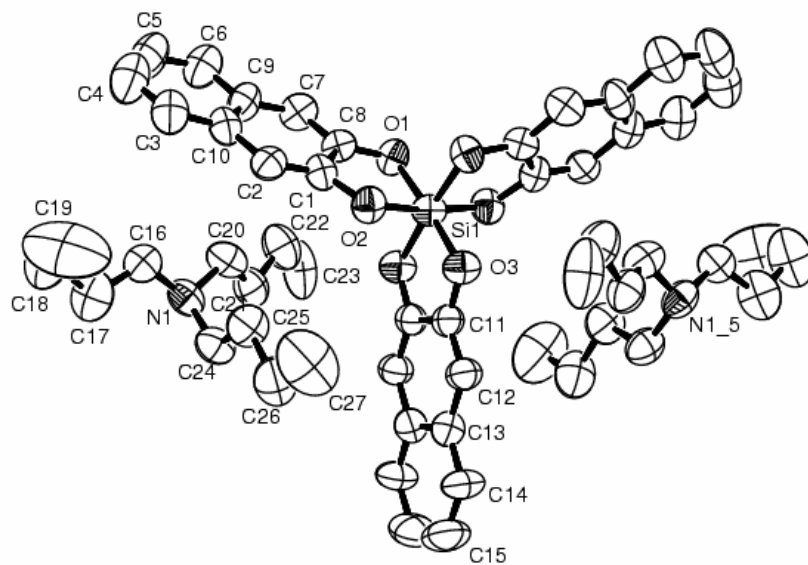


**Figure 4.4** ORTEP diagram of  $[(n\text{-C}_4\text{H}_9)_3\text{NH}_2][\text{Si}(\text{C}_{10}\text{H}_6\text{O}_2)_3]$

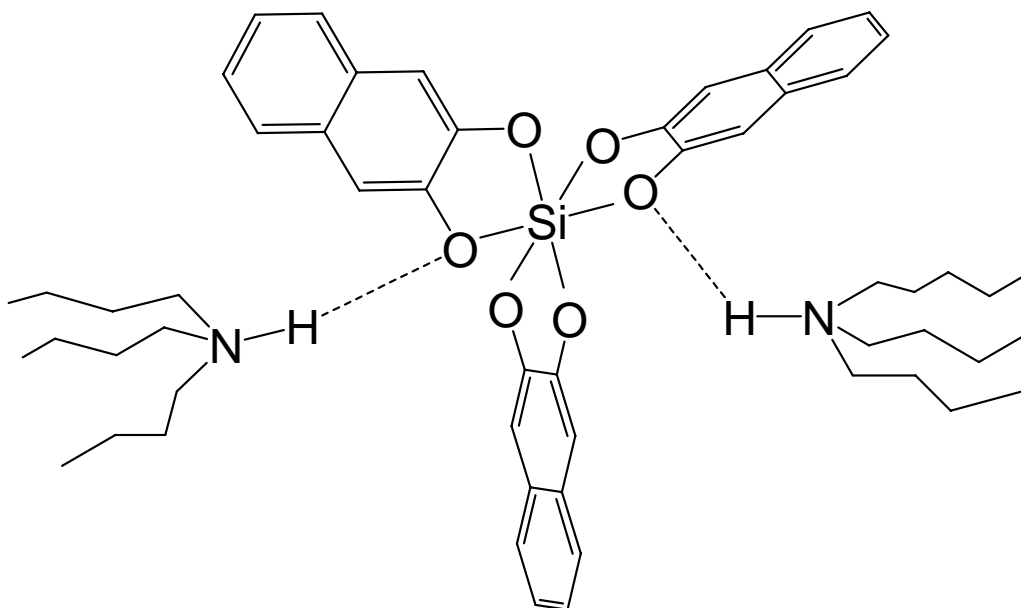


**Figure 4.5:** Representation of hydrogen bonding interaction between ion pairs

Tri-*n*-butylammonium counter cations and tris(2,3-dihydroxynaphthalato)silicate anion have been linked through N1-H1..O1 hydrogen bonding (N1-H1=0.911Å,

H1...O1=2.041Å and N1-H1...O1=157.42°) are given in the **Table 4.7**. The structure does not reveal any intermolecular hydrogen bonding between the silicate units.

**Table 4.7** Hydrogen bonds for [(n-C<sub>4</sub>H<sub>9</sub>)<sub>3</sub>NH]<sub>2</sub>[Si(C<sub>10</sub>H<sub>6</sub>O<sub>2</sub>)<sub>3</sub>] [Å and °].

D-H...A	d(D-H)	d(H...A)	d(D...A)	<(DHA)
N(1)-H(1)...O(1)#2	0.91	2.04	2.041 (6)	157.5

Symmetry transformations used to generate equivalent atoms: #1 -y+1,-x+1,-z+1/2 #2 -x+3/2, y+1/2

#### 4.3.4 Packing of bis(tri-*n*-butylammonium)tris(2,3-dihydroxynaphthalato)silicate

Four molecules of bis(tri-*n*-butylammonium)tris(2,3-dihydroxynaphthalato) silicate are present per unit cell as shown in the **Figure 4.6**. When we see the packing diagram in **Figure 4.3** the C<sub>2</sub> axis of symmetry along the diagonal is present. However, no such symmetry was observed in packing diagram that is shown in **Figure 4.6**.

Stabilization of the molecules in crystal lattice was due to hydrogen bond and van der Waals interaction between silicate and ammonium counter cations. The silicate and ammonium ions are held in the lattice by intra molecular hydrogen bonding. The interaction between two molecular units is only due to weak van der Waals force.



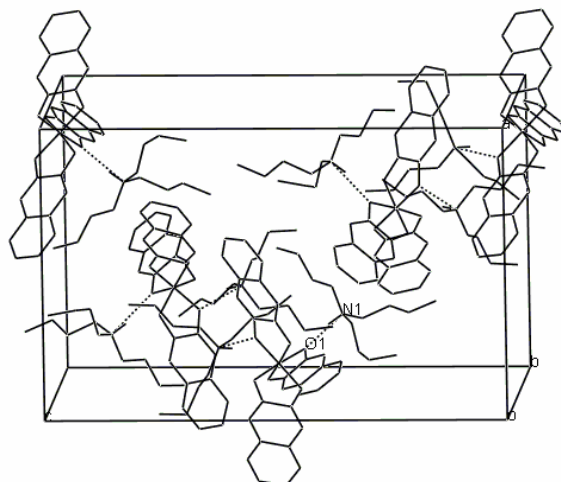


**Figure 4.6** Packing diagram of  $[(n\text{-C}_4\text{H}_9)_3\text{NH}]_2[\text{Si}(\text{C}_{10}\text{H}_6\text{O}_2)_3]$

#### 4.3.5 Effect of counter cation

The effect of counter cations on different properties of bis(ammonium)tris(2,3-dihydroxynaphthalato)silicates is considered.

##### 4.3.5.1 Solubility

With change in the substitution on ammonium counter cations of tris(2,3-dihydroxynaphthalato)silicate, solubility in organic solvents has shown variation. This observation can be attributed to the extent of hydrogen bonding in the presence of different ammonium ions (John, 1984).

##### 4.3.5.2 Stability of the crystals

Tri-*n*-butylammonium derivative crystal was quite stable in air without mother liquor whereas diisobutylammonium derivative loses its crystallinity when removed from the mother liquor. Stability of the tri-*n*-butylammonium may be due to the absence of solvent moiety in the lattice due to crowding of alkyl chains.

#### 4.4 Conclusions

- ✓ Bis(ammonium)tris(2,3-dihydroxynaphthalato)silicates with diisobutylammonium and tri-*n*-butylammonium counter cations have been structurally studied.
- ✓ In the case of bis(ammonium)tris(2,3-dihydroxynaphthalato)silicates, silicon is in distorted octahedral geometry irrespective of counter cation.
- ✓ Presence of solvent moiety in the crystal lattice depends on the bulkiness of the solvent moiety.
- ✓ There is no  $\pi$ - $\pi$  stacking among two silicate units with the aromatic ring of ligand
- ✓ It has been observed that counter cations and silicate anions are linked through hydrogen bonding with two different naphthalate moiety of tris(2,3-dihydroxynaphthalato)silicate.
- ✓ There is no extended network through hydrogen bonding between counter cation mediated by solvent moiety to silicate units unlike in other hexacoordinate silicates that are available in literature.

## **CHAPTER V**

### **PYROLYTIC AND HYDROLYTIC STABILITY OF BIS(AMMONIUM)TRIS(2,3-DIHYDROXYNAPHTHALATO) SILICATES: A STUDY WITH RELEVANCE FOR BIOSILIFICATION**

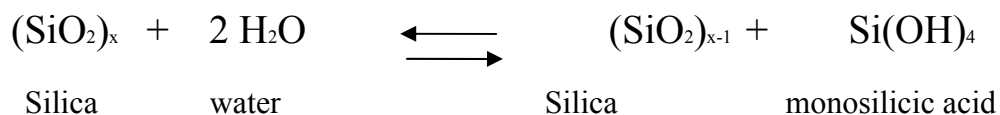
---

## 5.1 INTRODUCTION

Mesoporous silica was widely used as solid supports in various catalytic reactions. This has led to the development of numerous methods to synthesize such materials (Davis *et al*, 2002). In recent years considerable focus has been given to synthesize silica from organic-inorganic hybrid materials (Yin *et al*, 2005). In literature, metal oxalates were used as precursor for microporous materials (Decurtins *et al*, 1993) and thermal decomposition of silicon oxalate complexes resulted in silica with specific pore dimensions (Balkus *et al*, 1995). The sol-gel method was commonly employed to produce various amorphous silica morphologies such as tubular, organogels and crystalline mesoporous materials by molecular imprinting method (Jung *et al*, 2000; Szostak *et al*, 1998). In this sol gel process, formation of silica takes place in two stages, namely hydrolysis and condensation. When silica precursor has bulkier alkyl group that leads to slow hydrolysis and thereby play a role in particle size control (Brinker *et al*, 1990; Chen *et al*, 1996). Polymerization and aggregation of silica from monomeric silicon complex  $K_2[Si(C_6H_4O_2)_3]$  under approximately neutral pH condition and in presence of hemicellulose to evaluate the effect on polymerization were studied by Perry *et al*, in 1995. The counter ion effect of  $M[Si(C_6H_4O_2)_3]$  in hydrolytic studies has been studied (Santschi *et al*, 1974; Mc Cormick *et al*, 1989 ; P.W.J.G, 1990; Perry *et al*, 1995). The silicon species,  $K_2[Si(C_6H_4O_2)_3]$  has relevance in the transport of soluble silicon in certain plants (Peggs *et al*, 1988). It was found that, it yields transient hexacoordinate silicon species, as is evident from NMR studies (Kinrade *et al*, 1999). Hence the hexacoordinate silicates are of interest in synthesis of bio inspired silica materials.

The solubility of silica in aqueous solutions depends on many factors (Iller, 1979). However, the crucial factor that has greater influence on the solubility are (i) the particle size of silica, (ii) the degree of internal hydration in the silica and (iii) impurities present in the medium such as other ions, molecules and macromolecules. The impurities alter the degree and strength of the hydrogen bonding of silica in solution. Thus preventing or stimulating the dissolution of the silica can be depending on the nature of the impurities.

The dissolution of silica in water is slow and its depolymerization is gradual. It follows a reversible reaction as given below [Iller, 1979]



The scheme for formation of a silica sol (solution of colloidal particles of sizes 1-1000 nm, in a liquid) from the monosilicic acid is given in **Figure 5.1**.

So far, in the literature pentacoordinate and hexacoordinate silicates were used as a precursor for glasses, ceramic and porous materials respectively (Pallavi *et al*, 1994; Balkus *et al*, 1995). Recently, 2,3-dihydroxynaphthalene and catechol were used as template in the synthesis of tubular and globular silicates (Isayama *et al*, 1999). Aliphatic amines with long alkyl chain are popular templates or structure directing agents in zeolite synthesis (Ferracin *et al*, 1990).

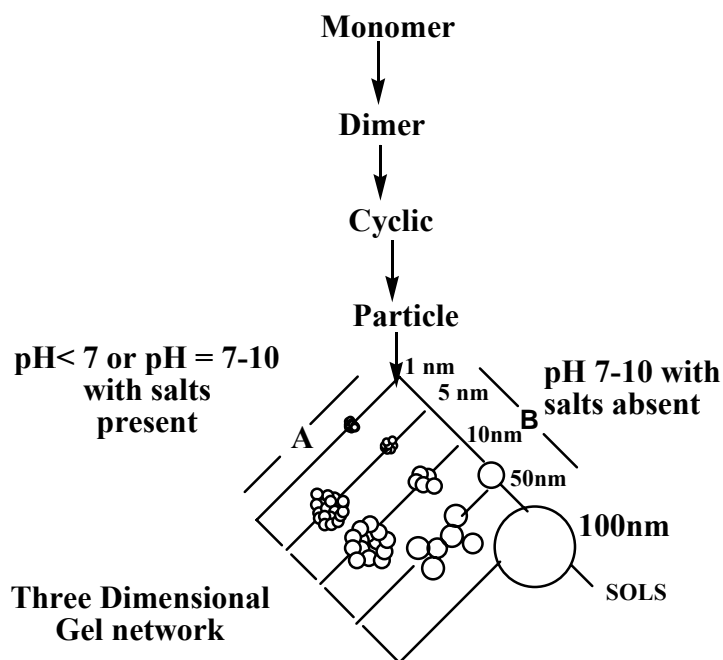


**Figure 5.1:** Polymerization behavior of silica in aqueous medium A = in the presence of salts/acidic medium; B = alkaline medium (reproduced from the work of Iller)

In this study the bis(ammonium)tris(2,3-dihydroxynaphthalato)silicate was used as precursor for the synthesis of silica. Ammonium counter ion can act as a template to obtain silica under both hydrolytic and pyrolytic conditions. Various ammonium ions were used in the present study to know their effect on the decomposition of the precursors and on the silica formed.

## 5.2 EXPERIMENTAL

### 5.2.1 Thermal stability of tris(2,3-dihydroxynaphthalato)silicate with ammonium counter cations (TGA and DTA studies)

Approximately 3.0 mg of these hexacoordinate silicates were heated in the temperature range of 298 – 1073 K at a heating rate of 283 K/min under nitrogen atmosphere in the

thermal analyzer. Representative TG and DT plots of tris(2,3-dihydroxynaphthalato)silicates are given in Figure 5.2 (a) and (b) respectively.

### **5.2.2 Bulk Pyrolysis**

1 gm of ammonium (*t*-butylammonium, diisopropylammonium and Tri-*n*-butylammonium) derivative of tris(2,3-dihydroxynaphthalato)silicate was taken in quartz boat and pyrolyzed in muffle furnace at 1073 K in air for 3 h. From TGA plot, it was inferred that all organic components of silicon complexes decompose completely by heating at 1073 K. The silica obtained is a white powder. Silica was characterized by IR and X-ray diffraction.

### **5.2.3 Hydrolytic stability of tris(2,3-dihydroxynaphthalato)silicate with ammonium counter cations**

The oligomerization reactions were carried out at room temperature of 293 K. Solutions (0.14 mmol<sup>-1</sup>) of complexes were prepared with a 4:1 mixture of ethanol and double distilled water in a plastic container. The resulting solution undergoes decomposition to give orthosilicic acid. The oligomerization of the newly formed silicic acid was measured as a function of orthosilicic acid concentration by modified molybdenum blue colorimetric method described by Iller, 1979. The details of this test were discussed in chapter 2.

The precipitated silica was removed from the system after 7 days and was washed well to remove traces of 2,3-dihydroxynaphthalene. The morphology of the silica was obtained using transmission electron microscopy. A small quantity of sample was placed in a vial and a suspension was made in chloroform. A small drop of this suspension was placed on a Formvar coated holey carbon-copper electron microscope grid and viewed with

transmission electron microscope operating at 200KeV. For SEM studies, lyophilized samples were dispersed on double-sided sticky tape and mounted on aluminum stubs with the edges of the tape being painted with quick drying silver paint to prevent charging of the sample. All loose aggregates were removed by tapping the stub before the silica samples were coated with a layer of platinum using a sputter coat.

The particle size was obtained from TEM micrographs of representative samples. A minimum of 50 particles per sample was measured. Measurement was complicated by the fact that most of the area of silica was comprised of overlapping and/or aggregated particles, which were difficult to separate from one another.

Surface area measurements were carried out by using 0.5 g quantities of precipitated silica obtained after 7 days of reaction. Single point measurements were performed and BET isotherms were obtained by sorptometer. Samples were degassed at 403 K for a minimum of 16 h before analysis at liquid nitrogen temperature (this has to be done in order to ensure that all surface water vapors were removed from the silica samples, although it is appreciated that there may have some effect on the structure of the material following this treatment). The specific surface area was obtained by the BET method, assuming nitrogen to have a cross-sectional area of  $0.16 \text{ nm}^2$ . Pore size distributions were calculated by application of the BJH method to the adsorption data. However, the materials under investigation showed a variety of adsorption/desorption hysteresis loops and for consistency, adsorption data were used for the calculations. This is mainly due to the fact that various shapes of the pores do not affect adsorption data to a great extent compare to desorption.



## 5.3 RESULTS AND DISCUSSION

The thermal studies on tris(catecholato)silicate revealed the counter ion plays a role on the thermal stability (Kingston *et al*, 2000). In the case of indium-tin oxide, a sensor material was prepared using new precursor by a one-pot thermal decomposition route (Hockensmith *et al*, 1999). The thermal study of ammonium derivatives of tris(2,3-dihydroxynaphthalato)silicate was carried out to know whether there will be any difference in their thermal behaviour when ligand environment around silicon was changed. The effect of counter cations on the hydrolytic stability of tris(2,3-dihydroxynaphthalato)silicate was studied by monitoring UV-Vis spectral changes of ethanol/water solution of bis(ammonium)tris(2,3-dihydroxynaphthalato)silicates over a period of time. The literature observations, triggered us to study the bis(ammonium)tris(2,3-dihydroxynaphthalato)silicate as precursor with ammonium ion in itself as a template and a one pot thermal decomposition route to obtain silica.

### 5.3.1 Thermal studies of tris(2,3-dihydroxynaphthalato)silicate with ammonium counter ion

Thermal stability of tris(2,3-dihydroxynaphthalato)silicate has varied with respect to difference in counter cations. The stability of bis(ammonium)tris(2,3-dihydroxynaphthalato)silicate follows the order  $3^{\circ} > 2^{\circ} > 1^{\circ} >$  cyclic amine, as deduced from the values of onset temperature of decomposition. A representative TG plot is given in **Figure 5.2(a)**. The complex undergoes decomposition mostly in three to four stages leading to formation of silica. The decomposition of this complex is exothermic in nature as inferred from DTA (**Figure 5.2(b)**).

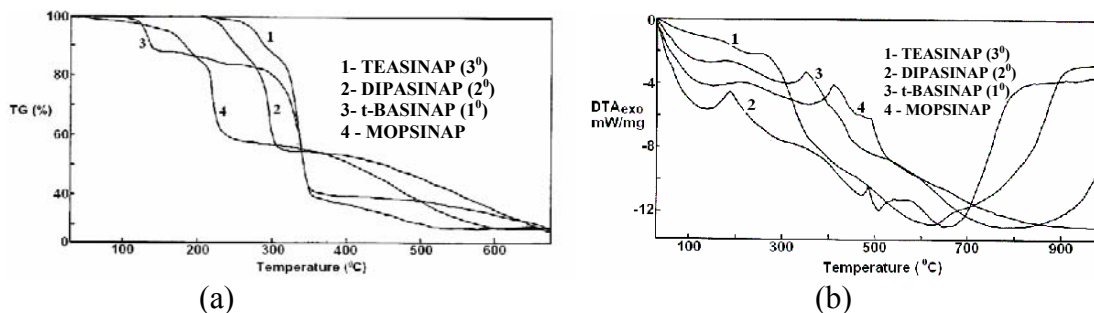
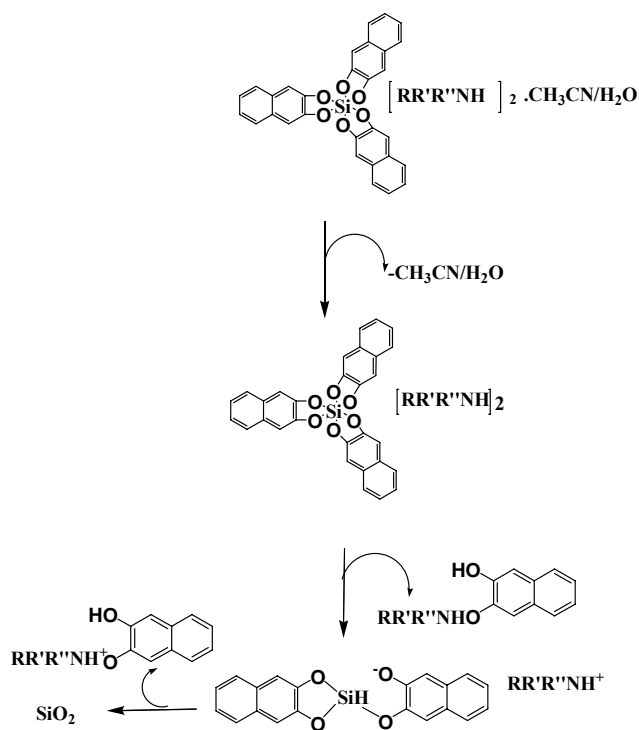


**Figure 5.2(a)** Representative TGA plot & (b) DTA plot of ammonium salt of tris(2,3-dihydroxynaphthalato)silicate

Three-stage decomposition is observed for compounds I, II, III, V, VI, VII, IX, X, XI & XII (see Table 5.3). In all these silicates, first stage of decomposition corresponds to loss of the solvent and/or corresponding amine and the second and third stages of decomposition are due to the loss of monoammonium naphthalate and monoammonium naphthalate with 2,3-dihydroxynaphthalene respectively leading finally to a silica residue. The possible mechanism of thermal decomposition based on percentage weight loss is depicted in **Scheme 5.1**. From TGA plot the percentage weight loss and stability temperature range for a particular fragment are listed in **Table 5.1**. On the other hand, with similar ammonium ion as counter cations, decomposition of the tris(catecholato)silicate leads to a loss of bisammonium catecholate and formation of spiro-silane was observed in all the cases (Kingston *et al*, 2000). In the present case, no such observation is seen in the analogues silicate of 2,3-dihydroxynaphthalene. In the case of tris(2,3-dihydroxynaphthalato)silicate, loss of ammoniumnaphthalate occurs in two to three stages leading to the formation of residual silica.



**Scheme 5.1:** Possible mechanism of thermolysis of different ammonium salt of tris(2,3-dihydroxynaphthalato)silicate

**Table 5.1:** Thermoanalytical data of tris(2,3-dihydroxynaphthalato)silicate with different counter ammonium ions

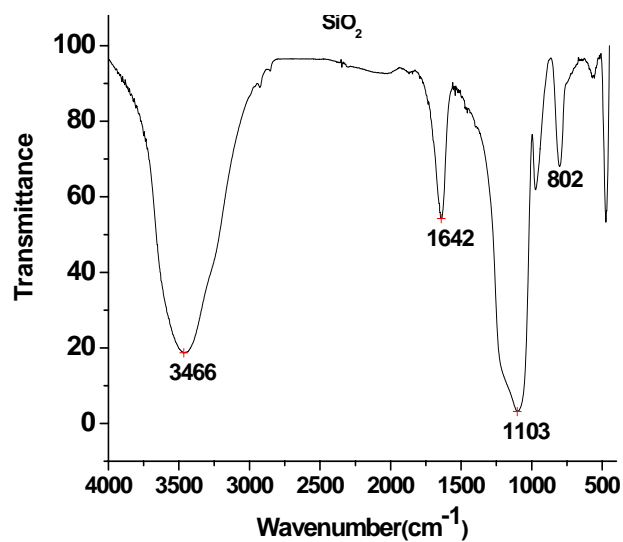
Compd.	Decomposition – I*			Decomposition – II <sup>#</sup>			Decomposition – III <sup>@</sup>		
	Temp. Range (°C)	Wt. Loss %	DTA peak (°C)	Temp. Range (°C)	Wt. Loss %	DTA peak (°C)	Temp. Range (°C)	Wt. Loss %	DTA peak (°C)
TnBASINAP	50-290	13.9 (12.9)	227	225-375	49.6 (47.8)	347.0	375-800	27.4 (26.5)	610.9
TEASINAP	50-280	11.9 (14.1)	150	280-425	52.8 (50.8)	2882.0	425-800	23.9 (24.2)	-
DIPASINAP	210-300	11.9 (12.5)	-	300-390	65.6 (67.8)	--	390-800	12.5 (11.9)	-
DIBASINAP	50-270	23.5 (22.5)	-	270-800	68.7 (67.9)	---	-	-	-
MOPSINAP	50-290	11.2 (10.8)	255	290-390	38.3 (37.8)	316.4	390-900	38.5 (37.8)	688.2

NMPSINAP	50-250	2.7 (2.45)	--	150-350	14.6 (13.9)	---	305-800	75.6 (73.5)	-
PIDASINAP	50-325	3.0 (2.8)	--	325-800	61.1 (60.7)	---	--	---	-
PYDASINAP	50-100	2.6 (2.4)	---	100-550	54.8 (53.4)	---	550-800	32.0 (31.9)	-
<i>Sec</i> BASINAP	50-145	3.4 (2.9)	--	145-294	30.9 (29.3)	--	294-800	48.1 (49.5)	-
<i>t</i> -BASINAP	50-220	18.7 (17.5)	212.6	220-480	65.6 (65.4)	382.1	480-800	23.1 (21.5)	660.0
2 <i>Am</i> PYSINAP	50-280	26.8 (27.9)	---	280-800	52.2 (51.9)	----	---	----	-

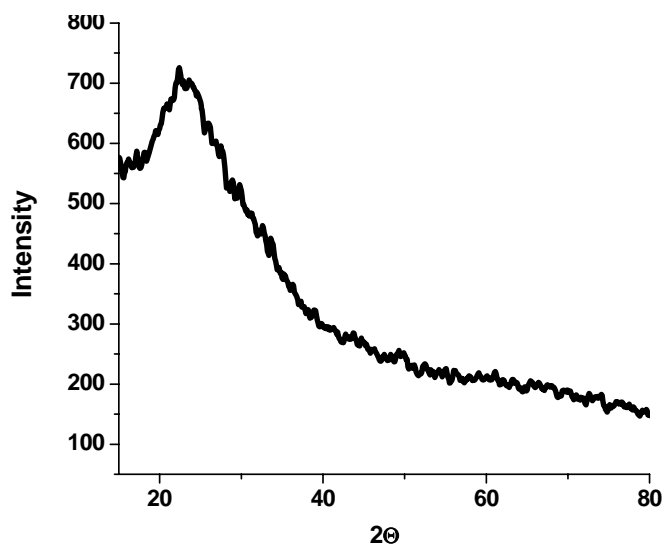
\* - loses solvent/amine; # - loses ammoniumnaphthalate; @ - loses ammoniumnaphthalate and 2,3-dihydroxynaphthalene

### 5.3.2 Bulk pyrolysis

Upon pyrolysis of bis(ammonium)tris(2,3-dihydroxynaphthalato)silicate [tri-*n*-butylammonium, diispropylammonium and *t*-butyl ammonium] at 1073 K yielded silica. It was characterized by IR spectroscopy where, peak at 1103 cm<sup>-1</sup> is characteristic of Si-O bond stretch of silica and broad peak at 3400 cm<sup>-1</sup> is due to hydrogen bonded water molecule (**Figure 5.3 a**). The IR stretching frequencies matched with that obtained in bioinspired silica mediated by poly(allylamine hydrochloride) (Parwardhan *et al*, 2002). Broad diffraction pattern in powder XRD around 2θ = 25° revealed the amorphous nature of silica obtained (**Figure 5.3.b**). The diffraction pattern of amorphous silica reported in literature matches with the silica diffraction pattern obtained in this study (Hamden *et al*, 1997).



(a)



(b)

**Figure 5.3**(a) IR spectra of the silica obtained from on pyrolysis (b) Powder XRD of silica obtained on pyrolysis

### 5.3.3 TEM of silica obtained by Pyrolysis

The silica obtained from tris(2,3-dihydroxynaphthalato)silicate of tri-*n*-butylammonium ion as counter ion gave the fine tubular aggregates with particle size of 5-8 nm (. Large spherical aggregates with particle size of 10-14 nm were obtained from tris(2,3-

dihydroxynaphthalato)silicate with diisopropylammonium counter ion as precursor. Disorganized silica with particle size 4-6 nm was obtained from precursor tris(2,3-dihydroxynaphthalato)silicate of *t*-butylammonium counter ion **Figure 5.4 a, b & c**). All the silica has pore size in the range of 8-10 Å.

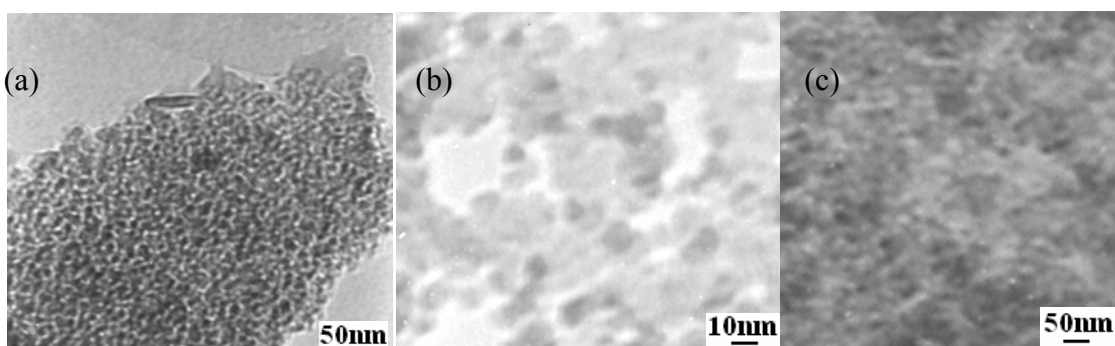


**Figure 5.4** TEM images of silica obtained under pyrolytic condition from (a) *Tn*BASINAP (b) DIPASINAP (c) *t*-BASINAP

That all the three compounds shows ill-defined SAD pattern further confirms the amorphous nature of silica (**Figure 5.5a**) and their compositions were also qualitatively confirmed from EDAX (**Figure 5.5b**).

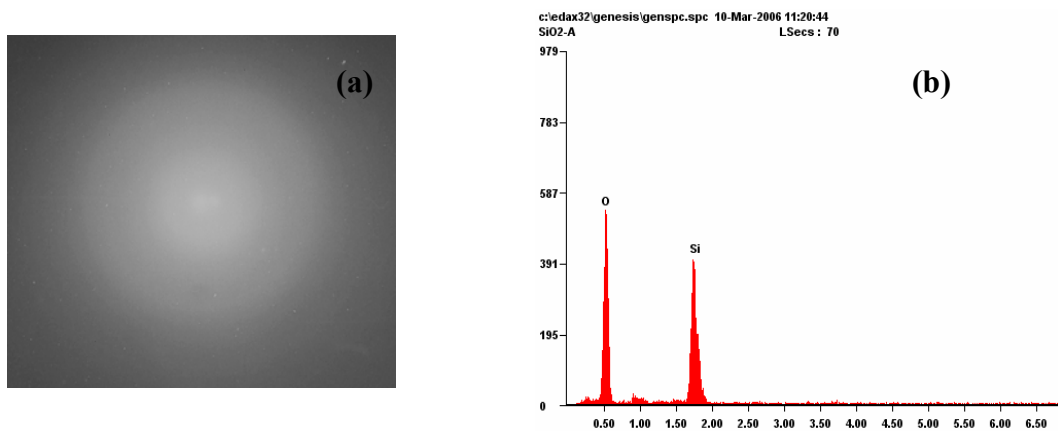


**Figure 5.5:** (a) Diffraction pattern of the silica (b) EDAX of the silica

Values of surface area of silica obtained from these silicon complexes under pyrolytic conditions are listed in **Table 5.2**. The surface area decreases with increase in bulkiness of the alkyl group on ammonium ion of the precursor bis(ammonium)tris(2,3-dihydroxynaphthalato)silicate. The surface area of silica obtained from tris(2,3-dihydroxynaphthalato)silicate is comparable to the reported values of tris(catecholato)silicates under hydrolytic condition (Harrison *et al*, 1995).

**Table 5.2** Surface area and pore volume of silica obtained by pyrolysis

Compound name	Surface area/m <sup>2</sup> g <sup>-1</sup>	Pore volume/cm <sup>3</sup> g <sup>-1</sup>
<i>t</i> -BASINAP	426.4	0.46
DIPASINAP	378.3	0.81
T <i>n</i> BASINAP	226.9	0.19

#### 5.3.4 SEM of silica obtained by Pyrolysis

The silica materials obtained from tris(2,3-dihydroxynaphthalato)silicate containing different counter cations (tri-*n*-butylammonium, diisopropylammonium & *t*-butylammonium ions) were examined under scanning electron microscopy (SEM) to monitor the changes in the morphology with respect to the change in the counter ions. The tubular silica along other particles is clearly observed from SEM image of silica obtained from tri-*n*-butylammonium derivative of tris(2,3-dihydroxynaphthalato)silicate shown in Figure 5.6(a). Representative micrographs of silica obtained by varying the counter cations are given in **Figure 5.6 (a, b & c)**.

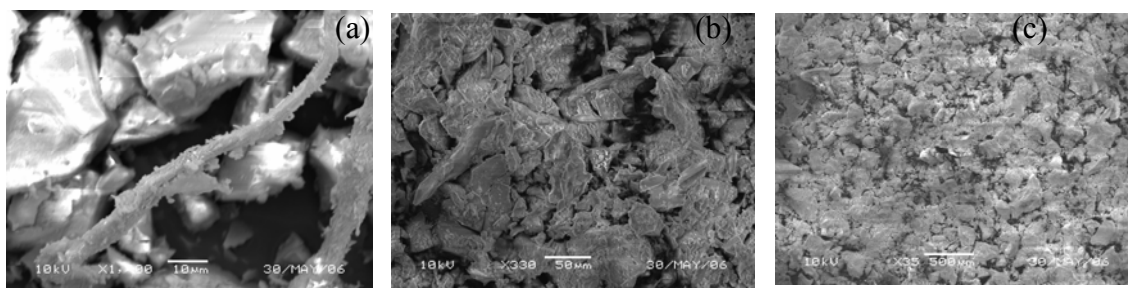


**Figure 5.6:** SEM images of silica obtained on pyrolysis of a) TnBASINAP (b) DIPASINAP (c) t- BASINAP

From the SEM and TEM we could arrive at the morphology and size distribution of the particles. A detail explanation will be included. Amorphous nature of silica was confirmed from the SAD shown in Figure 5.5a, their particle shapes were observed using SEM that are shown in Fig 5.6. Since the SEM and TEM images are not so clear to calculate pore volume, we used BJH for arriving at the pore volume and BET method for measurement of surface area. From the SEM picture we can observe the shape of silica which helps us to understand the surface area variation. Two of the derivatives that are having the spherical shape, hence a higher surface area compare to the tubular shape silica.

### 5.3.5 Hydrolytic stability

**Figure 5.7** shows the effect of time on the decomposition of the three silicon complexes present in ethanol-water mixture (1:4) solution under neutral condition. At the beginning of the experiment all the complexes start breaking down immediately even in neutral condition in presence of water. Under acidic condition, the decomposition is rapid when compared to basic conditions due to the fact that the increase of hydroxyl ion concentration reduces the chance of protonation of Si-O bond. **Figure 5.9.**



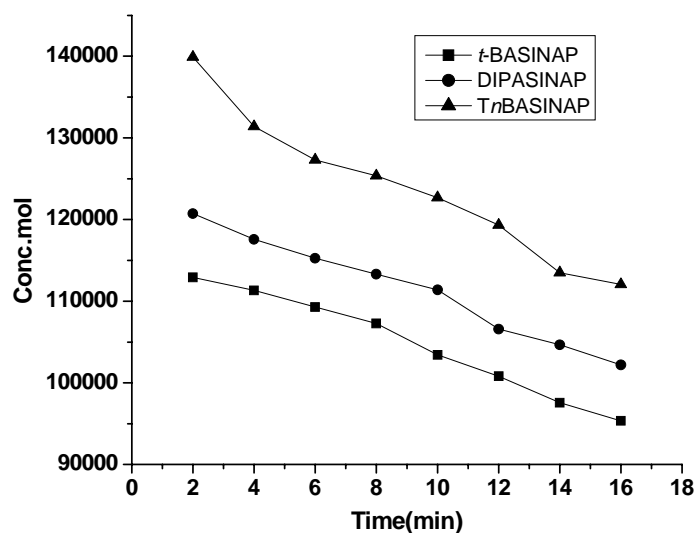
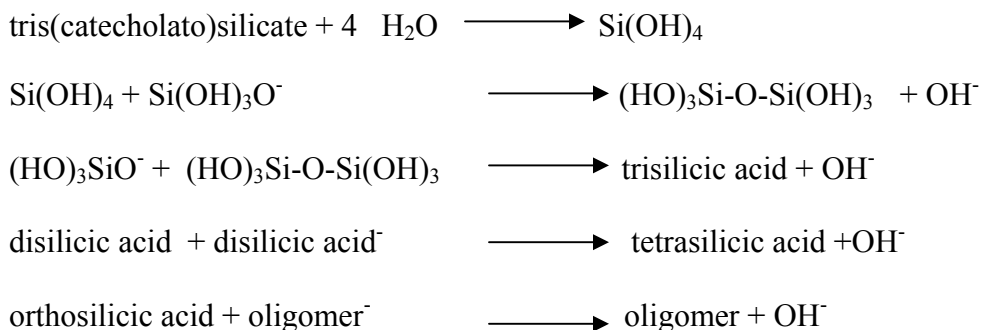


**Figure 5.7** : A plot of concentration of tris(2,3-dihydroxynaphthalato)silicate Vs. time

### 5.3.6 Colorimetric molybdate test

Tris(2,3-dihydroxynaphthalato)silicates undergo decomposition in presence of water to give the following products: 2,3-dihydroxynaphthalene, silica and corresponding alkylammonium hydroxide. The decomposition process of tris(2,3-dihydroxynaphthalato)silicate was characterized by UV-Vis absorption studies. Moreover, the increase in the concentration of 2,3-dihydroxynaphthalene is evident from the increase in the intensity of the peak at around 324 nm with time (Figure 5.8). Similarly, the silica obtained by the decomposition, was also tested by molybdate blue test. Silica in presence of water initially forms orthosilicic acid (monomer) and due to increase in concentration of ammonium hydroxide during decomposition of silicate. The suggested route to the formation of its oligomers in the case of tris(catecholato)silicate is shown in the following scheme(Perry et al, 1992).



The increase of hydroxyl ion concentration in the medium leads to rapid growth of oligomer. However one could not make any distinction between monomer and oligomers. The oligomers, during colorimetric molybdate test, in the presence of acidic ammonium molybdate undergo decomposition to give monomers. The formation of monomer has been monitored by the growth of the peak at 810 nm in UV-Vis spectrum with time.

Initially, for the first 20 min the concentration of monosilicic acid was gradually increasing and, saturation in the concentration was observed after 20 mins. Initially the shape of the plots varied according to the counter cations, since the initial concentration of the silicic acid varies with respect to varying counter cations. Decomposition in the cases of tris(2,3-dihydroxynaphthalato)silicate follows the order of tri-*n*-butylammonium cation < *t*-butylammonium cation < diisopropylammonium cation is shown in the **Figure 5.8**.

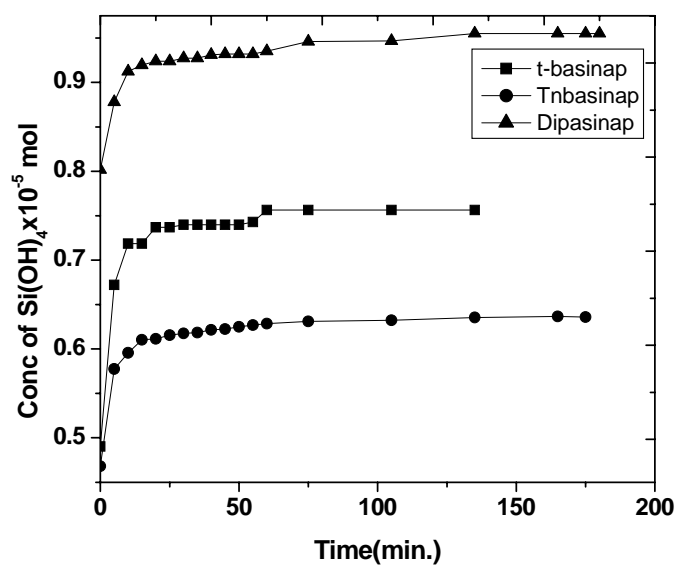
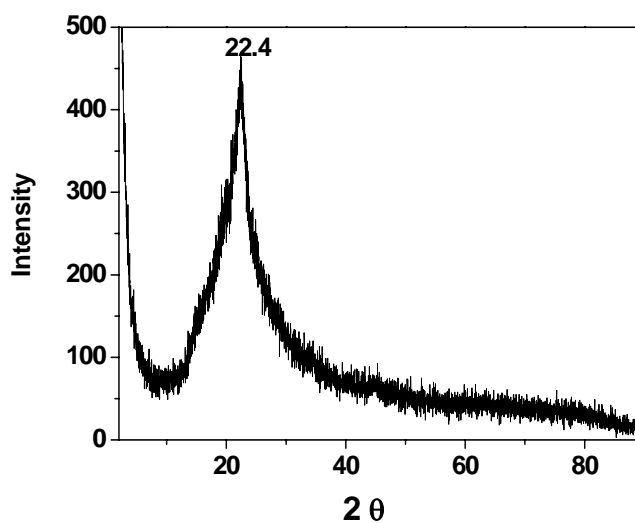


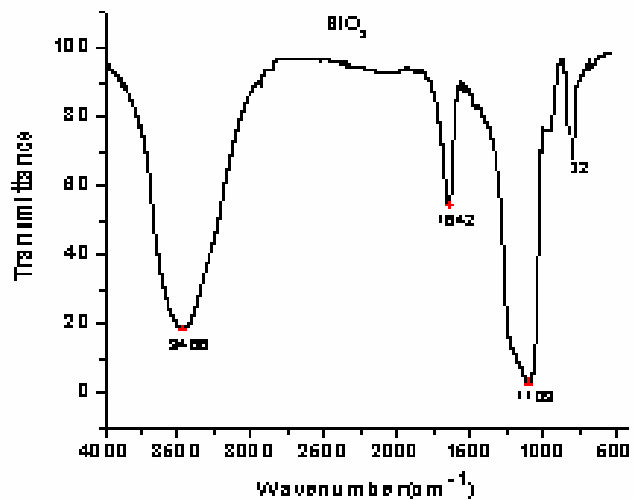
Figure 5.8: A plot concentration of silicic acid Vs time

### 5.3.7 Silica obtained on hydrolysis

Silica obtained on hydrolysis of tris(2,3-dihydroxynaphthalato)silicate with varying counter cations in ethanol-water mixture was characterized by IR and XRD. The characteristic features are observed in IR and XRD as shown in **Figure 5.9 a & b**.



(a)



(b)

**Figure 5.9**(a) IR spectra of the silica obtained on hydrolysis (b) Powder XRD of silica

### 5.3.8 Transmission Electron Microscopy

The silica obtained from tris(2,3-dihydroxynaphthalato)silicate of tri-*n*-butylammonium ion as counter ion gave the fine spherical aggregates with particle size of 8-9 nm. Fine aggregates with particle size of 6-8 nm for silica that was obtained from tris(2,3-dihydroxynaphthalato)silicate with diisopropylammonium counter ion. Irregularly aggregated silica with particle size 10-12 nm was obtained from tris(2,3-dihydroxynaphthalato)silicate with *t*-butylammonium counter ion(**Figure 5.10 (a, b & c)**). All the silica material has pore size in the range of 6-8 Å. Similar observations were reported for tris(catecholato)silicate (Harrison *et al*, 1995), but not as expected observation of obtaining tubular silicate using 2,3-dihydroxynaphthalene as template reported in literature (Isayama *et al*,2005).

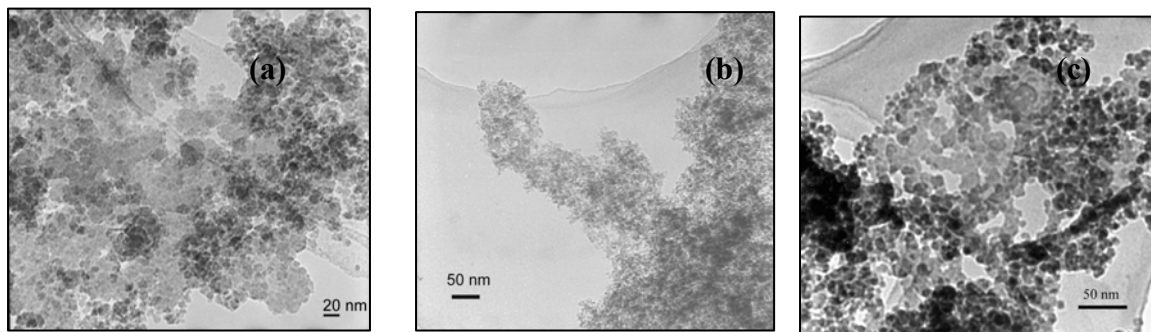


**Figure 5.10:** TEM images of silica obtained after 7 days in ethanol-water mixture for (a) *t*-butylammonium cation (b) diisopropylammonium cation (c) Tri-*n*-butylammonium cation containing tris(2,3-dihydroxynaphthalato)silicate

### 5.3.9 SEM of silica

SEM of the silica obtained on hydrolysis with varying counter cations are given in **Figure 5.11 (a, b & c)**. The wires like and spongy morphologies are seen for these mesoporous silica materials.

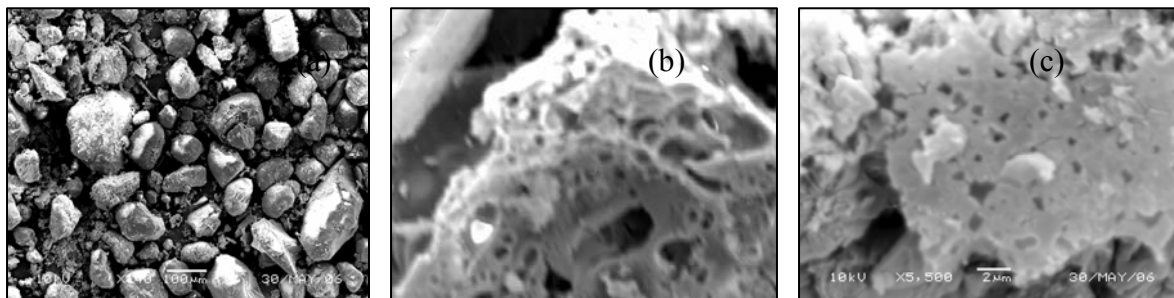


**Figure 5.11.** SEM images of silica obtained on hydrolysis of a) TnBASINAP (b) DIPASINAP (c) *t*-BASINAP

Values of surface area of silica obtained from these complexes under hydrolytic condition are given in **Table 5.3**. The values of surface area decreases with increase in bulkiness of alkyl group on ammonium counter ion of the precursor, bis(ammonium)tris(2,3-dihydroxynaphthalato)silicate.

**Table 5.3** surface area and pore volume of silica obtained by hydrolysis

Compound	Surface area/m <sup>2</sup> g <sup>-1</sup>	Pore volume/cm <sup>3</sup> g <sup>-1</sup>
t-BASINAP	336.4	0.76
DIPASINAP	298.3	0.81
TnBASINAP	196.9	0.19

#### 5.4 CONCLUSION

- ✓ The thermal study of tris(2,3-dihydroxynaphthalato)silicates shows that stability increases when counter ion varies from primary to tertiary ammonium ions. Thermal decomposition pattern varies as we change silicon environment from catechol to 2,3-dihydroxynaphthalene.
- ✓ Stability of silicate under hydrolytic condition increases as ammonium ion varies from primary to tertiary ions. The tris(2,3-dihydroxynaphthalato)silicates hydrolysed to yield ligand, alkyl ammonium hydroxide and silicic acid. Monosilicic acid undergoes oligomerization in presence of amine and depolymerized under molybdate blue test. The depolymerization rate increases as one goes from tris(2,3-dihydroxynaphthalato)silicate with counter cations tertiary to primary ammonium ions.
- ✓ Silica particles obtained under pyrolytic and hydrolytic conditions are mesoporous materials. Silica obtained by pyrolytic route is of the particle size of 2-8 nm unlike as in the case of hydrolytic route (6-15 nm). Thus silica material obtained in pyrolytic condition has higher surface area compared to the one obtained under hydrolytic condition.

**CHAPTER VI**  
**CYCLIC VOLTAMMETRIC STUDIES OF BIS(AMMONIUM)**  
**TRIS(2, 3-DIHYDROXYNAPHTHALATO)SILICATE**

---

---

## 6.1 INTRODUCTION

In order to understand the redox process in biological systems, modeling studies of function systems have been carried out to mimic photosystems (oxidation of water) and oxidation of aromatic diols in presence of enzymes (macromolecule). Several enzymes such as the copper-containing fungal laccase, superoxide dismutase, haem containing peroxidases and tyrosinase in plants, animals and bacteria are able to catalyse the oxidation of catechol to benzoquinone (Mason et al, 1961). Synthesis and redox behavior of catechol complexes of iron, manganese, vanadium, chromium, titanium, cobalt, actinium, molybdenum, rhenium are well studied (Jones et al, 1981; Chin et al, 1982; Triller, 2003; Pierpont et al, 1994). Manganese complexes of 3,5-di-*t*-butyl catechol bind reversibly to molecular oxygen which is analogous to what is found in the final step of oxidation of water to molecular oxygen in the photosystem II of green plant (Jones et al, 1981). The 2-methyl-1,4-naphthoquinones is a synthetic intermediate of vitamin K and was synthesized from 2-methylnaphthalene using chromium oxide (Yamazaki, 2001). Electrochemical syntheses of lead complexes of ortho-diols and ortho-quinone have been reported by Gareth et al in 2003. Electro-organic syntheses of Diels Alder and polymeric compounds have also been reported (Nematollahi et al, 2006; Plesu et al, 2003).

Redox behavior of these complexes was studied in which either the ligand or metal or both will be electroactive. In the current study, only ligand alone is active as a redox species.



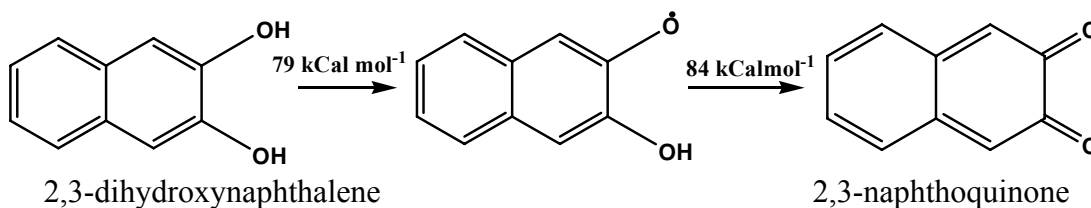
### 6.1.1 Redox Behavior of 2, 3 – Dihydroxynaphthalene

Similar to catechol the redox behavior of the extended systems like 2,3-dihydroxynaphthalene has also been studied. 2,3-Naphthoquinone is one of the three missing members in the family of naphthoquinones due to instability. The study of the oxidation of 2,3-dihydroxynaphthalene with Cobalt (III) indicated instability for the primary oxidation product, apparently the 2,3-naphthoquinone. The spontaneous chemical transformation of the 2, 3-naphthoquinone has been characterized as polymers. The only physicochemical information, which characterizes 2,3-naphthoquinone, was the polarographic half wave potential reported by Horner *et al* in 1981. Cyclic voltammetry in different aqueous buffers using graphite paste electrode showed only an anodic peak indicating a rapid depletion of 2,3-naphthoquinone on the electrode surface. This behavior is explained by a rapid dimerization or polymerization of the quinone (Horak *et al*, 1981).

The oxidation of 2,3-dihydroxynaphthalene with aqueous  $\text{KIO}_3$  resulted in the formation of 2,3-naphthoquinone, that in the presence of cyclopentadiene gave Diels-Alder [4+2] adduct which was characterized (Horak *et al*, 1981). The oxidation of 2,3-dihydroxynaphthalene with aqueous  $\text{KIO}_3$  and in the presence of solvents such as methanol, acetone and ethyl acetate, produced 1, 1'- dimer (Horak *et al*, 1981). Electrochemistry of complexes of 2,3-dihydroxynaphthalene for the elements such as boron, ruthenium and zinc were also reported (Lim *et al*, 2003; Yang *et al*, 1997 and Mabrouk *et al*, 1987).

2,3-dihydroxynaphthalene was chemically oxidized using hydrogen peroxide in presence of Mn(II) which was monitored using fluorescence spectroscopy. On addition of

ethylenediamine to this solution lead to the formation of quinoxaline derivative (Watanabe *et al*, 1995). Flueraru *et al* (2006) have studied cytotoxicity of quinones and naphthoquinones. It was concluded that formation of 2,3-naphthoquinones under experimental conditions does not take place. This proved that 2,3-dihydroxynaphthalene had lower cytotoxicity compared to other members of naphthalene. Energetic and structural changes for the naphthalenediol → naphthosemiquinone → naphthoquinone are given in the **Scheme 6.1**. Bond dissociation energy are given in  $\text{kCal mol}^{-1}$



**Scheme 6.1:** Energetic and structural changes in the naphthalenediol oxidation

### 6.1.2 Redox Behavior of other Silicon Complexes

So far, the redox behavior of silicon complexes with ligands porphyrine and phthalocyanine was studied (Lorenz *et al*, 1997). Silicon complexes with phenalenyl-based ligand had shown three-stage one electron reduction whose structural details were established by UV-Vis studies (Pal *et al*, 2005). In the present study, the redox behaviour of 2,3-dihydroxynaphthalene present in tris(2,3-dihydroxynaphthalato) silicates is studied with varying ammonium counter cations.

## 6.2 EXPERIMENTAL SECTION

Cyclic voltammograms were recorded at  $25 \pm 0.1$  °C with a microcomputer-controlled system at a scan rate of 100, 50, 25, 10 mV/s. Glassy carbon electrode (Tokai Carbon GC-30S), freshly polished with 0.1  $\mu\text{m}$  diamond slurry was used as the working electrode and a platinum wire served as the counter electrode. Ag/AgNO<sub>3</sub> (0.01 mol dm<sup>-3</sup> in CH<sub>3</sub>CN) was the reference electrode. Controlled potential electrolysis was carried at 480 mV Vs Ag/AgCl for tri-n-butylammonium derivative of silicate.

**Figure 6.2** shows cyclic voltammogram of 0.5 mM [(*sec*-C<sub>4</sub>H<sub>9</sub>)<sub>2</sub>NH<sub>2</sub>]<sub>2</sub>[Si(C<sub>10</sub>H<sub>6</sub>O<sub>2</sub>)<sub>3</sub>] in supporting electrolyte of tetrabutylammonium perchlorate in CH<sub>3</sub>CN was recorded in the scan rate of 25 mV/s. Three oxidation waves were observed. They are mostly ill-defined waves. In the reverse sweep, the corresponding reduction waves were not obtained. In addition, cyclic voltammogram of 0.5 mM 2,3-dihydroxynaphthalene in supporting electrolyte of tetrabutylammonium perchlorate in CH<sub>3</sub>CN was also recorded. It gave only an irreversible oxidation wave at around 851 mV (**Figure 6.1**). The effect of cations on the voltammetric behavior of [Si(C<sub>10</sub>H<sub>6</sub>O<sub>2</sub>)<sub>3</sub>]<sup>2-</sup> was studied by measuring voltammograms of tris(2,3-dihydroxynaphthalato)silicate with different ammonium counter ions and the peak potentials are given in the **Table 6.1**. The effect of scan rate on the current was also measured to study the kinetics. The stability of the silicates under electrochemical conditions was studied by repetitive cycling and electrochemical reaction nature studied by recording the voltammograms at different scan rates.

**Table 6.1:** Compounds considered for the study  $(R_3NH)_2(Si(C_{10}H_6O_2)_3)$

S.N o.	Ammonium ion	$[Si(C_{10}H_6O_2)_3]$ with $(R_3NH)_2$
1	Primary	<i>Sec</i> - $C_4H_9NH_3^+$ , <i>t</i> - $C_4H_9NH_3^+$
2	Secondary	<i>i</i> - $C_3H_7)_2NH_2^+$ , <i>i</i> - $C_4H_9)_2NH_2^+$
3	Tertiary	$(C_2H_5)_3NH^+$ , <i>n</i> - $C_4H_9)_3NH^+$
4	Cyclic	$O(CH_2)_4NH_2^+$ , $CH_3N(CH_2)_4NH_2^+$
5	Aromatic	$C_6H_5NH_3^+$ , $C_6H_4N(NH_3)^+$

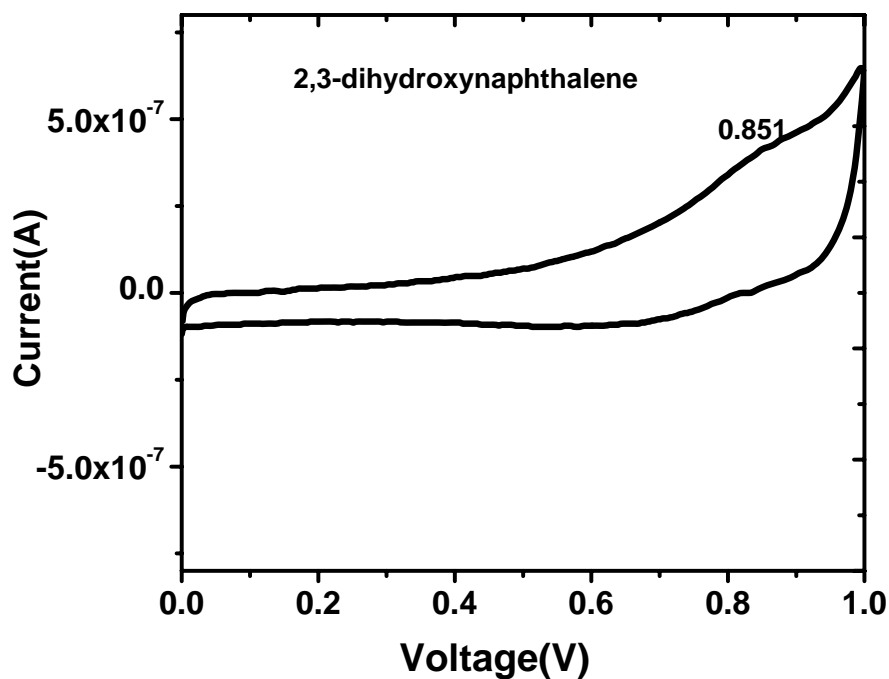


**Figure 6.1:** Cyclic Voltammogram of 2,3-dihydroxynaphthalene with TBAP in acetonitrile as supporting electrolyte

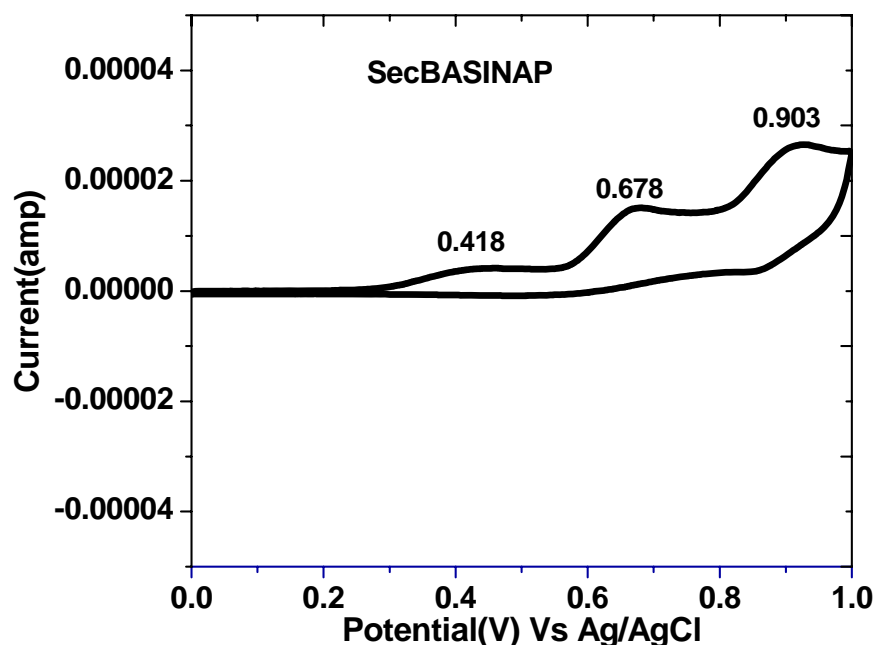


**Figure 6.2:** Cyclic voltammogram of bis(*sec*-butylammonium)tris(2,3-dihydroxynaphthalato)silicates

### 6.2.1 Chemical Oxidation

The chemical oxidation procedure employed for the present study is similar to that reported for 2,3-dihydroxynaphthalene by Horak et al (1981).

Bis(tri-*n*-butylammonium)tris(2,3-dihydroxynaphthalato)silicate (0.06 g) was dissolved in acetonitrile (3 mL) and the aqueous solution of  $\text{KIO}_3$  was added. Even after an hour no colour change was noticed. On addition of 1 mL of acetone induced development of a pink coloration in 15 min for which UV-Vis spectrum was recorded.

Acetone solution of tri-*n*-butylammonium containing tris(2,3-dihydroxynaphthalato)silicate resulted similar pink solution for which ESR and UV-Vis spectrum was recorded.

## 6.3 RESULTS AND DISCUSSION

Bodini et al have studied redox behavior of 1,2-dihydroxynaphthalene, 1,2-naphthoquinone and their metal complexes and their use as powerful oxidizing agent for organic or inorganic substrates (1997). In 2004, Okamoto et al reported that ammonium cations have acceleration effect on electron transfer reactions of quinones by hydrogen bonding with 1,4-naphthosemiquinone anion radicals. This has been structurally proved by ESR studies. Based on ESR studies, role of intramolecular hydrogen bonding was correlated to electrochemical stability of hydroxyl-quinones and semiquinone (Frontana et al, 2005). Since 2,3-naphthoquinones are unstable, not much of studies were carried out on electrochemical behavior.

### **6.3.1 Cyclic Voltammetric Study**

In order to study the redox behavior of tris(2, 3- dihydroxynaphthalato)silicates, cyclic voltammetric studies with conventional three electrode system were carried out. Tetrabutylammonium perchlorate in acetonitrile medium was used as supporting electrolyte. The experiments were carried out under nitrogen atmosphere to avoid the aerial oxidation of the ligand. Silicon complexes of 2,3-dihydroxynaphthalene with ammonium counter cation undergo three-step irreversible oxidation. The first oxidation potential was sensitive to the variation of the counter cation whereas, the other two-oxidation potentials did not show any shift with variation of counter cations. Whereas in the case of 1,2-naphthoquinones it was reported that it gave two reversible reductions (Bondini et al, 1997). Unlike 2,3-naphthoquinone, 1,2-naphthoquinones are stable (Scherbak et al, 2005). The cyclic voltammogram of the 2,3-dihydroxynaphthalene gives an ill-defined irreversible anodic peak around 0.851 V. The silicon complex of 2,3-dihydroxynaphthalene gave three irreversible anodic peaks at 0.2-0.4 V, 0.6 V and 0.9 V.

Horak et al, reported that only anodic peak was observed for the 2,3-dihydroxynaphthalene and it was accounted for instability of the 2,3-naphthoquinone (1981). The boron complex of 2,3-dihydroxynaphthalene was also reported to have ill-defined peak in cyclic voltammetric studies (Lim et al, 2003). Due to instability of the intermediate no structural correlation was derived for three stage anodic peaks. Since chemical oxidation was carried out in aqueous medium, no meaningful correlation could be achieved as the silicon complex cleaves in presence of water. The values of redox potentials of silicon complexes with different ammonium counter cations are given in Table 6.2. The cyclic voltammetric studies were carried out at different scan rates and the representative voltammogram for a bis(sec-butylammonium)tris(2,3-dihydroxynaphthalato)silicate is given in **Figure 6.2**.

**Table 6.2:** Redox potential of  $[\text{Si}(\text{C}_{10}\text{H}_6\text{O}_2)_3]^{2-}$  with different counter cation

$[\text{Si}(\text{C}_{10}\text{H}_6\text{O}_2)_3]^{2-}$ with counter cation	Oxidation Potential(V)		
	1 <sup>st</sup>	2 <sup>nd</sup>	3 <sup>rd</sup>
Sec-C <sub>4</sub> H <sub>9</sub> NH <sub>3</sub> <sup>+</sup>	0.435	0.652	0.943
t-C <sub>4</sub> H <sub>9</sub> NH <sub>3</sub> <sup>+</sup>	0.420	0.668	0.968
(i-C <sub>3</sub> H <sub>7</sub> ) <sub>2</sub> NH <sub>2</sub> <sup>+</sup>	0.409	0.670	0.968
(i-C <sub>4</sub> H <sub>9</sub> ) <sub>2</sub> NH <sub>2</sub> <sup>+</sup>	0.240	0.601	0.953
(C <sub>2</sub> H <sub>5</sub> ) <sub>3</sub> NH <sup>+</sup>	0.372	0.604	0.987
(n-C <sub>4</sub> H <sub>9</sub> ) <sub>3</sub> NH <sup>+</sup>	0.473	0.683	0.966
O(CH <sub>2</sub> ) <sub>4</sub> NH <sub>2</sub> <sup>+</sup>	0.339	0.695	0.973
CH <sub>3</sub> N(CH <sub>2</sub> ) <sub>4</sub> NH <sub>2</sub> <sup>+</sup>	0.428	0.634	0.961
(CH <sub>2</sub> ) <sub>5</sub> NH <sub>2</sub> <sup>+</sup>	0.355	0.621	0.955
(CH <sub>2</sub> ) <sub>4</sub> NH <sub>2</sub> <sup>+</sup>	0.355	0.592	0.968
C <sub>6</sub> H <sub>5</sub> NH <sub>3</sub> <sup>+</sup>	0.408	0.574	0.917
C <sub>6</sub> H <sub>4</sub> N(NH <sub>3</sub> ) <sup>+</sup>	0.487	0.693	0.966

### 6.3.2 Chemical Oxidation

UV-Vis spectra of both the solutions obtained from aqueous  $\text{KIO}_3$  and acetone gave absorption at 500 nm. The spectra are shown in **Figure 6.3 a and b**

ESR of the pink solution obtained for acetone solution of tris(2,3-dihydroxynaphthalato)silicate gave a single peak with g value of 2.0048 as shown in Figure 6.4. Since splitting patterns are not observed it did not help to understand the structure of the radical formed.

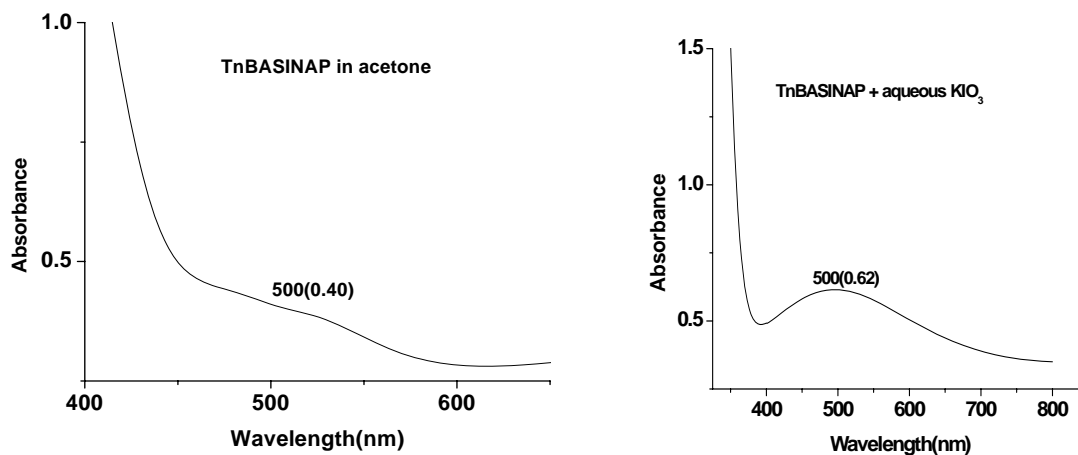


**Figure 6.3:** UV-Vis spectra of (a) TnBASINAP in acetone (b) TnBASINAP in aqueous  $\text{KIO}_3$

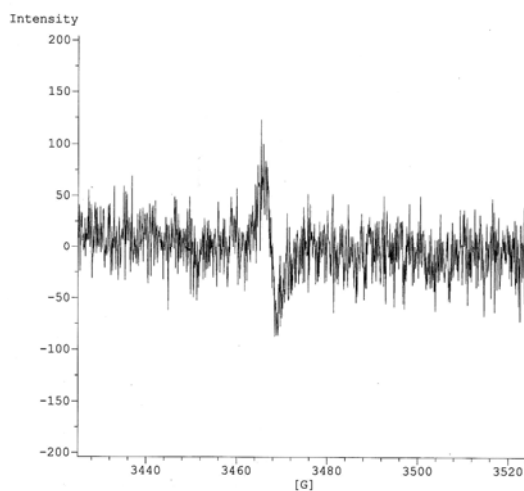


**Figure 6.4:** EPR spectrum of anionic radical obtained from acetone solution of TnBASINAP



### 6.3.3 Controlled Potential Electrolysis

The controlled potential electrolysis was carried out in an attempt to study the structure of the intermediate formed in the redox process. The resulted solution monitored for the product formed using UV-Vis spectrometry. The absorption at 500 nm that was observed for chemically oxidized product was absent. So no structural detail on the intermediate that formed during first step oxidation process for the tris(2,3-dihydroxynaphthalato)silicate could be obtained.

### 6.3.4 Nature of Redox Process

The Plot of Current Vs Voltage at different scan rates is given in the Figure 6.5. It was observed that as the scan rate increases the current of three anodic peaks increases. This observation can be correlated based on the Randles-Sevick equation in which the Peak current ( $I_p$ ) is directly proportional to the square root of the scan rate( $v^{1/2}$ ) that is clear from the plot of peak anodic current Vs square root of the scan rate, which shows a linear relationship as given in the Figure 6.6.

It was observed that the oxidation process was diffusion controlled based on analysis employing Randles-Sevick equation. The equation is given below

***Randles-Sevick equation:***

$$I_p = 0.4463 nFA (nF/RT)^{1/2} D^{1/2} v^{1/2} C_{\text{analyte}}$$

$I_p$  = Peak current;  $C_{\text{analyte}}$  = bulk conc.;  $A$  = electrode area;  $n$  = number of electrons;  $D$  = diffusion coefficient;  $v$  = scan rate. Peak current has to be directly proportional to the square root of scan rate.

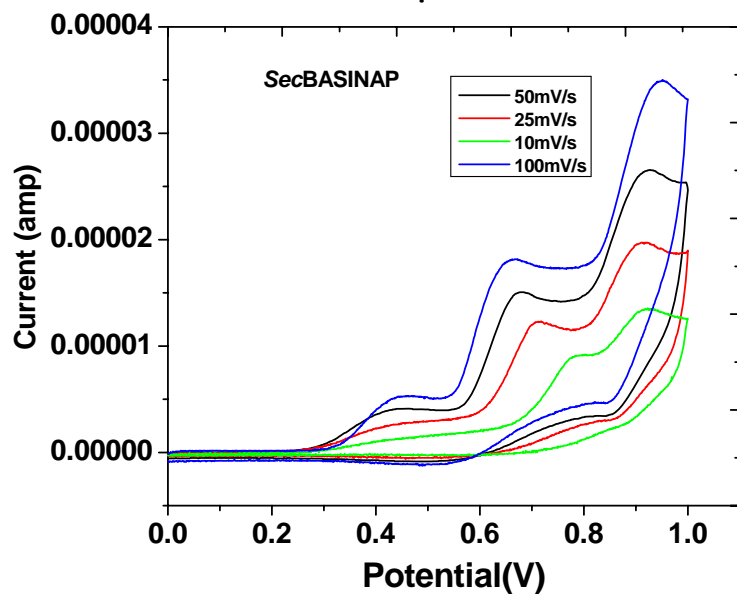


**Figure 6.5:** Cyclic voltammogram of bis(*sec*-butylammonium)tris(2,3-dihydroxy naphthalato)silicates at different scan rates

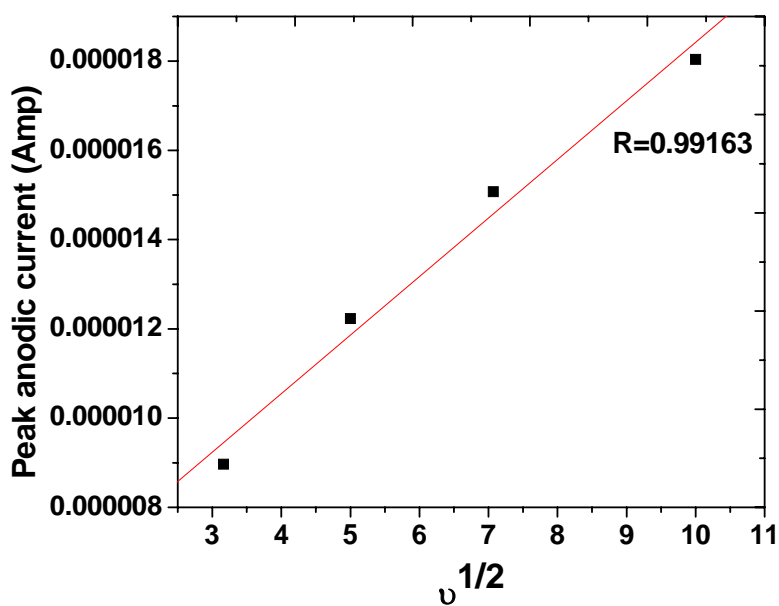


**Figure 6.6:** Plot of scan rates  $v$  vs anodic peak current to represent the Randles-Sevick relation

### 6.3.5 Stability of Silicate Under Electrochemical Condition

Cyclic voltammetric study of the tris(2,3-dihydroxynaphthalato)silicate with tri-*n*-butylammonium ion and *t*-butylammonium ion was carried out in repetitive cycles to understand the stability of these silicates under electrochemical conditions. It is observed that the current drops for the second cycle and after that the change in current is insignificant irrespective of the counter cations. A representative voltammogram is given in **Figure 6.7**.

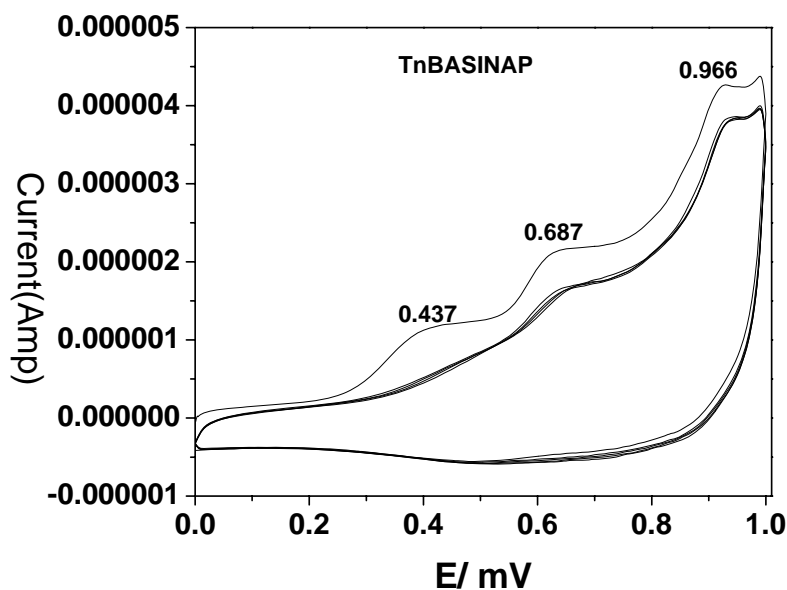


**Figure 6.7:** Multiple cycle voltammogram of tri-*n*-butylammonium containing tris(2,3-dihydroxynaphthalato)silicate recorded at sweep rate of 50 mV/s

### 6.4 CONCLUSION

- ✓ Cyclic voltammetric studies of the silicon complexes with different counter cations have been carried out.
- ✓ Tris(2,3-dihydroxynaphthalato)silicate gave three anodic peaks.

- ✓ The redox process is diffusion controlled that is derived from Randles servick equation.
- ✓ It is evident from the study that counter cation has an effect on the redox behaviour of the 2,3-dihydroxynaphthalene in tris(2,3-dihydroxynaphthalato)silicate.
- ✓ Due to instability of the intermediate formed under electrochemical condition, no structural information could be arrived.
- ✓ The stability of tris(2,3-dihydroxynaphthalato)silicate under electrochemical conditions is not affected by counter cations.

**CHAPTER VII**  
**SYNTHESIS AND THERMAL STUDIES ON TRIS(2, 3-**  
**DIHYDROXYNAPHTHALATO)SILICATE WITH TRANSITION**  
**METAL COMPLEXES AS COUNTER IONS**

---

---

## 7.1 INTRODUCTION

Amorphous silica finds application as support for the catalytic materials. For example, Yoshida *et al* reported that  $V_2O_5$  was photocatalytically active only when supported on silica (1981). Moreover he also observed that supported silica was catalytically inactive but promotes thermal-, photo- and photo oxidation reactions. Hence silica-metal oxide composites have applications in various fields including that of magnetic, optics, electronics as well as catalysis (Scott *et al*, 1994). Incipient wetness impregnation method has been used to prepare silica supported manganese oxide. Silica supported manganese oxide was used as catalyst in oxidation of acetone (Reed *et al*, 2005). Silica supported metal oxides have also been used in methanol oxidation (Jih-Mim *et al*, 1996).  $CrO_3/SiO_2$  was used as a catalyst in ethylene polymerization (Hogan *et al*, 1981).

Pyrolysis is a single step method to synthesize structured silica (Jang *et al*, 2006). Ethylenediamine complexes of transition metal derivatives of tris(catecholato)silicates on pyrolysis leads to transition metal orthosilicate/metaloxide-silica mixture with good catalytic activity. Bis(ammonium)tris(catecholato)silicates reacts with transition metal complexes to yield ion exchanged transition containing tris(catecholato)silicates (Bindu *et al*, 2004 ; Sackerer *et al*, 1977). Like catechol, 2, 3-dihydroxynaphthalene was also used as a template for preparation of structured tubular silicates (Isayama *et al*, 2005). Guo *et al* synthesized ZnO nanomaterial by pyrolysis of zinc ethylenediamine complexes in presence of air at lower temperature (2006).

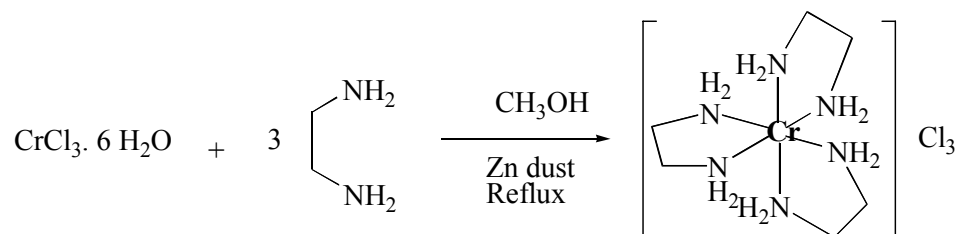
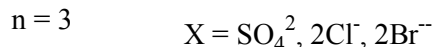
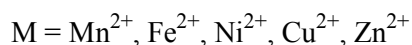
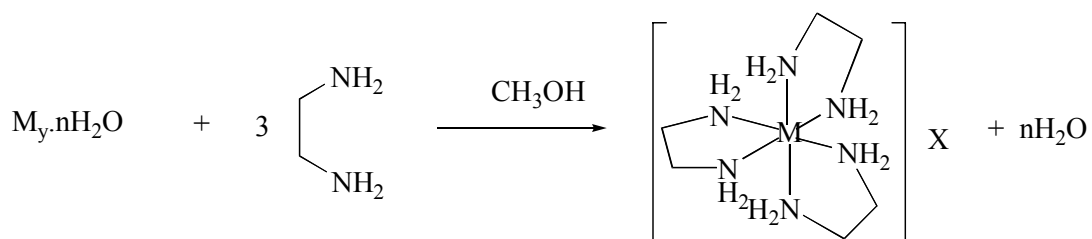
In this chapter, synthesis and characterization of ethylenediamine metal derivatives of tris(2,3-dihydroxynaphthalato)silicates was achieved by using bis(ammonium)tris(2,3-

dihydroxynaphthalato)silicate as precursors. The attempt has been made to synthesize metal silicates/metal oxide-silica under milder condition using ethylenediamine complexes of transition metal derivatives of tris(2,3-dihydroxynaphthalato)silicate by pyrolysis method.

## 7.2 EXPERIMENTAL SECTION

### 7.2.1 Synthesis of Ethylenediamine Complexes of 3d-Transition Metals

The synthesis procedure reported in Vogel *et al*, 1975 was adopted in this work for the synthesis of ethylenediamine complexes of 3d-transition metals (**Scheme 7.1**). The procedure is given in chapter 2. The experimental details are given in **Table 7.1**.



**Scheme 7.1:** Synthesis of ethylenediamine complexes of 3d-transition metal

**Table 7.1:** Experimental details for the precursor - ethylenediamine complexes of 3d-transition metals

Metal salts (g, mmol.)	Ethylenediamine (g, mmol.)	Yield (%)	Ref.
CrCl <sub>3</sub> .6H <sub>2</sub> O (1, 4.30)	0.78, 12.8	95	Whuler <i>et.al</i> , 1975
MnCl <sub>2</sub> .6H <sub>2</sub> O (1, 4.27)	0.69, 11.6	85	Vogel, 1975
FeSO <sub>4</sub> .7H <sub>2</sub> O (1, 3.85)	0.70, 11.5	92	Vogel, 1975
CoCl <sub>2</sub> .6H <sub>2</sub> O (1, 4.20)	0.75, 12.6	95	Whuler <i>et al</i> , 1975
NiCl <sub>2</sub> .6H <sub>2</sub> O (1, 4.20)	0.75,12.6	98	Vogel, 1975
CuCl <sub>2</sub> .2H <sub>2</sub> O (1, 5.87)	1.0, 17.5	95	Fijta <i>et al</i> , 1983
ZnBr <sub>2</sub> (1,4.47)	0.81, 13.4	97	Vogel, 1975

### 7.2.2 Synthesis of Tris(ethylenediamine)nickle(II) tris(2,3-dihydroxynaphthalato)silicate from Bis(diisopropylammonium)tris(2,3-dihydroxynaphthalato)silicate (Compound XVIII)

To a stirred solution of bis(diisopropylammonium)tris(2,3-dihydroxynaphthalato)silicate (1 g; 1.416 mmol) in acetonitrile (15 mL), a slurry of [Ni(en)<sub>3</sub>]Cl<sub>2</sub> (0.43 g; 1.416 mmol) in methanol (10 mL) was added at room temperature. A pale purple precipitate was formed during addition. After 30 min, the mixture was filtered, washed successively with methanol (3x5 mL), ether (3x5 mL) and acetonitrile (2x5 mL) successively and was dried in vacuum. The percentage yield of compound XVIII was 81 %.



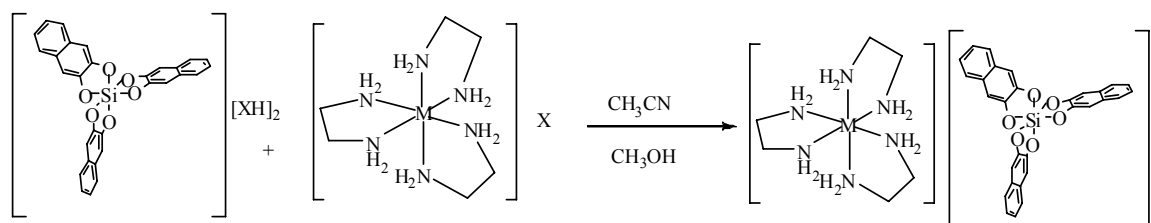
The colorless filtrate was concentrated and cooled at 273 K for 2 days to isolate a water soluble white solid (0.79g, 6.4mmol). The solid melted above 523K and was identified as  $(C_3H_7)_2NH_2Cl^-$  based on spectral characteristics. IR( $cm^{-1}$ ): 600(vs,br), 2480(vs,sh), 1480(vs,br), 1440(vs,br), 1390(vs,sh), 1380(vs,sh), 1320(m,sh), 1170(vs,sh), 1080(s,sh), 1030(vs,sh), 840(m, sh), 800(s, sh), 780(w) and 720(w).

Analogous reactions of other transition metal complexes viz.,  $[Cr(en)_3]Cl_3$ ,  $[Mn(en)_3]Cl_2$ ,  $[Fe(en)_3]SO_4$ ,  $[Co(en)_3]Cl_3$ ,  $[Cu(en)_3]Cl_2$ ,  $[Zn(en)_3]Br_2$  with TnBASINAP were carried out in  $CH_3CN/CH_3OH$  medium at room temperature in 1:1 mole ratio as shown in the **Scheme 7.2** to obtain the corresponding salts, namely,  $[Cr(en)_3]Cl.[Si(C_{10}H_6O_2)_3]$ ,  $[Fe(en)_3][Si(C_{10}H_6O_2)_3]$ ,  $[Co(en)_3]Cl.[Si(C_{10}H_6O_2)_3]$ ,  $[Cu(en)_3][Si(C_{10}H_6O_2)_3]$ ,  $[Zn(en)_3][Si(C_{10}H_6O_2)_3]$ . The designations of these complexes along with the precursors employed and the yields obtained are given in the **Table 7.2**.

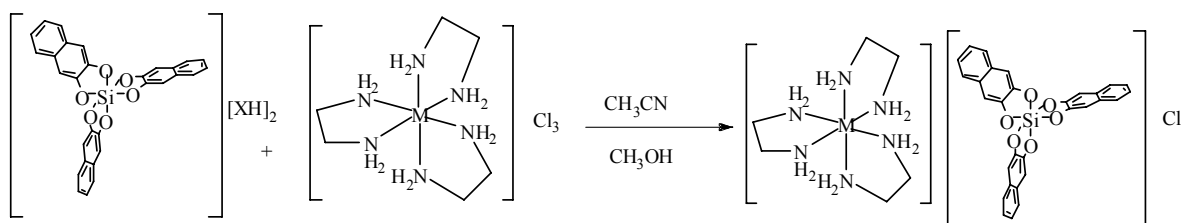
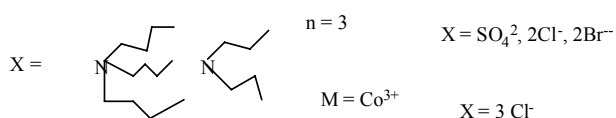
**Table 7.2:** Synthesis detail transition metal containing silicates

Compd No.	Compound name	Compound Formula*	Precursor (g)	Colour	% Yield
XIV	CrSINAP	$[Cr(en)_3]Cl.[Si(C_{10}H_6O_2)_3]$	$[Cr(en)_3]Cl_3(0.48g)$	Pale yellow	42
XV	MnSINAP	$[Mn(en)_3][Si(C_{10}H_6O_2)_3]$	$[Mn(en)_3]Cl_2(0.43g)$	Dull white	81
XVI	FeSINAP	$[Fe(en)_3][Si(C_{10}H_6O_2)_3]^{\#}$	$[Fe(en)_3]SO_4(0.38g)$	pale purple	94
XVII	CoSINAP	$[Co(en)_3]Cl.[Si(C_{10}H_6O_2)_3]$	$[Co(en)_3]Cl_3(0.49g)$	Pale yellow	78
XVIII	NiSINAP	$[Ni(en)_3][Si(C_{10}H_6O_2)_3]^{\#}$	$[Ni(en)_3]Cl_2(0.35g)$	Pale purple	81
XIX	CuSINAP	$[Cu(en)_3][Si(C_{10}H_6O_2)_3]$	$[Cu(en)_3]Cl_2(0.44g)$	Pale purple	67
XX	ZnSINAP	$[Zn(en)_3][Si(C_{10}H_6O_2)_3]$	$[Zn(en)_3]Cl_2(0.57g)$	Dull white	89

\* - (1g, 1.416mmol) of DIPASINAP except XVI and XVIII; # - (1g, 1.144mmol) of TnBASINAP



M = Mn<sup>2+</sup>, Fe<sup>2+</sup>, Ni<sup>2+</sup>, Cu<sup>2+</sup>, Zn<sup>2+</sup>



**Scheme 7.2:** Synthesis of transition metal containing tris(2,3-dihydroxynaphthalato)silicates

The transition metal containing silicates obtained were characterized using IR, MALDI-MS, UV-Vis, elemental analysis and ICP analysis that confirm the composition of the metal containing tris(2,3-dihydroxynaphthalato)silicates. EPR and magnetic measurements were carried to study the effect of bulky silicate counter anion on metal. The spectral and analytical data are given in the **Table 7.3** and **Table 7.4**.

### 7.2.3 Thermal Analysis

Thermogravimetric and Differential thermal analysis were carried out on a NETZSCH thermal analyzer for all the transition metal containing silicates with alumina as external reference under N<sub>2</sub> atmosphere in the temperature range of 198 K – 1073 K at a heating rate of 10 °C/min. A representative TGA plot for [Ni(en)<sub>3</sub>][Si(C<sub>10</sub>H<sub>6</sub>O<sub>2</sub>)<sub>3</sub>] is showed in the **Figure 7.4**.

### 7.2.4 Bulk Pyrolysis

Bulk pyrolysis was carried out in a muffle furnace under static air for all the complexes. A typical method of performing pyrolysis has been described below.

About one gram of compound **XIV-XX** was separately heated in a porcelain crucible to 1073 K for 3 h in muffle furnace under static air atmosphere. After 3 h, the crucible along with residues were brought to room temperature and weighed. The products obtained were characterized using powder XRD (**Table 7.5**). The materials obtained on pyrolysis were examined under scanning electron microscope (SEM). The surface area values of the pyrolysed materials were obtained using Brunauer, Emmett, and Teller method. The pore volume was obtained using Barrett, Joyner and Halenda method. The XRD data obtained for the pyrolyzed products together with surface area and pore volume are given in **Table 7.5**. The data extracted from thermogravimetric analysis for these complexes are given in **Table 7.6**.

## 7.3 RESULTS AND DISCUSSION

### 7.3.1 Synthesis

Synthesis of tris(2,3-dihydroxynaphthalato)silicate with transition metal complexes was achieved by displacement reaction of bis(ammonium)tris(2,3-dihydroxynaphthalato)silicate with ethylenediamine complexes of 3d-transition metals (Cr, Mn, Fe, Co, Ni, Cu and Zn).

The reaction time ranges from 0.5 h to 1 h depending on the nature of the metal complexes used. The products were obtained as dull colored powders, and their yields are in the range of 45-94 %. The products are quite insoluble in any of the common organic solvents and are high melting solids. Interestingly, complexes having both the silicate and chloride ions were isolated when trivalent metal complexes (Cr and Co) were employed for the reaction. Prior to this study, only two reports are available for transition metal containing higher coordination silicates. In 1977 Sackerer *et al* reported the isolation and structural characterization of  $[\text{Cu}(\text{en})_3][\text{Si}(\text{C}_6\text{H}_4\text{O}_2)_3]$ . Subsequently, in 2004, Bindu *et al*, reported on isolation of ethylenediamine complexes of 3d transition metal derivatives with tris(catecholato)silicate anion and their thermal studies.

### 7.3.2 Characterization

#### 7.3.2.1 IR spectral Analysis

IR spectra of all these silicates were similar and provide an unambiguous clue to the presence of tris(2,3-dihydroxynaphthalato)silicate ion by showing all the strong peaks at 1585, 1470, 1260, 1165, 870, 850, 750, 640, 590, and 420  $\text{cm}^{-1}$  of the  $[\text{Si}(\text{C}_{10}\text{H}_6\text{O}_2)_3]^{2-}$  ion, where the peak at around 1260  $\text{cm}^{-1}$  corresponds to Si-O stretch was without much

shift compared to the precursor, refer to **Table 7.3**. A representative IR spectrum is given in **Figure 7.1**.

Miller *et al* have reported that the characteristic IR peaks of the transition metal complexes of ethylenediamine appear in the region of 1000-800  $\text{cm}^{-1}$ . In the case of tris(2,3-dihydroxynaphthalato)silicate derivatives overlap of naphthalene ring's bending and stretching frequencies with the characteristic peaks of make it difficult to distinguish (1981). The expected NH stretching frequencies in the region 3360–3150  $\text{cm}^{-1}$ , reveals the presence of the ligand around transition metal and it matches with those reported for similar metal complex derivatives of tris(catecholato)silicate (Bindu *et al*, 2004).

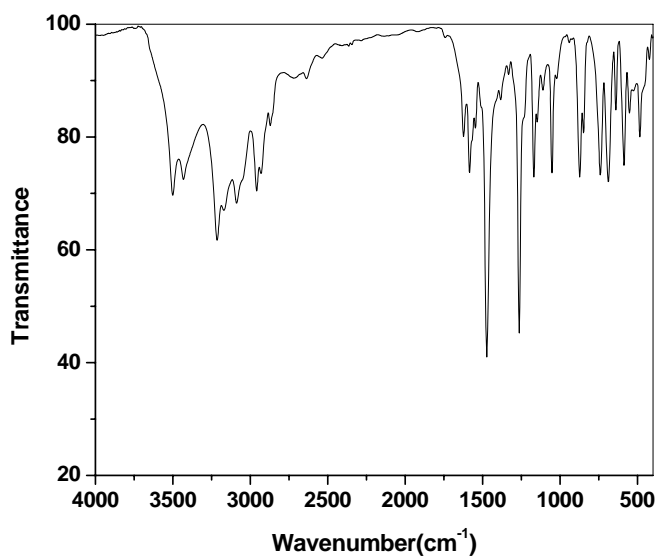


**Figure 7.1:** IR spectrum of  $[\text{Cr}(\text{en})_3][\text{Si}(\text{C}_{10}\text{H}_6\text{O}_2)_3]$

### 7.3.2 2 Optical Spectral Analysis

Electronic spectra of these metal-containing silicates (recorded as Nujol mulls) also provide useful clues in characterization. The d-d transition was observed as broad peak

in the visible region for the corresponding transition metal ion in its octahedral geometry. A representative spectrum is shown in the **Figure 7.2**. A small shift compared to ethylenediamine complexes of this metal precursor was observed in the  $\lambda_{\max}$  and intensity is suggestive of interaction between the oppositely charged ions. The  $\lambda_{\max}$  values of these series lie in the same region as that of transition metal ethylenediamine derivative of tris(catecholato)silicates as reported by Bindu *et al*, 2004. The  $\lambda_{\max}$  values observed for transition metal containing tris(2,3-dihydroxynaphthalato)silicate was given along with literature data of similar tris(catecholato)silicate for comparison in **Table 7.3**.

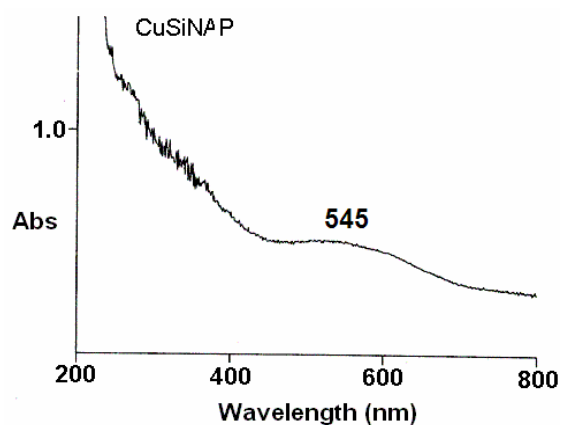


**Figure 7.2:** UV-Vis spectrum of  $[\text{Cu}(\text{en})_3][\text{Si}(\text{C}_{10}\text{H}_6\text{O}_2)_3]$  in nujol mull

**Table 7.3:** IR and UV-Vis spectral data of transition metal containing silicates

Compd. No.	UV-Vis(nm)#	IR( $\text{cm}^{-1}$ )
XIV	457 (470)	3214 (s, br), 3088 (s, br), 2959 (m, sh), 1584 (m, sh), 1473 (m, br), 1264 (m, sh), 1168 (s, sh), 1110 (m, sh), 873 (s, sh), 740 (s, sh), 587 (s, sh), 423 (s, sh)
XV	617 (667)	3331 (s, sh), 3270 (s, sh), 2930 (s, sh), 1585 (m, sh), 1473 (s, sh), 1263 (s, sh), 1167 (m, sh), 1111 (s, sh), 870(s, sh), 755 (s, sh), 585 (s, sh), 485 (s, sh)
XVI	570 (550)	3322 (s, sh), 3254 (s, br), 2934 (s, sh), 1586 (m, sh), 1474 (m, br), 1264 (m, sh), 1167 (s, sh), 1111 (m, sh), 871 (s, sh), 755 (s, sh), 690 (s, sh), 585 (s, sh), 485 (s, sh)
XVII	488 (465)	3330 (s, br), 3274(s, br), 2936 (m, sh), 1585(m, sh), 1475 (m, br), 1264 (m, sh), 1168 (m, sh), 1110 (s, sh), 871 (s, sh), 755 (s, sh), 690 (s, sh), 583(s, sh), 485 (s, sh)
XVIII	550 (525)	3300 (s, br), 3221(s, br), 3021 (m, sh), 1586 (m, sh), 1473 (m, sh), 1263 (m, sh), 1167(s, sh), 1111 (s, sh), 871(s, sh), 756 (s, sh), 690 (s, sh), 588 (s, sh), 485 (s, sh)
XIX	545 (530)	3312 (s, sh), 3219 (s, br), 2924 (s, sh), 1584 (m, sh), 1473 (m, br), 1264 (m, sh), 1166 (m, sh), 1112 (m, sh), 871 (s, sh), 756 (s, sh), 686 (s, sh), 588 (s, sh), 485 (s, sh)
XX	--	3336(s, sh), 3276 (s, br), 2937(s,sh), 1585 (m, sh), 1473 (m, br), 1264 (m, sh), 1167 (m, sh), 1111(m, sh), 870 (s, sh), 755 (s, sh), 688 (s, sh), 585 (s, sh), 486 (s, sh)

#- Values given in bracket are literature values of derivatives of tris(catecholato)silicates

### 7.3.2.3 MALDI Mass Spectral Analysis

MALDI mass spectral analysis was useful to identify the ion pairs from the data obtained by positive and negative mode.

#### 7.3.2.3.1 Negative Mode

The presence of tris(2,3-dihydroxynaphthalato)silicate is revealed from the parent ion peak in negative mode at around  $m/z = 503$  (100%) as in the case of bis(ammonium)tris(2,3-dihydroxynaphthalato)silicate that corresponds to  $[(C_{10}H_6O_2)_3Si]H^-$  and their further fragmentation was also observed. Irrespective of counter ion the tris(2,3-dihydroxynaphthalato)silicate ion is stable species under negative mode of MALDI mass spectral condition. The stable species  $[(C_{10}H_6O_2)_3Si]H^-$  is observed in all the transition metal containing derivatives are given in the **Table 7.3**.

#### 7.3.2.3.2 Positive Mode:

The  $M^+$  peak was observed for the corresponding ethylenediamine metal complexes except in the cases of XV and XVII. The absence of molecular ion peak of cationic part of the silicate derivative (XV and XVII) may be attributed to the less stable nature of these species under MALDI conditions.

The data obtained for all the transition metal containing silicates from mass spectral analysis are given in **Table 7.3**.

#### 7.3.2.4 Elemental Analysis

The compositions of the transition metal containing silicates were confirmed from elemental analysis. The CHN experimental values are match with the calculated values based on the proposed composition. ICP<sup>wet</sup> method was employed to estimate metal content of transition metal complex derivatives of tris(2,3-dihydroxynaphthalato) silicate. From which the weight percentage of metal was calculated based on the proposed



composition matches well with theoretical values. The results of these studies are given in **Table 7.4**.

**Table 7.4:** Analytical data of transition metal containing silicates

Comp No	MALDI-MS		Elemental Analysis (%)			
	Positive	Negative	C	H	N	M
XIV	234	502.9	56.14 (56.32)	5.45 (5.64)	10.91 (10.67)	6.68 (6.75)
XV	61.8	503.3	57.96 (58.62)	5.41 (5.69)	10.98 (11.39)	7.38 (7.45)
XVI	235	503.3	55.86 (55.93)	5.43 (5.62)	10.86 (11.02)	7.28 (7.56)
XVII	61.8	503.5	55.61 (55.36)	5.41 (5.46)	10.81 (10.67)	7.32 (7.58)
XVIII	239	-	58.32 (58.63)	5.63 (5.69)	11.3 (11.54)	8.12 (7.92)
XIX	61.8 184	503.0	57.98 (57.92)	5.67 (5.46)	11.26 (11.34)	8.33 (8.52)
XX	184	503.0	58.14 (57.80)	4.89 (5.62)	11.05 (11.24)	8.48 (8.75)

### 7.3.2.5 EPR Spectral Analysis

X-band polycrystalline EPR spectra of  $[\text{Cu}(\text{en})_3]^{2+}$  was recorded both at 300 and 77 K. A single broad signal without hypersplitting was observed. Hyperfine coupling is not resolved in polycrystalline samples due to higher exchange coupling between copper centers (Procter *et al*, 1968). The  $g_{\text{iso}}$  was 2.085, that was found to be well within the range of the reported value for tris(catecholato)silicate derivatives. Whereas, the  $g_{\text{iso}}$  of powder sample of precursor compound  $[\text{Cu}(\text{en})_3]\text{SO}_4$  was reported by Rajan *et al*, in 1963

to be 2.120. When the temperature was lowered  $[\text{Cu}(\text{en})_3]^{2+}$  of tris(2,3-dihydroxynaphthalato)silicate did not show any appreciable change in the EPR signal pattern. The broad nature of the signal is presumably due to the dipolar broadening caused by the presence of the bulky anionic tris(2,3-dihydroxynaphthalato)silicate moiety. Typical EPR spectrum of  $[\text{Cu}(\text{en})_3][\text{Si}(\text{C}_{10}\text{H}_6\text{O}_2)_3]$  is shown in the **Figure 7.3**.

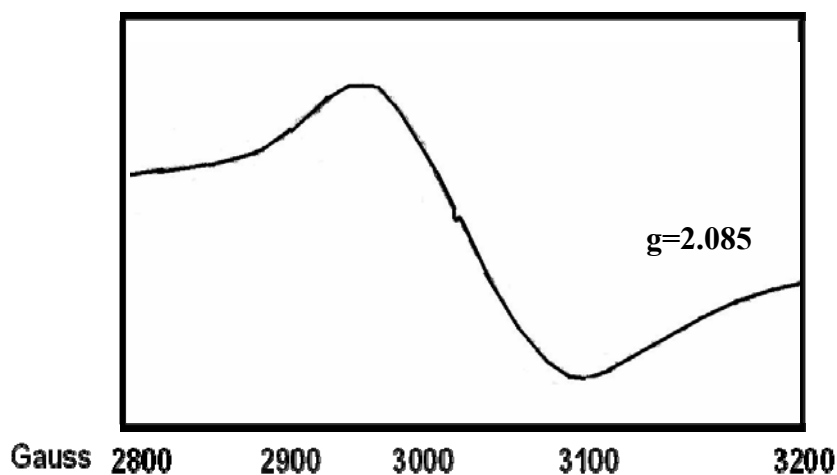


**Figure 7.3:** EPR spectrum of  $[\text{Cu}(\text{en})_3][\text{Si}(\text{C}_{10}\text{H}_6\text{O}_2)_3]$

### 7.3.2.6 Magnetic Susceptibility Analysis

Magnetic susceptibility measurements at 300 K for ethylenediamine complexes of cobalt, manganese and copper derivatives of tris(2,3-dihydroxynaphthalato)silicates were carried out and calculated magnetic moments. In all cases, the values agreed with anticipated value for the corresponding oxidation state and geometry of each of the metal ion was observed (Carlin *et al*, 1977; Sacconi *et al*, 1987; Hathway *et al*, 1987 and Fowles *et al*, 1958). Cobalt exists in +3 oxidation state that is diamagnetic in nature. A comparison of the observed value for  $[\text{Mn}(\text{en})_3]^{2+}$  and  $[\text{Cu}(\text{en})_3]^{2+}$  are 5.08MB and 1.98BM respectively

that are in good agreement with the reported values of corresponding derivatives of tris(catecholato)silicate(Bindu *et al* 2004).

### 7.3.2.7 Thermal Studies

Thermogravimetric (TG) analysis of all these silicates with ethylenediamine transition metal complexes as cations was carried out to understand the influence of the bulky hypervalent silicate anionic moiety on the thermal behaviour of these complexes. The results obtained are given in **Table 7.5**. The thermograms of all these silicates recorded in the temperature range of 300 to 1073 K in air. The offset temperature in decomposition of various complexes indicates thermal stability. A representative TGA plot of  $[\text{Ni}(\text{en})_3]^{2+}$  is as shown in the **Figure 7.4**.

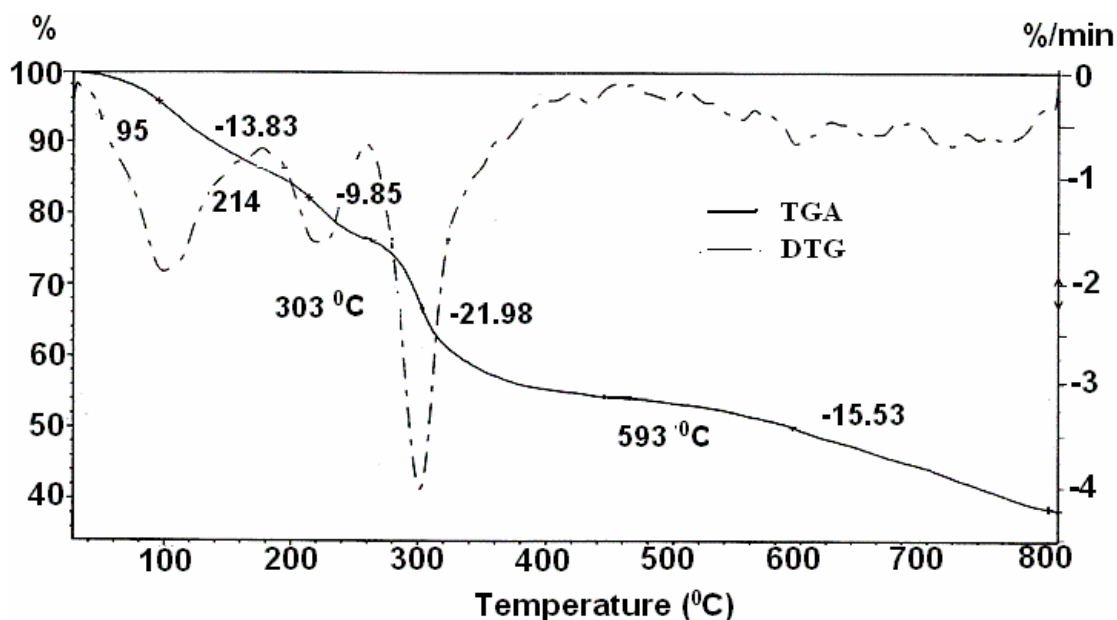


**Figure 7.4 :** TGA plot of  $[\text{Ni}(\text{en})_3][\text{Si}(\text{C}_{10}\text{H}_6\text{O}_2)_3]$

In the case of transition metal derivatives of naphthalatosilicate all the compound's onset temperature is at 50° C. Unlike in the case of tris(catecholato)silicate among the complexes  $\{\text{Ni}(\text{en})_3\}^{2+}$  was the most stable and  $[\text{Mn}(\text{en})_3]^{2+}$  is found to be least stable. A

noteworthy feature was that the ligand en coordinated to Ni(II) in Ni(en)<sub>3</sub> does not get expelled even at high temperature and its onset decomposition temperature was found to be well above 473K for tris(catecholato)silicate. No such interesting observation is seen in naphthalatosilicate. The TGA plots revealed that these complexes do not form spiro-silane. Further, DTA plots reveal the exothermic nature of these processes.

TGA-DTA studies of these complexes revealed that they undergo decomposition with complete loss of organic moiety at 1073 K leaving residue of metal oxide and silica mixture.

**Table 7.5:** Thermal studies data of transition metal containing silicates

Comp No.	Decomposition I <sup>@</sup>			Decomposition II <sup>*</sup>			Decomposition III <sup>#</sup>		
	Temp range. (°C)	wt.loss (%)	DTA (°C)	Temp range. (°C)	wt.loss (%)	DTA (°C)	Temp range. (°C)	wt.loss (%)	DTA (°C)
XIV	50- 185	16.39 (18.25)	-	185-275	6.9 (6.5)	-	275-800	39.8 (35.9)	-
XV	50- 125	5.75 (4.75)	106	125-400	23.4 (25.6)	596	400-789	23.1 (23.4)	666
XVI	50- 175	5.63 (6.75)	106	175-475	38.7 (37.5)	310	475 -790	17.6 (16.9)	-
XVII	50- 150	10.58 (11.59)	130	150-270	9.1 (8.89)	233	270-780	41.1 (40.3)	-
XVIII	50- 280	10.37 (12.58)	146	280-420	12.6 (11.8)	349	420-700	36.9 (37.4)	840
XIX	50- 275	3.48 (2.84)	-	275-450	49.3 (47.5)	336	400-700	14.9 (12.9)	-
XX	50- 275	12.96 (13.41)	136	275-400	24.3 (26.1)	359	400-700	34.6 (33.5)	590

@- elimination ethylenediamine/solvent

\* - loss of ethylenediamine/ethylenediammoniumnaphthalate

# - loss of 2, 3-dihydroxynaphthalene

### 7.3.2.8 Bulk Pyrolytic Studies

Silica supported metal oxide was obtained by two stage i) silica material by sol-gel and followed by ii) impregnation method. Precursor for silica used was tetraethoxysilane and ammonium salt of metal oxides (Tanaka *et al*, 2005)

Pyrolysis of these metal-containing silicates was carried out in muffle furnace in presence of air at 1073 K. The residue obtained in all the cases is a mixture of silica and metal oxides. They were characterized using powder XRD. The silica residue obtained during the pyrolysis was amorphous, as revealed by a broad peak around  $2\theta = 25$ . The XRD peaks observed agree with the reported peaks for the metal oxides (**Table 7.6**).

### 7.3.2.9 Surface Area Measurement of pyrolysed product

Surface area measurement and pore size distribution studies were carried out. The silica-metal oxide materials are mesoporous in nature since the pore size analysed by BJH method are in the range of 2 to 50 nm. These pore size and surface area data are given in **Table 7.6**. Bis(ammonium)tris(2,3-dihydroxynaphthalato)silicates were used as precursor in the earlier part of this work. The surface area observed was in the range 200-400 m<sup>2</sup>/g that is higher than the one obtained on including the metal oxide in mesoporous silica material. This may be due to the metal oxides occupies the pore volume of mesoporous silica material that leads to decrease of surface area compared to pure silica obtained from similar precursor. Zhao *et al* reported such observation in similar silica metal oxide material (2004).

**Table 7. 6:** Surface area, powder XRD and Pore volume of residue of pyrolytic product

Compd	Surface Area(m <sup>2</sup> /g)	Specific pore volume(cm <sup>3</sup> /g)	d <sub>hkl</sub> (Å)#	
			Observed	lit for MO
Cr <sub>2</sub> O <sub>3</sub> +SiO <sub>2</sub>	94	0.18	2.664, 2.476, 3.629	2.668, 2.476, 3.628
MnO+SiO <sub>2</sub>	9.8	0.02	2.561, 2.309, 2.298,	2.565, 2.319, 2.161
Fe <sub>2</sub> O <sub>3</sub> +SiO <sub>2</sub>	3.7	0.7	3.685, 2.705, 2.520	3.684, 2.704, 2.523
Co <sub>2</sub> O <sub>3</sub> +SiO <sub>2</sub>	205	0.36	2.870, 2.300, 1.780	2.868, 2.302, 1.780
CuO+SiO <sub>2</sub>	200	0.47	2.450, 2.122, 1.500	2.454, 2.128, 1.505
NiO+SiO <sub>2</sub>	113	0.19	2.411, 2.088	2.414, 2.100
ZnO+SiO <sub>2</sub>	55	0.28-	2.478, 2.607, 2.817	2.479, 2.608, 2.820

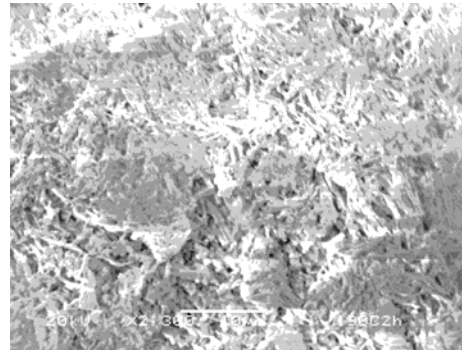
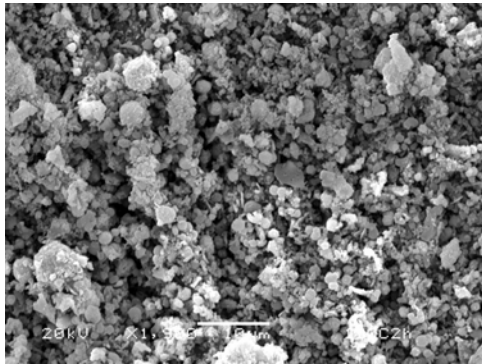
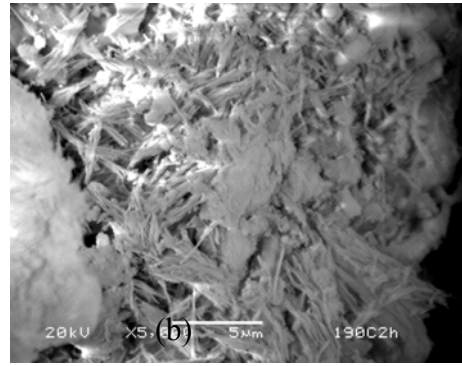
#-Silica is amorphous and 100, 80 and 60% peaks alone considered

### 7.3.2.10 Electron Micrographs of Silica-Metal Oxides

All the metal containing silicates were pyrolysed under the identical conditions, but interestingly they ended up in a unique morphology for each of the metal derivatives except in two of the cases Co and Ni. The morphologies as seen by the electron microscopic analysis are shown in **Figure 7.5**. In this experiment, the interesting observation is that though the composition of these metal complexes was almost the same except for the variation of the metal ion there is unique morphology for each of them. It is that the template of the complexes affects the morphology (Isayama *et al*, 2005).

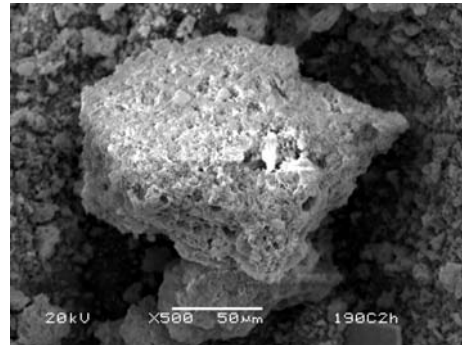
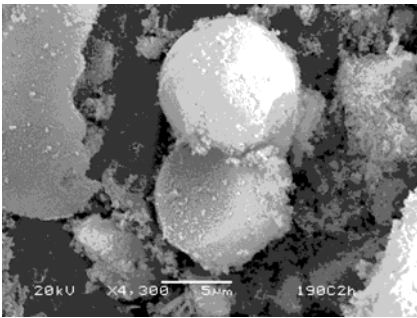
In the case of [Cr(en)<sub>3</sub>]<sup>2+</sup> containing silicate as precursor on pyrolysis yielded Cr<sub>2</sub>O<sub>3</sub>-SiO<sub>2</sub> mixture which was confirmed by XRD data. The SEM micrograph for the residue is shown in **Figure 7.5 (e)**. It is seen that metal oxide particle with silica coating are

spherical in shape with particle size 10-15  $\mu\text{m}$ . In the case of  $[\text{Mn}(\text{en})_3]^{2+}$  containing silicate as precursor on pyrolysis yielded  $\text{MnO-SiO}_2$  composition was confirmed using XRD data. The SEM micrograph of the residual mixture showed that the particles are irregular in shape with silica coating. The particle size is in the range 2-5  $\mu\text{m}$  (**Figure 7.5(g)**). In the case of  $[\text{Fe}(\text{en})_3]^{2+}$  containing silicate  $\text{Fe}_2\text{O}_3\text{-SiO}_2$  mixture was obtained on Pyrolysis which was confirmed by XRD data. SEM picture of this mixture showed spherical particles with thick coating of  $\text{SiO}_2$  (**Figure 7.5(c)**). The particle size lies in the range 2-5  $\mu\text{m}$ . In the case of  $[\text{Co}(\text{en})_3]^{2+}$  containing silicate as precursor, on pyrolysis yielded  $\text{Co}_2\text{O}_3\text{-SiO}_2$  mixture which was confirmed by XRD data. The SEM picture of this mixture showed fibrous metal oxide with silica coating (**Figure 7.5 (d)**). The particle size is in the range 10-12  $\mu\text{m}$ . In the case of  $[\text{Ni}(\text{en})_3]^{2+}$  containing silicate as precursor, on pyrolysis yielded  $\text{NiO-SiO}_2$  which was confirmed by XRD data. The SEM picture of this mixture showed fibrous particles with silica coating (refer **Figure 7.5 (b)**). The particle size is in the range of 2-5  $\mu\text{m}$ . In the case of  $[\text{Cu}(\text{en})_3]^{2+}$  containing silicate as precursor, on pyrolysis yielded  $\text{CuO-SiO}_2$  which was confirmed by XRD data. The SEM picture of  $\text{CuO-SiO}_2$  mixture showed rod like particles with silica coating (refer **Figure 7.5 (a)**). The particle size is in the range 10-15  $\mu\text{m}$ . In the case of  $[\text{Zn}(\text{en})_3][\text{Si}(\text{C}_{10}\text{H}_6\text{O}_2)_3]$  as precursor, on pyrolysis yielded  $\text{ZnO-SiO}_2$  which was confirmed by XRD data. The SEM picture is shown in **Figure 7.5(f)**. It is seen that the particles are fibrous in nature with silica coating. The particle size is in the range 2-5  $\mu\text{m}$ .



(c)

(d)



(e)

(f)

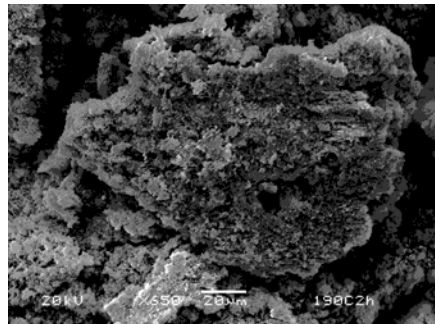


**Figure 7.5 :** SEM micrograph of (a)  $\text{CuO}+\text{SiO}_2$  (b)  $\text{NiO}+\text{SiO}_2$  (c)  $\text{Fe}_2\text{O}_3$  (d)  $\text{Co}_2\text{O}_3+\text{SiO}_2$  (e)  $\text{Cr}_2\text{O}_3+\text{SiO}_2$  (f)  $\text{ZnO}+\text{SiO}_2$  and (g)  $\text{MnO}+\text{SiO}_2$



## 7.4 CONCLUSIONS

- ✓ In this study, transition metal containing silicates were synthesised and characterized by MALDI-MS and EPR.
- ✓ The thermal stability of tris(2,3-dihydroxynaphthalato)silicate were found not depend on the counter metal ion.
- ✓ Residue obtained during the thermal studies was metal oxide-silica mixture. The obtained silica supported metal oxide were characterized by XRD, SEM, TEM.
- ✓ Surface area values of metal oxide-silica material are found to be lesser compare to pure silica obtained from similar silicate due to blocking of metal oxides in mesoporous silica.
- ✓ The morphology of the materials are found to have different shapes, such as rod, spherical, fibres for different silicate-metal complexes.

## **SUMMARY AND CONCLUSIONS**

---

In the introductory chapter the significance of silicon, silicates and their availability in nature are discussed in detail. The existence of higher coordinate silicates and their possible role in the biosilicification have been elaborated. A brief summary and important finding on the various classes of higher coordinate silicates with synthetic methods adopted, structural findings and stability are presented. Microwave methods for the synthesis of such higher coordinate silicates reported to date are discussed. The studies on the decomposition of silicon complexes, electrochemical studies of dihydroxyaryl compound and higher coordinate silicates as precursor for metal oxide-silica synthesis described in the previous reports are discussed in detail.

In contrast to catechol based ligands, 2,3-dihydroxynaphthalene, a similar ortho - diol but of a fused aromatic system has been used for obtaining pentacoordinated derivatives of silicon with the exception of a scanty report on a hexacoordinate species. Interestingly, such higher coordinated silicate systems of 2,3-dihydroxynaphthalene have potential application in the field of reprography but synthesis of such useful materials and their properties were not studied in detail so far. In this thesis work, an effective synthetic route has been formulated for tris(2,3-dihydroxynaphthalato)silicate with different ammonium counter cations. The effect of counter ion on thermal, electrochemical and hydrolytic stability of tris(2,3-dihydroxynaphthalato)silicate was studied. Bis(ammonium)tris(2,3-dihydroxynaphthalato)silicate was used as precursor to synthesise ethylenediamine complexes of Cr, Mn, Fe, Co, Ni, Cu and Zn containing tris(2,3-dihydroxynaphthalato)silicate by ion-exchange reaction. These silicates have

been utilized for the synthesis of catalytic materials such as meso-porous silica and metal silicates.

The experimental conditions used for the characterization of silicates have been discussed. Orthosilicic acid concentrations measured using modified molybdenum blue colorimetric method has been considered in Chapter 2 where other details of experimental methodology are outlined.

Chapter 3 deals with synthesis of hexacoordinate silicon complexes with 2,3-dihydroxynaphthalene as ligand using tetraethoxysilane has been demonstrated. Silicates with various ammonium counter ions have been synthesized, in three different (room temperature, microwave and conventional heating) conditions. Microwave assisted synthesis was found to be an effective route to achieve bis(ammonium)tris(2,3-dihydroxynaphthalato)silicates in shorter reaction time. Microwave technique has been used to achieve bis(ammonium)tris(2,3-dihydroxynaphthalato)silicates in a green process, without using solvent.

Bis(ammonium)tris(2,3-dihydroxynaphthalato)silicates with diisobutylammonium and tri-*n*-butylammonium counter cations have been structurally studied. In the case of bis(ammonium)tris(2,3-dihydroxynaphthalato)silicates, silicon was in distorted octahedral geometry irrespective of counter cation. Presence of solvent moiety in the crystal lattice depends on the bulkiness of the solvent moiety. There is no  $\pi$ - $\pi$  stacking between two silicate units with the aromatic ring of ligand. It has been observed that counter cations and silicate anion are linked through hydrogen bonding with two different naphthalate moiety of tris(2,3-dihydroxynaphthalato)silicate. There is no extended network through

hydrogen bonding between counter cations mediated by solvent moiety to silicate units unlike in other hexacoordinate silicates that are available in literature.

The thermal study of tris(2,3-dihydroxynaphthalato)silicates shows that stability increases when counter ion is varied from primary to tertiary ammonium ions. Thermal decomposition pattern was found to vary with the change in silicon environment from catechol to 2,3-dihydroxynaphthalene. Stability of silicates increases as ammonium ion varies from primary to tertiary ions under hydrolytic condition. The tris(2,3-dihydroxynaphthalato)silicates hydrolysed to yield the corresponding ligand, alkyl ammonium hydroxide and silicic acid. Monosilicic acid undergoes oligomerization in presence of amine and depolymerize under molybdate blue test. The depolymerization rate increases as one goes from tertiary to primary ammonium ions of tris(2,3-dihydroxynaphthalato)silicate. Silica particles obtained under pyrolytic and hydrolytic conditions are mesoporous materials. The particle size of silica obtained by pyrolytic route is around 2-8 nm unlike the one obtained from hydrolytic route (6-14 nm). Thus silica material obtained in pyrolytic conditions has higher surface area compared to the one obtained under hydrolytic condition.

Cyclic voltammetric studies of the silicon complexes with different counter cations have been carried out. Tris(2,3-dihydroxynaphthalato)silicate gave three anodic peak potentials. It was evident from the study that counter cation has an effect on the redox behaviour of the 2,3-dihydroxynaphthalene in silicon complexes. Due to instability of the intermediate formed no structural correlation could be arrived. The stability of tris(2,3-dihydroxynaphthalato)silicates under electrochemical conditions was not affected by counter cations.

In this study, ethylenediamine complexes of transition metal (Cr, Mn, Fe, Co, Ni, Cu, and Zn) containing silicates were synthesised and characterized using MALDI-MS, UV-Vis spectral techniques and CHN analysis. The bulkier silicate anion has effect on spectral property of ethylenediamine complexes of 3d transition metal ions. The thermal stability of tris(2,3-dihydroxynaphthalato)silicate was found to depend on the nature of counter ion. Residue obtained during the thermal studies was a mixture of metal oxide and silica. The obtained silica - metal oxide materials were characterized by powder XRD. Surface area values are found to be lesser compared to pure silica obtained from bis(ammonium)tris(2,3-dihydroxynaphthalato)silicates. This may be due to blocking of the pores by metal oxides in mesoporous silica. The morphology of the materials is found to be different such as rods, spheres and fibres for different silica-metal oxides.

## REFERENCES

---

- 1 **Angel, D.** and **A. Moreno** (2005) Microwaves in organic synthesis. Thermal and non-thermal microwave effects. *Chem. Soc. Rev.*, **34**, 164 – 178.
- 2 **Antonio, C.** and **R. T. Deam** (2005) Comparison of linear and non-linear sweep rate regimes in variable frequency microwave technique for uniform heating in materials processing. *J. Mat. Proc. Tech.*, **169**, 234 – 241.
- 3 **Arsenova, N. H., H. Bludau, R. Schumacher, W. O. Haag, H. G. Karge, E. Brunner** and **U. Wild** (2000) Catalytic and sorption studies related to the para selectivity in the ethylbenzene disproportionation over H-ZSM-5 catalysts. *J. Catal.*, **191**, 326 – 331.
- 4 **Atkins, P. W., D. E. Shriver** and **C. H. Longford** (1990) Inorganic chemistry. Ed. W.H. Freeman, New York, pp38.
- 5 **Avdeef, A., S. R. Sofen, T. L. Bregante** and **K. N. Raymond** (1978) Coordination chemistry of microbial iron transport compounds. 9. Stability constants for catechol models of enterobactin. *J. Am. Chem. Soc.*, **100**, 5362 – 5370.
- 6 **Bailey, S. W.** (1984) Classification and structure of the micas, in *Micas (Reviews in Mineralogy 13*, Ed. S. W. Bailey (Mineralogical Society of America) 1 – 12.
- 7 **Balkus, K. J., S. Gabruekiva** and **S. G. Bott** (1995) Tris(Oxalato) complexes of silicon as precursors to porous silicate materials: Synthesis and structure. *Inorg Chem.*, **34**, 5776 – 5780.
- 8 **Barnum, D. W., J. M. Kelley** and **B. Poocharoen** (1973) Magnesium and guanidinium salts of a silicon-catechol coordination complex. *Inorg. Chem.*, **12**, 497 – 498.
- 9 **Barrett, E. P., L. G. Joyner** and **P. H. Halenda** (1951) The determination of pore volume and area distributions in porous substances. I. Computations from nitrogen isotherms. *J. Am. Chem. Soc.*, **73**, 373 – 380.
- 10 **Bassindale, A. R., M. S. Borbaruah, J. D. Glynn, J. Parker** and **P. G. Taylor** (1999) Modelling nucleophilic substitution at silicon in solution, using hypervalent silicon compounds based on 2-pyridones. *J. Chem. Soc. Per. Trans.*, **2**, 2099 – 2109.
- 11 **Bassindale, A. R., M. S. Borbaruah, J. D. Glynn, J. Parker** and **P. G. Taylor** (2000) Modelling nucleophilic substitution at silicon using hypervalent silicon compounds based on di and tri halosilanes. *J. Org. Chem.*, **606**, 125 – 131.



- 12 **Bassindale, A. R. and T. Sout** (1984) The preparation and observation by  $^{29}\text{Si}$ -NMR spectroscopy of simple, acyclic, five-coordinate silicon salts. *J. Chem. Soc. Chem. Commun.*, 1387 – 1389.
- 13 **Biller, A., C. Burschka, M. Penka and R. Tacke** (2002) Dianionic complexes with hexacoordinate silicon (IV) or germanium (IV) and three bidentate ligands of the hydroximato(2-) type: Syntheses and structural characterization in the solid state. *Inorg. Chem.*, **41**, 3901 – 3908.
- 14 **Bindu, P., J. V. Kingston and M. N. Sudheendra Rao** (2004) Dianionic silicate derivatives of transition metals: synthesis by a facile ion exchange route, characterisation and thermolysis. *Polyhedron*, **23**, 679 – 686.
- 15 **Bindu, P., B. Varghese and M. N. Sudheendra Rao** (2003) Six-coordinate Tris(catecholato)silicates of primary amine residues: Synthesis, characterization, and thermolysis studies. X-ray structures of  $[n\text{-C}_3\text{H}_7\text{NH}_3]_2[\text{Si}(\text{C}_6\text{H}_4\text{O}_2)_3] \cdot 1/2(\text{C}_6\text{H}_{14}\text{N}_2)$  and of a bulky secondary ammonium ion,  $[(i\text{-C}_4\text{H}_9)_2\text{NH}_2]_2[\text{Si}(\text{C}_6\text{H}_4\text{O}_2)_3] \cdot \text{H}_2\text{O}$ . *Phosphorus Sulfur Silicon Relat. Elem.*, **178**, 2373 – 2386.
- 16 **Bodini, M. E. and V. Arancibia** (1997) Redox chemistry of 1,2-dihydroxynaphthalene, 1,2-naphthoquinone and 1,2-naphthoquinone and their complexes with manganese(II) and manganese(III). *Transit. Met. Chem.*, **22**, 150 – 155.
- 17 **Bock, H.** (1989) Fundamentals of silicon chemistry: Molecular states of silicon containing compounds. *Angew. Chem. Int. Ed. Engl.*, **28**, 1627 – 1650.
- 18 **Boer, F. P. and F. P. Remoortere** (1970) Structural studies of pentacoordinate silicon VI. Cyclobis(benzamidodimethylsilane). *J. Am. Chem. Soc.*, **92**, 801 – 807.
- 19 **Bolton, J. L., M. A. Trush, T. M. Penning, G. Dryhurst and T. J. Monks** (2000) Role of quinones in toxicology, a review. *Chem. Res. Toxicol.*, **13**, 135 – 160.
- 20 **Bordwell, F. G.** (1988) Equilibrium acidities in dimethyl sulfoxide solution. *Acc. Chem. Rev.*, **21**, 456 – 463.
- 21 **Borgias, B. A., R. S. Cooper, Y. B. Koh and K. N. Raymond** (1984) Synthetic, structural, and physical studies of titanium complexes of catechol and 3,5-di-tert-butylcatechol. *Inorg. Chem.*, **23**, 1009 – 1016.
- 22 **Boudin, G., Cerveau, C. Chuit, R. J. P. Corriu and C. Reye** (1986) Reactivity of anionic pentacoordinated silicon complexes towards nucleophiles. *Angew. Chem. Int. Ed. Engl.*, **25**, 473 – 474.

- 23 **Brinker C. J. and G. W. Scherer** (1990) Sol-gel Science: The Physics and Chemistry of Sol-gel Processing Academic Press, Boston.
- 24 **Brook, M. A.** (2000a) Silicon in organic, organometallic, and polymer chemistry. John Wiley& Sons, Inc. 379 – 442.
- 25 **Brook, M. A.** (2000b) Silicon in organic, organometallic, and polymer chemistry. John Wiley& Sons, Inc. 256 – 298.
- 26 **Bishop G. R. and V. L. Davidson** (1997) Catalytic role of monovalent cations in the mechanism of proton transfer which gates an interprotein electron transfer reaction. *Biochemistry*, **36**, 13586 – 13592.
- 27 **Brunauer, S. P., H. Emmett and E. Teller** (1938) Adsorption of gases in multimolecular layers. *J. Am. Chem. Soc.*, **60**, 309 – 319.
- 28 **Bugg, T. D. H. and C. J. Winfield** (1998) Enzymic cleavage of aromatic rings: mechanistic aspects of the catechol dioxygenases and later enzymes of bacterial oxidative cleavage pathways. *Nat. Prod. Rep.*, **15**, 513 – 530.
- 29 **Carlin R. L. and A. J. van Duynveldt** (1977) Magnetic properties of transition metal compounds, Springer, New York.
- 30 **Carr, F., G. Cerveau, C. Chuit, R. J. P. Corriu and C. Reye** (1992) Comparative study of the reactivity of different hexacoordinate silicon species towards nucleophiles reagents. *New J. Chem.*, **16**, 63 – 69.
- 31 **Casey, W. H., S. D. Kinrade, C. T. G. Knight, D. W. Rains and E. Epstein** (2004) Aqueous silicate complexes in wheat, *Triticum aestivum* L. *Plant Cell Envir.*, **27**, 51 – 54.
- 32 **Caulfield, M. J., T. R. Solomon and H. David** (2001) Complexes of benzene-1,2-diol Mannich bases. I. Novel hexacoordinate zwitterionic silicon (IV) complexes. *Aus. J. Chem.*, **54**, 375 – 381.
- 33 **Ceintrey, C.** Reprography materials containing silicon or phosphorus derivatives of 2,3-dihydroxynaphthalene. Brit. UK Pat. Appl. (1979), 27 pp.
- 34 **Cella, J. A., J. D. Cargioli and E. A. Williams** (1980) Silicon-29 NMR of five- and six-coordinate organosilicon complexes. *J. Organomet. Chem.*, **186**, 13 – 17.
- 35 **Cerveau, G., C. Chuit, E. Colomer, R. J. P. Corriu and C. Reye** (1990) Ferrocenyl compounds containing two hypervalent silicon species electrochemical studies. *Organometallics*, **9**, 2415 – 2417.

- 36 **Chandrasekhar, V., S. Nagendran, Samiksha and G. T. Senthil Andavan** (1998) Hypervalent tris(catecholato)silicate derived from rice husk ash. *Tetrahedron. Lett.*, **39**, 8505 – 8508.
- 37 **Chin, D. H., S. E. Jones, L. E. Leon, P. Bosserman, M. D. Stallings and D. T. Sawyer** (1982) Redox chemistry of the 3,5-di-tert-butylcatecholato and o-semiquinonato complexes of transition metal ions in aprotic media. *Adv. Chem. Ser.*, **201**, 675 – 707.
- 38 **Chuit, C., R. J. P. Corriu, C. Reye and J. C. Young** (1993) Reactivity of penta- and hexa-coordinate silicon compounds and their role as reaction intermediates. *Chem. Rev.*, **93**, 1371 – 1448.
- 39 **Comotti, A., M. C. Gallazzi, R. Simonutti and P. Sozzani** (1998) <sup>13</sup>C and <sup>31</sup>P magic-angle spinning nuclear magnetic resonance spectroscopy of tris(2,3-naphthalenedioxy)cyclotriphosphazene inclusion compounds. *Chem. Mat.*, **10**, 3589 – 3596.
- 40 **Corey, J. Y. and R. West** (1963) Triphenyl(bipyridyl)siliconium ion. *J. Am. Chem. Soc.*, **85**, 4034 – 4035.
- 41 **Corriu R. J. P. and J. C. Young** (1989) The chemistry of organic silicon compounds. Eds. Patai, S., Rappoport, Z., Wiley, New York, Chapter 20.
- 42 **Corriu, R. J. P.** (1990) Hypervalent species of silicon: Structure and reactivity. *J. Organomet. Chem.*, **400**, 81 – 106.
- 43 **Davis, A. V., T. K. Firman, B. P. Hay and K. N. Raymond** (2006) d-orbital effects on stereochemical non-rigidity: Twisted Ti<sup>IV</sup> intramolecular dynamics. *J. Am. Chem. Soc.*, **128**, 9484 – 9496.
- 44 **Davis, M. E.** (2002) Ordered porous materials for emerging applications. *Nature* **417**, 813 – 821.
- 45 **Dean, J. A.** (1987) Handbook of organic chemistry McGraw Hill Co., New York.
- 46 **Dean, P. A. W., D. F. Evans and R. F. Phillips** (1969) Trisoxalato-complexes of silicon, germanium, tin, and titanium. *J. Chem. Soc. A.*, **3**, 363 – 366.
- 47 **Decurtins. S., H. W. Schmalle, P. Schmeuwly and H. R. Oswald** (1993) Photochemical synthesis and structure of a 3-dimensional anionic polymeric network of an iron (II) oxalato complex with tris(2,2'-bipyridine)iron(II) cations. *Inorg. Chem.*, **32**, 1888 – 1892.

- 48 **Denekamp, C. I. F., D. F. Evans, A. M. Z. Slawin, D. J. Williams, C. Y. Wong and J. D. Woollins** (1992) Synthesis, nuclear magnetic resonance and crystallographic studies of six-co-ordinate bis(bidentate ligand)-dihalogenotin(IV) complexes. *J. Chem. Soc., Dalton Trans.*, 2375 – 2382.
- 49 **Denmark S. E. and R. F. Sweis** (2002) Design and implementation of new, silicon-based, cross-coupling reactions: Importance of silicon-oxygen bonds. *Acc. Chem. Res.*, **35**, 835 – 846.
- 50 **Diwu, Z. J. and J. W. Lown** (1993) Photosensitization with anticancer agents. 15. Perylenequinonoid pigments as potential photodynamic therapeutic agents: formation of semiquinone radicals and reactive oxygen species on illumination. *J. Photochem. Photobiol., B: Biol.*, **18**, 131 – 143.
- 51 **Dilthey, W.** (1903) Silicon compounds. *Berichte der Deutschen Chemischen Gesellschaft*, **36**, 923 – 930.
- 52 **Eberson, L.** (1985) The Marcus Theory of electron transfer, a sorting device for toxic compounds. *Adv. Free Radic. Biol. Med.*, **1**, 19 – 90.
- 53 **Ekkehardt, F., M. K. Hahn and K. N. Raymond** (1995) Catecholate complexes of silicon: Synthesis and molecular and crystal structures of [Si(cat)<sub>2</sub>].THF and Li<sub>2</sub>[Si(cat)<sub>3</sub>].3.5 dme (cat = catecholato dianion). *Inorg. Chem.*, **34**, 1402 – 1407.
- 54 **El-Hendawy, A. M., W. P. Griffith, C. A. O'Mahoney, and D. J. Williams** (1989) Complexes of naphthalene-2,3-diol (H<sub>2</sub>ND) with group VI and group VIII metals, and the X-ray crystal structure of *cis*-(NH<sub>4</sub>)<sub>2</sub>[Mo<sub>2</sub>O<sub>5</sub>(ND)<sub>2</sub>].2H<sub>2</sub>O. *Polyhedron*, **8**, 519 – 525.
- 55 **Ennis, C.** (2002) Silicon-based life! *Chemistry Review*, **12**, 2 – 6.
- 56 **Evans, D. F., J. Parr and E. N. Coker** (1990) Nuclear magnetic resonance studies of silicon(IV) complexes in aqueous solution—I. Tris-catecholato complexes *Polyhedron*, **9**, 813 – 823.
- 57 **Frontana, C., A. Bernardo and I. Frontana-Urbe** (2004) Electrochemical and ESR study on the transformation processes of  $\alpha$ -hydroxy-quinones *J. Elec. Chem.*, **573**, 307 – 314.
- 58 **Feig, A. L. and S. J. Lippard** (1994) Reactions of non-heme Iron(II) centers with dioxygen in biology and chemistry. *Chem. Rev.*, **94**, 759 – 805.

- 59 **Ferracin, L. C., M. Ionashiro and M. R. Davolos** (1990) Manufacture of silica by thermal decomposition of triethylammonium tris(oxalato)silicate(IV). *An. Congr. Bras. Ceram.*, **34**, 203 – 208.
- 60 **Fujita, T. and H. Ohtaki** (1983) An X-ray-diffraction study on the structures of bis(ethylenediamine)copper(ii) and tris(ethylenediamine)copper(II) complexes in solution. *Bul. Chem. Soc. jpn.*, **56**, 3276 – 3283.
- 61 **Flueraru, M., A. L. L. Chichirau, W. G. Chepelev, T. Willmore, Durst, M. Charron, L. R. C. Barclay and J. S. Wright** (2005) Cytotoxicity and cytoprotective activity in naphthalenediols depends on their tendency to form naphthoquinones. *Free Radic. Biol. Med.*, **39**, 1368 – 1377.
- 62 **Flynn, J. J. and F. P. Boer** (1969) Structural studies of hexacoordinate silicon Tris(O-phenylenedioxy)siliconate. *J. Am. Chem. Soc.*, **91**, 5756 – 5761.
- 63 **Fowles, G. W. A. and W. R. Mc Gregor** (1958) Amine compounds of the transition metals. III. The reaction of some transition metal chlorides with anhydrous ethylenediamine and propylenediamine. *J. Chem. Soc.*, 136 – 140.
- 64 **Frye, C. L.** (1964) Pentacoordinate silicon derivatives II. Salts of bis(O-arylenedioxy)organosiliconic acid. *J. Am. Chem. Soc.*, **91**, 5756 – 5761.
- 65 **Frye, C. L.** (1970) Pentacoordinate silicon derivatives II. Alkylammonium siliconate salts derived from aliphatic 1,2-diol. *J. Am. Chem. Soc.*, **96**, 1205 – 1210.
- 66 **Fujdala, K. L. and T. D. Tilley** (2003) Design and synthesis of heterogeneous catalysts: the thermolytic molecular precursor approach. *J. Catal.*, **216**, 265 – 275.
- 67 **Fujdala, K. L. and T. D. Tilley** (2001) Thermolytic transformation of tris(alkoxy)siloxochromium(IV) single-source molecular precursors to catalytic chromia-silica materials. *Chem. Mat.*, **13**, 1817 – 1827.
- 68 **Furin, G. G., D. A. Vyazankina, B. A. Gostevsky and N. S. Vyazankin** (1988) Synthetic aspects of the use of organosilicon compounds under nucleophilic catalysis conditions. *Tetrahedron*, **44**, 2675 – 2749.
- 69 **Gareth, B. M., M. A. Brown, H. E. Mabrouk, B. R. McGarvey and G. T. Dennis** (2003) Synthetic routes to lead(II) derivatives of aromatic 1,2-diols and orthoquinones. *Inorg. Chim. Acta*, **349**, 142 – 148.
- 70 **Gay-Lussac, J. L. and L. J. Thenard** (1809) *Mem. Phy. Chem. Soc.*, Arcueil, **2**, 317 – 319.

- 71 **Gibbs, G.V.** (1982) Molecules as models for bonding in silicates. *Amer. Min.*, **67**, 421 – 450.
- 72 **Gigant, K., A. Rammal and M. Henry** (2001) Synthesis and Molecular Structures of Some New Titanium (IV) Aryloxides. *J. Am. Chem. Soc.*, **123**, 11632 – 11637.
- 73 **Gillespie, R., and B. Silvi**, (2002) The octet rule and hypervalence: two misunderstood concepts. *Coord. Chem. Rev.*, **233-234**, 53 – 62.
- 74 **Gillespie, R. J. and E. A. Robinson** (1995) Hypervalence and the octet rule. *Inorg. Chem.*, **34**, 978 – 979.
- 75 **Gmelin** (1984) Handbook of Inorganic Chemistry, 8th Ed.; Springer-Verlag: New York, Silicon, Part A1, History, pp 7 – 50.
- 76 **Go, Y.** (2005) Curing accelerators, epoxy resin compositions therewith, and semiconductor devices sealed therewith. Jpn. Kokai Tokkyo Koho, JP 2005048110, pp 29.
- 77 **Guo, Y., R. Weiss, R. Boese and M. Epple** (2006) Synthesis, structural characterization and thermochemical reactivity of tris(ethylenediamine)zinc tetracyanozincate, a precursor for nanoscale ZnO. *Thermochim. Acta.*, **446**, 101 – 105.
- 78 **Hahn, F. E., M. Keck and K. N. Raymond** (1995) Catechol complexes of silicon. Synthesis and molecular and crystal structure of  $[\text{Si}(\text{cat})_2] \cdot 2\text{THF}$  and  $\text{Li}_2[\text{Si}(\text{cat})_3] \cdot 3.5\text{dme}(\text{cat}=\text{catecholato dianion})$ . *Inorg. Chem.*, **26**, 760 – 765.
- 79 **Hall, R. D. and S. Henry** (2003) Mobius bis and tris-spiroaromatic systems. *Org. Biomol. Chem.*, **1**, 182 – 185.
- 80 **Hardemare, A .D., S. Torelli, G. Serratrice and J. L. Pierre** (2006) Design of Iron chelators: Syntheses and iron (III) complexing abilities of tripodal tris-bidentate ligands. *Biometals*, **19**, 349 – 366.
- 81 **Hamdan, H.** (1997) Si-29 MAS NMR, XRD and FESEM studies of rice husk silica for the synthesis of zeolites. *J. Non. Cry. Solid.*, **211**, 126 – 131.
- 82 **Harrison, C. C. and N. Loton** (1995) Novel routes to designer silicas: studies of the decomposition of  $(\text{M}^+)_2 [\text{Si}(\text{C}_6\text{H}_4\text{O}_2)_3] \cdot \text{X H}_2\text{O}$ . Importance of  $\text{M}^+$  identity of the kinetics of oligomerization and the structural characteristics of the silicas produced. *J. Chem. Soc. Far. Trans.*, **91**, 4287 – 4297.
- 83 **Hemmert, C., A. Maestrin, M. Renz, H. Gornitzka and B. Meunier** (2000) Second generation of a polypyridine ligand to mimic enzymes containing non-heme iron centers. *C.R. Acad. Sci., Ser. IIc: Chim*, **3**, 735 – 741.

- 84 **Jang, H. D., H. Chang, Y. Suh and K. Okuyama** (2006) Synthesis of SiO<sub>2</sub> nanoparticles from sprayed droplets of tetraethylorthosilicate by the flame spray pyrolysis. *Cur. Appl. Phys.*, **6**, e110 – e113
- 85 **Hathaway, B. J.** (1987) Comprehensive coordination chemistry, vol. 5, Pergamon Press, Oxford, New York.
- 86 **Henry, M.** (1998) Retrosynthesis in inorganic crystal structures: application to nesosilicate and inosilicate networks. *Coord. Chem. Rev.*, **178**, 1109 – 1163.
- 87 **Hensen, K., M. Kettner, T. Stumpf and M. Bolte** (2000) Syntheses and crystal structure determination of hexacoordinated silicon-complexes with dimethylpyridines. *Z. Natur. B. A. J. Chem. Sci.*, **55b**, 901 – 906.
- 88 **Herreros, B., S. W. Carr and J. Klinowski**, (1994) Five coordinate silicon compounds as intermediates in the synthesis of silicates in non-aqueous media. *Science*, **263**, 1585 – 1587.
- 89 **Hockensmith, C. M., J. C. Goldsby and T. Kacik** (1999) Thermal studies of new precursors to indium-tin oxides for use as sensor materials in the detection of NO<sub>x</sub>. *Thermochim. Act.*, **340 – 341**, 315 – 322.
- 90 **Hogan, J. P., D. D. Norwood and C. A. Ayres** (1981) Phillips petroleum company loop reactor polyethylene technology. *J. Appl. Polym. Sci.*, **36**, 49 – 60.
- 91 **Holmes, R. R.** (1996) Comparison of phosphorus and silicon: Hypervalency, stereochemistry, and reactivity. *Chem. Rev.*, **96**, 927 – 950.
- 92 **Holmes, R. R., R. O. Day, V. Chandrasekhar and J. M. Holmes** (1985) Pentacoordinated molecules. 61. Synthesis and molecular structure of five-coordinated spirocyclic anionic silicates containing tert-butyl groups. Hydrogen-bonding effects. *Inorg. Chem.*, **24**, 2009 – 2015.
- 93 **Holmes, R. R.** (1990) The stereochemistry of nucleophilic substitution at tetracoordinated silicon. *Chem. Rev.*, **90**, 17 – 31.
- 94 **Hoppe, M. L., R. M. Lain, J. Kampf, M. S. Gordon and L. W. Burggraf** (2002) Ba[Si(OCH<sub>2</sub>CH<sub>2</sub>O)<sub>3</sub>], a hexaalkoxysilicate synthesized from SiO<sub>2</sub>. *Angew. Chem. Int. Ed. Engl.*, **32**, 287 – 289.
- 95 **Horak, V., F. V. Foster, R. de Levie, J. W. Jones and P. Svoronos** (1981) Generation and trapping of 2,3-naphthoquinone. *Tetrahedron. Lett.*, **22**, 3577 – 3578.

- 96 **Horimoto, A. and Y. Goh** (2005) Latent catalysts and epoxy resin compositions useful for encapsulating semiconductor device containing them. U.S. Pat. Appl. Publ., US 2005075474, 19.
- 97 **Horner, L. and E. Geyer** (1965) *o*-Quinones. XXVII. Redox potentials of pyrocatechol derivatives. *Chem. Ber.*, **98**, 2016 – 2045.
- 98 **Hosmane, N. S., P. De Meester, U. Siriwardane, M. S. Islam and S. S. C. Chu** (1986) Reductive and non-reductive insertions of silicon atoms into carborane cages: Synthesis and structure of a carbaborane analogue of bis(cyclopentadienyl)silicon. *J. Chem. Soc. Chem. Commun.*, 1421 – 1422.
- 99 **Iller, R. K.** (1979) *The chemistry of silica: Solubility, Polymerization, colloid and surface properties and biochemistry.* John Wiley & Sons, New York.
- 100 **Ingo, R., M. Penka and R. Tacke** (2002) The hexacoordinate silicate dianions *mer*-Tris[glycolato(2-)-O<sub>1</sub>,O<sub>2</sub>]silicate and *fac*-Tris[benzilato(2-)-O<sub>1</sub>,O<sub>2</sub>]silicate: Syntheses and structural characterization. *Inorg. Chem.*, **41**, 3950 – 3955.
- 101 **Irons, R. D. and R. Sawahata** (1985) Phenols, catechols, and quinones in Bioactivation of Foreign Compounds. Ed., Anders, M.W.. San Diego: Academic Press, 259 – 279.
- 102 **Isayama, M., K. Nomiyama and T. Yamaguchi** (2005) Templated synthesis of mesoscopic tube silicates using aqueous mixtures of naphthalenediol and ammonium surfactants. *Chem. Lett.*, **34**, 462 – 463.
- 103 **Ishii, Y.** (1991) Toners for electrostatic image development using silicon-containing complex charge-controlling agent. Jpn. Kokai Tokkyo Koho, JP 03276166, pp 8.
- 104 **Jacobsen, S. D., J. R. Smyth and R. J. Swope** (2003) Thermal expansion of hydrated six-coordinate silicon in thaumasite, Ca<sub>3</sub>Si(OH)<sub>6</sub>(CO<sub>3</sub>)(SO<sub>4</sub>).12H<sub>2</sub>O *Physics and Chem. Min.*, **30**, 321 – 329.
- 105 **Jih-Mim J. B., A. Hungchun Hu, A. Xingtao Gao and E. W. Israel** (1996) The dynamic states of silica-supported metal oxide catalysts during methanol oxidation. *Catal. Today*, **28**, 335 – 355.
- 106 **John, B.** (1984) Solubility Parameters: Theory and application AIC Book and Paper Group Annual, Ed, C. Jensen, **3**, 13 – 58.
- 107 **Jones, D. W. and R. L. Wife** (1972) *o*-Quinonoid compounds. V. Derivatives of 2,3-naphthoquinone dimethide. *J. Chem. Soc., Perkin Trans. I*, **21**, 2722 – 2727.



- 108 **Jones, S. E., D. Chin, and D. T. Sawyer** (1981) Redox chemistry of metal-catechol complexes in aprotic media. 2. 3,5-Di- *tert*-butylcatecholato complexes of manganese (IV) and manganese (III). *Inorg. Chem.*, **20**, 4257 – 4262.
- 109 **Jorgensen, E. G.** (1955) Solubility of the silica in diatoms *Physiologia Plantarum*, **8**, 846 – 851.
- 110 **Joshi, J. D., S. Sharma and G. V. Patel** (2002) Synthesis and characterization of nickel(II), zinc(II), and cadmium(II) mixed-ligand complexes with 2,2'-bipyridylamine and phenols. *Synth. React. Inorg. Met.-Org. Chem.*, **32**, 1729 – 1741.
- 111 **Jung, J. H., Y. Ono and S. Shinkai** (2000) Novel Silica structures, which are prepared by transcription of various superstructures, formed in organogels *Langmuir*, **16**, 1643 – 1649.
- 112 **Jutzi, P., D. Kanne and C. Kruger** (1986) Decamethylsilicocene - Synthesis and structure *Angew. Chem. Int. Ed. Engl.*, **25**, 164 – 164.
- 113 **Kluefers, P., X. Kaestele, F. Kopp, J. Schuhmacher and M. Vogt** (2005) Polyol metal complexes. Part 51. Silicon chelation in aqueous and nonaqueous media: The furanoidic diol approach. *Chem.-A Eur. J.*, **11**, 6326 – 6346.
- 114 **Kalka, K., H. F. Merk and H. Mukhtar** (2000) Photodynamic therapy in dermatology. *J. Am. Acad. Dermatol.*, **42**, 389 – 413.
- 115 **Kano, N., F. Komatsu, M. Yamamura and T. Kawashima** (2006) Reversible photo switching of the coordination numbers of silicon in organosilicon compounds bearing a 2-(phenylazo)phenyl group. *J. Am. Chem. Soc.*, **128**, 7097 – 7109.
- 116 **Kansal, P. and R. M. Laine** (1994) Pentacoordinate silicon complexes as precursors to silicate-glasses and ceramics. *J. Am. Ceram. Soc.*, **77**, 875 – 882.
- 117 **Keilin, D. and T. Mann** (1940) Properties of laccase from the latex of lacquer trees. *Nature*, **145**, pp304.
- 118 **King, R. B.** (1995) *Hypervalent Compounds* “Encyclopedia of inorganic chemistry”, John Wiley and Sons, New York, **3**, 1496 – 1511.
- 119 **Kingston, J. V. and M. N. Sudheendra Rao** (1997) High yield synthesis of cyclic phosphite, phosphates, sulphites and sulphates of catechol and glycol mediated by hypervalent silicon centers. *Tetrahedron Lett.*, **38**, 4841 – 4844.
- 120 **Kingston, J. V.** (1999) Studies on hypervalent silicates-synthesis, structure and reactivity. Ph.D thesis, Indian Institute of Technology Madras, Chennai.

- 121 **Kingston, J. V., B. Gostevskii, I. Kalikhman and D. Kost** (2001) Equilibrium between neutral hexacoordinate silicon complexes and ionic pentacoordinate siliconium salts through fast dissociation-recombination of the Si-Cl bond. *Chem. Comm.*, **14**, 1272 – 1273.
- 122 **Kingston, J. V. and J. G. Verkade** (2005) P[N(<sup>i</sup>Bu)CH<sub>2</sub>CH<sub>2</sub>]<sub>3</sub>N: A versatile non-ionic base for the synthesis of higher coordinate silicates. *Inorg. Chem. Comm.*, **8**, 643 – 646.
- 123 **Kingston, J. V., V. Babu and M. N. Sudheendra Rao** (2000) Synthesis and characterization of tris(catecholato) silicates, [(C<sub>6</sub>H<sub>4</sub>O<sub>2</sub>)<sub>3</sub>Si]<sup>2-</sup> with different counter cations - first pyrolysis study and X-ray structure of [ {(CH<sub>3</sub>)<sub>2</sub>CH }<sub>2</sub>NH<sub>2</sub>]<sub>2</sub>[(C<sub>6</sub>H<sub>4</sub>O<sub>2</sub>)<sub>3</sub>Si] . 2 CH<sub>3</sub>CN . H<sub>2</sub>O. *Main Group Chemistry*, **3**, 79 – 90.
- 124 **Kinrade S. D., J. W. Del Nin, A. S. Schach, T. A. Sloan, K. L. Wilson and C. T. Knight** (1999) Stable five- and six-coordinated silicate anions in aqueous solution. *Science*, **285**, 1542 – 1545.
- 125 **Kinrade, S. D., A. S. Schach, R. J. Hamilton and C. T. Knight** (2001a) NMR evidence of pentaoxo organosilicon complexes in dilute neutral aqueous silicate solutions. *Chem. Comm.*, **17**, 1564 – 1565.
- 126 **Kinrade, S. D., E. W. Deguns, A. E. Gillson and C. T. Knight** (2003) Complexes of pentaoxo and hexaoxo silicon with furanoidic vicinal cis-diols in aqueous solution. *J. Chem. Soc., Dalton Trans.*, **19**, 3713 – 3716.
- 127 **Kinrade, S. D., R. J. Hamilton, A. S. Schach and C. T. Knight** (2001b) Aqueous hypervalent silicon complexes with aliphatic sugar acids. *J. Chem. Soc., Dalton Trans.*, **7**, 961 – 963.
- 128 **Kinrade, S. D. and T. W. Swaddle** (1988) Silicon-29 NMR studies of aqueous silicate solutions. 1. Chemical shifts and equilibria. *Inorg. Chem.*, **27**, 4253 – 4259.
- 129 **Kinrade, S. D., A. M. E. Gillson and C. T. G. Knight** (2002) Silicon-29 NMR evidence of a transient hexavalent silicon complex in the diatom *Navicula pelliculosa*. *J. Chem. Soc., Dalton Trans.*, **3**, 307 – 309.
- 130 **Kinrade, S. D. and D. L. Pole** (1992) Effect of alkali-metal cations on the chemistry of aqueous silicate solutions. *Inorg. Chem.*, **31**, 4558 – 4563.

- 131 **Kinzel, A. B.** (1933) Silicon: its applications in modern metallurgy. *Mining and Metallurgy*, **14**, 489 – 492.
- 132 **Kira, M., K. Sato, C. Kabuto and H. Sakurai** (1989) Preparation and X-ray molecular structure of the first pentacoordinate silylsilicates. *J. Am. Chem. Soc.*, **111**, 3737 – 3748.
- 133 **Kira, M., L. C. Zhang, C. Kabuto and H. Sakurai** (1995) Synthesis and structure of hexacoordinate organosilicon compounds having troponato ligands. *Chem. Lett.*, 659 – 660.
- 134 **Klaur, W., N. Mocigemba, A. Weber-Schuster, R. Bell, W. Frank, D. Mootz, W. Poll and H. Wunderlich** (2002)  $[(C_5H_5)Co\{P(O)(OH)_2\}_3H]$ : A novel organometallic tris-phosphonic acid that dissolves glass to form a six-coordinate silicon complex. *Chem.-A Eur. J.*, **8**, 2335 – 2340.
- 135 **Kocher, N., C. Selinka, D. Leusser, D. Kost, I. Kalikhman and D. Stalke** (2004) Experimental charge density studies of cyclotetrasilazane and metal complexes containing the di- and tetraanion. *Z. Anorg. Allg. Chem.*, **630**, 1777 – 1793.
- 136 **Kost, D. and I. Kalikhman** (2004) Hydrazide-based hypercoordinate silicon compounds. *Adv. Organomet. Chem.*, **50**, 1 – 106.
- 137 **Kriegisch, V. and C. Lambert** (2005) Synthesis and linear optical properties of tris(catecholato)metal(III,IV) complexes with acceptor-substituted ligands. *Eur. J. Inorg. Chem.*, **22**, 4509 – 4515.
- 138 **Kriesel, J. W. and T. D. Tilley** (2001) A new molecular precursor for magnesia-silica materials. *Mat. Chem.*, **11**, 1081 – 1085.
- 139 **Kumada, M., K. Tamao and J. I. Yoshida** (1982) Chemistry of organopentafluorosilicates. *J. Organomet. Chem.*, **239**, 115 – 132.
- 140 **Kummer, D. and T. Seshadri** (1977) Contributions to the chemistry of halosilane adducts. IX. Hexa(pyridine N-oxide)silicon tetraiodide, a complex of silicon with six neutral ligands. *Z. Anorg. Allg. Chem.*, **432**, 147 – 152.
- 141 **Laine, R. M., K. Y. Blohowiak, T. R. Robinson, M. L. Hoppe, P. Nardi, J. Kampf and J. Uhm** (1991) Synthesis of pentacoordinate silicon complexes from  $SiO_2$ . *Nature*, **353**, 642 – 644.
- 142 **Lorenz, C. R., H. D. Dewald and F. R. Lemke** (1997) Electrochemistry of hexacoordinated silicon (IV) porphyrin complexes. *Electroanalysis*, **9**, 1273 – 1277.

- 143 **Larkins, T. H. and M. M. Jones** (1963) Some new asymmetric octahedral complexes of arsenic (V). *Inorg. Chem.*, **2**, 142 – 145.
- 144 **Levin E. M., C. R. Robbins and H. F. McMurdie** (1969) Phase Diagrams for Ceramists Vol 1 2<sup>nd</sup> Ed., American Ceramic Society.
- 145 **Lidstorm, P., T. Jason, W. Berhard and J. Westman** (2001) Microwave assisted organic synthesis—a review. *Tetrahedron*, **57**, 9225 – 9283.
- 146 **Lim, H. J., S. M. Kim, S. J. Lee, S. Jung, Y. K. Kim and Y. Ha** (2003) Synthesis of new boron complex containing aromatic moieties and their application to organic luminescent devices. *Opt. Mat.*, 211 – 215.
- 147 **Loo, C., A. Lowery, N. Halas, J. West and R. Drezek** (2005) Immunotargeted nanoshells for integrated cancer imaging and therapy. *Nano Lett.*, **5**, 709 – 711.
- 148 **Maanju, S., A. Chaudhary and R. V. Singh** (2006) Microwave assisted Synthesis, spectroscopic elucidation and antimicrobial activity of organosilicon (IV) derivatives of thiosemicarbazone. *Main Group Met. Chem.*, **29**, 31 – 38.
- 149 **Mabrouk, H. E., D. G. Tuck and M. A. Khan** (1987) The direct electrochemical synthesis of zinc and cadmium catecholates and related compounds. *Inorg. Chim. Acta*, **129**, 75 – 80.
- 150 **Marsann, H.** (1981) <sup>29</sup>Si-NMR spectroscopic results in NMR basic principles and progress, Springer Verlag, Berlin, **17**, 65 – 235.
- 151 **Martin, J. C.** (1983) Frozen transition states: pentavalent carbon. *Science*, **221**, 509 – 514.
- 152 **Martin, J. C. and E. F. Perozzi** (1976) Isolable oxysulfurones in organic chemistry. *Science*, **191**, 154 – 159.
- 153 **Manach, C.; A. Mazur and A. Scalbert** (2005), Polyphenols and prevention of cardiovascular diseases. *Curr. Opin. Lip.*, **16**, 77 – 84.
- 154 **Martin, M., H. Mangold, M. Oswald, K. Schumacher and H. Lach** (2004) Manufacture of silica by pyrolysis and dispersions. PCT Int. Appl. WO 2004054929, pp 30.
- 155 **Mason, H.S., E. Spencer and I. Yamazaki** (1961) Identification by electron spin resonance spectroscopy of the primary product of tyrosinase-catalyzed catechol oxidation. *Biochem. Biophys. Res. Commun.*, **4**, 236 – 238.
- 156 **Matzanke, B. F., G. Mueller-Matzanke and K. N. Raymond** (1989) Siderophore - mediated iron transport. *Phys. Bioinorg. Chem. Ser.*, **5**, 1 – 121.

- 157 **Merhrdad, E. and A. B. P. Lever** (1999), Ruthenium complexes of quinone related ligands: A Study of the electrochemical properties of 2-aminothiophenolatobis(2,2'-bipyridine)ruthenium(II). *Inorg. Chem.*, **38**, 467 – 474.
- 158 **Mc Garvey, B. R.** (1966) Transition Metal Chemistry – A Series of Advances vol. **3**, Marcel Dekker, New York.
- 159 **McCormick, A. V., A. T. Bell and C. J. Radke** (1989) Gas-phase overtone spectral investigation of structurally and conformationally nonequivalent carbon-hydrogen bonds in trimethylbenzenes. *J. Phy. Chem.*, **93**, 1737 – 1739.
- 160 **Meyer, H. and G. Nagersen** (1979) Structural and reactivity of the orthocarbonic and orthosilicic acid esters of pyrocatechol. *Angew. Chem. Int. Ed. Eng.*, **18**, 551 – 554.
- 161 **Meyer, H., G. Nagorsen and A. Wiess** (1968) Tris(o-arylenedioxo)- and bis(o-arylenedioxo-)organosilicic acid containing hexacoordinated and pentacoordinated silicon. *Angew. Chem. Int. Ed. Eng.*, **7**, 826 – 826.
- 162 **Miller, S. and A. H. Donald** (1981) Infrared spectroscopic studies on the conformation of  $[M(en)]^{3+}$  cations in the solid state: scope and limitation. *Inorg. Chim. Acta*, **157**, 29 – 32.
- 163 **Milsmann, C., A. Levina, H. H. Harris, G. J. Foran, P. Turner and P.A. Lay** (2006) Charge distribution in chromium and vanadium catecholato complexes: X-ray absorption spectroscopic and computational studies *Inorg. Chem.*, **45**, 4743 – 4754.
- 164 **Michael A., G. Hogarth and D. T.W. Oscroft** (2004) Organometallic chemistry in a conventional microwave oven:the facile synthesis of group 6 carbonyl complexes.*J. Organomet. Chem.*, **689**, 2429 – 2435.
- 165 **Moleski, R., E. Leontidis and F. Krumeich** (2006) Controlled production of ZnO nanoparticles from zinc glycerolate in a sol-gel silica matrix. *J. Col. Interfac. Sci.*, **302**, 246 – 253.
- 166 **Mosset, A., P. Baules and P. Lecante** (1996) A new solution route to silicates .4. Submicronic zircon powders. *J. Mat. Chem.* **6**, 1527 – 1532.
- 167 **Muetterties, E.L.** (1960) Stereochemistry of complexes based on metal tetrafluorides. *J. Am. Chem. Soc.*, **82**, 1082 – 1087.
- 168 **Mothilal, K. K., J. J. Inbaraj, C. F. Chignell, R. Gandhidasan and R. Murugesan** (2004) Photosensitisation with naphthoquinones and

- binaphthoquinones: EPR spin trapping and optical studies-formation of semiquinone radical and reactive oxygen species on photoillumination. *J. Photochem. Photobiol. A-Chem.*, **163**, 141 – 148.
- 169 **Muller, R.** and **L. Heinrich** (1961) Der Nachweis und die Abtrennung Von Alkoxo-und Aroxo-Verbindungen mit Funfbindigen silicium. *Chem. Ber.*, **94**, 1943 – 1951.
- 170 **Musher, J. I.** (1969) The chemistry of hypervalent molecules. *Angew. Chem. Int. Ed. Eng.*, **8**, 54 – 68.
- 171 **Nishio-Hamane, D., T. Nagai, K. Fujino, Y. Seto** and **N. Takafuji** (2005) Fe<sup>3+</sup> and Al solubilities in MgSiO<sub>3</sub> perovskite: implication of the Fe<sup>3+</sup>AlO<sub>3</sub> substitution in MgSiO<sub>3</sub> perovskite at the lower mantle condition. *Geophy. Res. Lett.*, **32**, L16306/1 – L16306/4.
- 172 **Nematollahi, D, M. S Workentin** and **E. Tammari** (2006) Electrochemical oxidation of catechol in the presence of cyclopentadiene. Investigation of electrochemically induced Diels - Alder reactions. *Chem. Commun.*, **15**, 1631 – 1633.
- 173 **Nazeri, A., E. Bescher** and **J. Mackenzie** (1993) Ceramic composites by the sol-gel method: a review. *Pub. in Ceramic Engineering & Science Proceedings*; **14**; 1 – 19.
- 174 **Oestreich, M.** (2006) Chirality transfers from silicon to carbon. *Chem. A- Eur. J.*, **12**, 30 – 37.
- 175 **Okamoto, K., K. Ohkubo, K. M. Kadish** and **S. Fukuzumi**, (2004) Remarkable accelerating effects of ammonium cations on electron-transfer reactions of quinones by hydrogen bonding with semiquinone radical anions *J. Phys. Chem. A.*, **108**, 10405 – 10413
- 176 **Ossowski, P., T. A. L Pipka** and **D. Jeziorek** (2000) Electrochemical and UV-spectrophotometric study of oxygen and superoxide anion radical interaction with anthraquinone derivatives and their radical anions. *Electrochimica Acta.*, **45**, 3581 – 3587.
- 177 **Olah, G. A., K. S. Prakash, R. E. Williams, L. D. Field** and **K. Wade** (1987) *Hypercarbon Chemistry*. Wiley-Interscience. New York.
- 178 **Pak, J. J., J. Greaves, D. J. McCord** and **K. J. Shea** (2002) Diastereoselective self-assembly of a pentacoordinate silicate tetraanionic molecular square. a mechanistic investigation. *Organometallics*, **21**, 3552 – 3561.

- 179 **Pal, S. K., F. S. Tham, R. W. Reed, R. T. Oakley and R. C. Haddon** (2005) Synthesis and characterization of germanium (IV) and silicon (IV) complexes derived from 9-hydroxyphenalenone: X-ray crystal and molecular structure of tris-(9-oxophenalenone)-germanium (IV) and silicon (IV) salts. *Polyhedron*, **24**, 16 – 17.
- 180 **Patwardhan, S. V., K. Shiba, C. Raab, N. Huesing and S. J. Clarson** (2005) Protein-mediated bioinspired mineralization *Pol. Biocat. Biomat. ACS Symposium Series*, 900, 150 – 163.
- 181 **Parr, J., M. Z. Alexandra, S. J. D. Woollins and D. J. Williams** (1994) The preparation and x-ray structure of  $K_2[Ge(cat)_3 \cdot 3H_2O \cdot 2EtOH]$ . A new potassium-aryl linked molecular array. *Polyhedron*, **13**, 3261 – 3263.
- 182 **Paul, L. D. and L. Ronan** (1996) Ultrasonic activation of  $SiO_2$  and  $GeO_2$  in basic solutions of diols. *Polyhedron*, **15**, 1975 – 1979.
- 183 **Pauling, L.** (1980) The nature of silicon-oxygen bonds. *Amer. Min.*, **65**, 321 – 323.
- 184 **Pak, J. J., Greaves, J. D. J. McCord and K. J. Shea** (2002) Diastereoselective self-assembly of a pentacoordinate silicate tetraanionic molecular square. A mechanistic investigation. *Organometallics*, **21**, 3552 – 3561.
- 185 **Perrin, D. D., W. L. F. Aramarego and D. R. Perrin** (1980) Purification of laboratory chemicals. Pergamon press, Oxford.
- 186 **Perry C. C. and T. Keeling-Tucker** (2000) Model studies of the precipitation of silica in the presence of aluminium; implications for biology and industry. *J. Inorg. Biochem.*, **78**, 331 – 339.
- 187 **Pierpont, C. G. and C. W. Lange** (1994) The chemistry of transition metal complexes containing catechol and semiquinone ligands. *Pro. Inorg. Chem.*, **41**, 331 – 442.
- 188 **Perreuse, L. and A. Loupy** (2001) A tentative rationalization of microwave effects in organic synthesis according to the reaction medium, and mechanistic considerations. *Tetrahedron*, **57**, 9199 – 9223.
- 189 **Perry, C. C., E. J. Moss and R. J. P. Williams** (1990) A staining agent for biological silica. *Proc. R. Soc. London B*, **241**, 47 – 50.

- 190 **Perry, C. C. and Y. Lu** (1992) Preparation of silicas from silicon complexes: role of cellulose in polymerization and aggregation control. *J. Chem. Soc. Far. Trans.*, **88**, 2915 – 2921.
- 191 **Pike, R. M. and R. R. Luongo** (1966) The structure of bis(2,4-pentanediono)diacetatosilicon(IV). *J. Am. Chem. Soc.*, **88**, 2060 – 2061.
- 192 **Plesu, N., A. Kellenberger, N. Vaszilcsin and I. Manoviciu** (2004) Electrochemical polymerisation of aniline on skeleton nickel electrodes. *Mol. Cryst. liq. Cryst.*, **416**, 127 – 135.
- 193 **Pimentel, G. C.** (1951) The bonding of trihalide and bifluoride ions by the molecular orbital method. *J. Chem. Phys.*, **19**, 446 – 448.
- 194 **Preggs, A. and H. Bowen** (1984) Inability to detect organo-silicon compounds in Equisetum and Thuja. *Phytochemistry*, **23**, 1788 – 1789.
- 195 **Procter, I. M.; B. J. Hathaway and P. Nicholls** (1968) Electronic properties and stereochemistry of the copper (II) ion. I. Bis(ethylenediamine)copper (II) complexes. *J. Chem. Soc. A*, **7**, 1678 – 1684.
- 196 **Rajan, R. and T. R. Reddy** (1963) Electron spin resonance in ethylenediamine complexes of copper(II) sulfate. *J. Chem. Phys.* **39**, 1140 – 1142.
- 197 **Ravi, B. G., V. Praveen, M. Selvam and K. J. Panneer Rao** (1998) Microwave - assisted preparation and sintering of mullite and mullite-zirconia composites from metal organics. *Mater. Res. Bull.*, **33**, 1527 – 1536.
- 198 **Ramil-Marcelo, L., A. Chandrasekaran, R. O. Day and R. R. Holmes** (1999) Synthesis and structure of cyclic zwitterionic silicates. Formation via Si-N donor interaction. *Organometallics*, **18**, 1686 – 1692.
- 199 **Readio, J., I. J. Borowitz, N. Pollack, J. Porter, L. Weiss and G. B. Borowitz** (1981) Metal complexes of N,N,N',N'-tetrakis(n-propyl)-1,2-phenylenedioxydiacetamide and related ligands. *J. Coord. Chem.*, **11**, 135 – 42.
- 200 **Reed, A. E. and P. V. R. Schleyer** (1990) Chemical bonding in hypervalent molecules. The dominance of ionic bonding and negative hyperconjugation over d-orbital participation. *J. Am. Chem. Soc.*, **112**, 1434 – 1445.
- 201 **Reed, C., Y. Xi and S. T. Oyama** (2005) Distinguishing between reaction intermediates and spectators: A kinetic study of acetone oxidation using ozone on a silica -supported manganese oxide catalyst. *J. Catal.*, **235**, 378 – 392.



- 202 **Rees, A. E. and P. V. R. Schleyer** (1990) Synthesis and molecular structure of noval bis( $\eta^5$ -di carbollide)silicon sandwich compound  $3,3'$ -Si(C<sub>2</sub>B<sub>9</sub>H<sub>11</sub>)<sub>2</sub>. *J. Am. Chem. Soc.*, **108**, 5369 – 5379.
- 203 **Ringwood, A. E. and M. Seabrook** (1963) High-pressure phase transformations in germanate pyroxenes and related compounds. *J. Geophys. Res.*, **68**, 4601 – 4609.
- 204 **Roesenheim, A., B. Raibmann, and G. Schendel** (1931) Complex pyrocatechol of quadrivalent elements. *Z. Anorg. Allg. Chem.*, **196**, 160 – 176.
- 205 **Rosenheim, A. and I. Baruttschisky** (1925) Bismuth pyrocatecholates. *Ber. Deut. Chem. Gesellschaft [Abteilung] B: Abhandlungen*, **58B**, 891– 893.
- 206 **Rundle, R. E.** (1993a) Implications of some recent structure of chemical valence theory. *Survey Progr. Chem.*, **1**, 81 – 131.
- 207 **Rundle, R. E.** (1993b) On the probable structure of XeF<sub>4</sub> and XeF<sub>2</sub>. *J. Am. Chem. Soc.*, **85**, 112 – 113.
- 208 **Sackerer, V. D. and G. Nagorsen** (1977) Die kristall struckut von Bis(athylendiamin)kufer(II)-tris(brenzcatechino)silicat. *Z. Anorg. Allg. Chem.*, **437**, 188 – 192
- 209 **Sahai, N. and J. A. Tossell** (2002) <sup>29</sup>Si NMR shifts and relative stabilities calculated for hypercoordinated silicon-polyalcohol complexes. Role in sol-gel and biogenic silica synthesis. *Inorg. Chem.*, **41**, 748 – 756.
- 210 **Santschi, P. H. and P. W. Schindler** (1974) Complex formation in the ternary systems calcium(II)- and magnesium(II)-orthosilicic acid-water. *J. Chem. Soc., Dalton Trans.*, **2**, 181-184.
- 211 **Saskia, A. G.** (1997) Microwave chemistry. *Chem. Soc. Rev.*, **26**, 233 – 238.
- 212 **Scherbak, N., A. Strid and L.A. Eriksson** (2005) Non-enzymatic oxidation of NADH by quinones. *Chem. Phys. Lett.*, **414**, 243 – 247.
- 213 **Schley, M., J. Wagler and G. Roewer** (2005) Crystallization by slow halogen exchange in hypercoordinate silicon chelates and the first X-ray structure of a trans-featured hexacoordinate difluorosilicon-bis-chelate. *Z. Anorg. Allg. Chem.*, **631**, 2914 – 2918.
- 214 **Schramb, J. and J. M. Bellama** (1976) Silicon-29 nuclear magnetic resonance. *Determ. Org. Struct. Phys. Meth.*, **6**, 203 – 209.

- 215 **Schweigert, N., J. L. Acero, S. Z. von Gunten, A. J. B. Canonica and R. I. L. Eggen** (2000) DNA degradation by the mixture of copper and catechol is caused by DNA-copperoxo complexes, probably DNA-Cu (I) OOH. *Environ. Mol. Mutagen*, **36**, 5 – 12.
- 216 **Sclar, C. B., L. C. Carrison and G.G. Cocks** (1964) Stishovite: thermal dependence of crystal habit. *Science*, **144**, 833 – 835.
- 217 **Scott S. I. and J. M. Basset** (1994) Stoichiometric and catalytic reactivity of organometallic fragments supported on inorganic oxides. *J. Mol. Cat.*, **86**, 5 – 22.
- 218 **Scott, B. J., G. Wirnsberger and G. D. Stucky** (2001) Mesoporous and mesostructured materials for optical applications, *Chem. Mater.* **13**, 3140 – 3150.
- 219 **Sebastian R. and M. Oestreich** (2005) Hypervalent silicon as a reactive site in selective bond forming processes, *Synthesis*, **11**, 1727 – 1747
- 220 **Seganish, W. M. and P. DeShong** (2004) Palladium-catalyzed cross-coupling of Aryl Triethylammonium Bis(catecholato)silicates with Aryl bromides using microwave irradiation *Org. Lett.*, **6**, 4379 – 4381.
- 221 **Sacconi, L., F. Mani and A. Bencini** (1987) Comprehensive coordination chemistry, vol. **5**, Pergamon Press, Oxford, New York.
- 222 **Seiler, O., C. Burschka, M. Fischer, M. Penka and R. Tacke** (2005) Behavior of tri(n-butyl)ammonium bis[citrato(3-)-O1,O3,O6]silicate in aqueous solution: analysis of a sol-gel process by small-angle neutron scattering. *Inorg. Chem.*, **44**, 2337 – 2342 .
- 223 **Seiler, O., C. Burschka, M. Penka and R. Tacke** (2004) Dianionic complexes with hexacoordinate silicon (IV) or germanium (IV) and three bidentate ligands of the salicylato(2-) type: Syntheses and structural characterization in the solid state and in solution. *Silicon Chemistry*, **1**, 355 – 365.
- 224 **Seiler, O., C. Burschka, M. Penka and R. Tacke** (2002) Dianionic tris[oxalato(2-)]silicate and tris[oxalato(2-)]germanate complexes: Synthesis, properties, and structural characterization in the solid state and in solution. *Z. Anorg. Allg. Chem.*, **628**, 2427 – 2434.
- 225 **Seiler, O., M. Penka and R. Tacke** (2004) [Benzilato(2-)-O1,O2]bis[1,3-diphenylpropane-1,3-dionato(1-)-O,O]silicon(IV): a neutral heteroleptic hexacoordinate silicon(IV) complex with an SiO<sub>6</sub> skeleton. *Inorg. Chim. Acta.*, **357**, 1955 – 1958.

- 226 **Seyferth, D.** (2001) Dimethyldichlorosilane and the Direct Synthesis of Methylchlorosilanes. The Key to the Silicones. Industry. *Organometallics*, **202**, 4978 – 4992.
- 227 **Sheldrick, G. M.** (1985) SHELXS-86 program for the solution of crystal structures. Univ. of Goettingen, Germany.
- 228 **Sheldrick, G. M.** (1993) SHELXS - 93 program for the refinement of crystal structures. Univ. of Goettingen, Germany.
- 229 **Shin, D., S. Sato, R. Takahashi and T. Sodesawa** (2002) Silica-coated metal oxide powders with high surface area. *J. Cera. Soc. Jpn.*, **110**, 1097 – 1099.
- 230 **Shioi, S., T. Tsuchida and A. Miyake** (1988) Thermal recording materials. Jpn. Kokai Tokkyo Koho, JP 63137888, pp 9.
- 231 **Shriver, D. F. and M. A. Drezdon** (1986) The manipulation of air sensitive compounds, John Wiley and sons, New York.
- 232 **Singh, R. V., M. Jain and C. N. Deshmukh** (2005) Microwave-assisted synthesis and insecticidal properties of biologically potent organosilicon(IV) compounds of a sulfonamide imine. *Appl. Organometal. Chem.*, **19**, 879 – 886.
- 233 **Sinha, B. K. and E. G. Mimnaugh** (1990) Free radicals and anticancer drug-resistance - oxygen free-radicals in the mechanisms of drug cytotoxicity and resistance by certain tumors. *Free Radic. Biol. Med.*, **8**, 567 – 581.
- 234 **Sperlich, J., J. Becht, M. Muehleisen, S. A. Wagner, G. Mattern and R. Tacke** (1993) Zwitterionic bis[*vic*-arenediolato(2-)][(morpholino)alkyl]silicates: synthesis and structural characterization in solution and in the crystal. *Z. Natur., B: Chem. Sci.*, **48**, 1693 – 1706.
- 235 **Steenken, S. and P. Neta** (1979) Electron transfer rates and equilibria between substituted phenoxide ions and phenoxyl radicals. *J. Phys. Chem.*, **83**, 1134 – 1137.
- 236 **Stintzi, A., C. Barnes, J. Xu and K. N. Raymond** (2000) Microbial iron transport via a siderophore shuttle: A membrane ion transport paradigm *Proc. Natl. Acad. Sci. U. S. A.*, **97**, 10691 – 10696.
- 237 **Strohmann, C., R. Tacke, G. Mattern and W. F. Kuhs** (1991) Bis(2,3-naphthalenediolato)[2-(pyrrolidinio)ethyl]silicate: synthesis and structural characterization of a zwitterionic  $\lambda$ -5-spirosilicate. *J. Organomet. Chem.*, **403**, 63 – 71.
- 238 **Su, K. and T. D. Tilley** (2001) Molecular routes es metal oxides sand metal silicates, synthesis and thermal decomposition studies of eclipsed

$\text{Mo}_2[\text{O}_2\text{Si}(\text{O}(\text{t})\text{Bu})_2]_3$  and  $\text{W}_2(\text{NHMe}_2)_2[\text{O}_2\text{Si}(\text{O}^t\text{Bu})_2]_2[\text{OSi}(\text{OH})(\text{O}^t\text{Bu})_2]_2$ . *Chem. Mat.*, **9**, 588 – 595.

- 239 **Sugata, K., S. Sugawara and S. Yamanaka** (1992) Aromatic silicon complex as charge-controlling agents and electrostatic image-developing toners. (Orient Chemical Industries, Ltd., Japan). JP 04318561, pp11.
- 240 **Sinha, B. K. and E. G. Mimnaugh** (1990) Free – radical and anticancer drug resistance – oxygen free radicals in the mechanisms of drug cytotoxicity and resistance by certain tumors. *Free Radic. Biol. Med.*, **8**, 567 – 581.
- 241 **Tacke, R. and R. Ingo** (2003) Higher-coordinate silicates for use in pharmaceutical, cosmetic, and dietary food stuff. PCT Int. Appl., WO 003061640, pp19.
- 242 **Tacke, R., R. Bertermann, C. Burschka and S. Dragota** (2004) Hexacoordinate silicon(IV) complexes with  $\text{SiO}_6$  skeletons and multidentate ligands derived from citric acid or malic acid. *Z. Anorg. Allg. Chem.*, **630**, 2006 – 2012 .
- 243 **Tacke, R., M. Muehleisen, A. Lopez- Mras and W. S. Sheldrick** (1995) Synthesis and crystal structure analysis of new zwitterionic spirocyclic(amminoorganyl)bis(VIC-Arenedialato(2-)) Silicates – Studies on the structure of the Lambda –S1- 5 Coordination polyhedral. *Z. Anorg. Allg. Chem.*, **621**, 779 – 788.
- 244 **Tacke, R., M. Plum and B. Wagner** (1999) Zwitterionic pentacoordinate silicon compounds. *Adv. Organomet. Chem.*, **44**, 221 – 273.
- 245 **Tacke, R., A. Stewart, J. Becht, C. Burschka and R. Ingo** (2000) Di(hydroxyalkyl)dimethylammonium] tris[benzene- 1,2- diolato(2-)] silicates and their germanium analogs: Synthesis, crystal structure analyses and NMR studies. *Can. J. Chem.*, **78**, 1380 – 1387.
- 246 **Tacke, R., A. Lopez- Mras, W. S. Sheldrick and A. Sebald** (1993) Synthesis, single- crystal X-ray analyses and solid state  $^{29}\text{Si}$  NMR studies of zwitterionic  $\lambda$ 5- spirosilicate and a cage like octa(silasesquioxane). *Z. Anorg. Allg. Chem.*, **619**, 347 – 358.
- 247 **Tacke, R. and O. Seiler** (2003) Higher-coordinate silicon compounds with  $\text{SiO}_5$  and  $\text{SiO}_6$  skeletons. Peter Jutzi, Ulrich Schubert Eds. *Silicon Chemistry, From atom to extended systems*, 324 – 337.
- 248 **Tacke, R., A. Lopez-Mras, W. S. Sheldrick and A. Sebald** (1993) Syntheses, single-crystal X-ray analyses and solid-state silicon-29 NMR studies of a zwitterionic  $\lambda$ - 5-spirosilicate and a cage-like octa(silasesquioxane). *Z. Anorg. Allg. Chem.*, **619**, 347 – 358.

- 249 **Tacke, R., A. Stewart, J. Becht, C. Burschka and I. Richter** (2000) Di[(hydroxyalkyl)dimethylammonium] tris[benzene-1,2-diolato(2-)]silicates and their germanium analogs: syntheses, crystal structure analyses and NMR studies. *Can. J. Chem.*, **78**, 1380 – 1387.
- 250 **Tacke, R., J. Sperlich, C. Strohmam and G. Mattern** (1991) Bis[2,3-naphthalenediolato(2-)](pyrrolidiniomethyl)silicate-acetonitrile adduct: synthesis and crystal and molecular structure of zwitterionic  $\lambda$ -5-spirosilicate. *Chem. Ber.*, **124**, 1491 – 1496.
- 251 **Tacke, R., M. Muehleisen, A. Lopez-Mras and W. S. Sheldrick** (1995) Syntheses and crystal structure analyses of new zwitterionic spirocyclic (ammonioorgano)bis[*vic*-arenediolato(2-)]silicates: studies on the structure of the  $\lambda^5$ -Si coordination polyhedra. *Z. Anorg. Allg. Chem.*, **621**, 779 – 788.
- 252 **Tacke, R. and O. Seiler** (2005) Higher-coordinate silicon compounds with SiO<sub>5</sub> and SiO<sub>6</sub> skeletons. *Chem. Inform.*, **36**, 450 – 500.
- 253 **Tacke, R., R. Bertermann, C. Burschka and S. Dragota** (2004) Hexacoordinate silicon(IV) complexes with SiO<sub>6</sub> skeletons and multidentate ligands derived from citric acid or malic acid. *Z. Anorg. Allg. Chem.*, **630**, 2006 – 2012.
- 254 **Tacke, R., R. Bertermann, M. Penka and O. Seiler** (2003) Bis[acetylacetonato(1-)-O,O]di(cyanato-N)silicon(IV): a neutral hexacoordinate silicon complex with two cyanato-N ligands. *Z. Anorg. Allg. Chem.*, **629**, 2415 – 2420.
- 255 **Tacke, R., M. Penka, F. Popp and R. Ingo** (2002) Bis[citrato(3-)-O1,O3,O6]silicate: a dianionic complex with hexacoordinate silicon(IV) and two tridentate dioato(2-)olato(1-) ligands. *Eur. J. Inorg. Chem.*, **5**, 1025 – 1028.
- 256 **Tacke, R., M. Willeke and M. Penka** (2001) Synthesis and structural characterization of cationic complexes with hexacoordinate silicon(IV) and three bidentate 1-oxopyridine-2-olato(1-) ligands. *Z. Anorg. Allg. Chem.*, **627**, 1236 – 1240.
- 257 **Takeuchi, H. and K. Sukata** Nucleation inhibitor, crystalline resin composition and method of controlling crystallization of crystalline resin composition.(2004), PCT Int. Appl. WO 2004005389, pp194.
- 258 **Tanaka, K., T. Nagatsuka and T. Takahashi** (1995) Magnetic toner for electrostatographic developer and image forming method (Canon KK, Japan). JP 07295287, pp 12.

- 259 **Tanaka, K. K.** (2005) Preparation of acetylcellulose/ silica composites by sol - gel method and their mechanical properties. *J. Mater. Sci.*, **40**, 5199 – 5206.
- 260 **Tandura, S. N., M. G. Voronkov and N. V. Alekseev** (1986) Molecular and electronic structure of penta- and hexa- coordinate silicon compounds. *Top. Curr. Chem.*, **131**, 99 – 189.
- 261 **Tarafder, P. K., S. Durani, R. Saran and G. V. Ramanaiah** (1994) Rapid spectrophotometric method (aqueous and extractive) for the determination of titanium in silicate rocks. *Talanta*, **41**, 1345 – 1351.
- 262 **Triller, M. U., D. Pursche, W. Hsieh, V. L Pecoraro, A. Rompel and B. Krebs** (2003) Catalytic oxidation of 3,5-di-tert-butylcatechol by a series of mononuclear manganese complexes: synthesis, structure, and kinetic investigation. *Inorg. Chem.*, **42**, 6274 – 6283.
- 263 **Thomas, J. M., J. M. Gonzalez-Calbert, C. A. Fyre, G. C. Gobbi and M. Nicol** Identifying the coordination of silicon by magic-angle-spinning NMR: Stishovite and quartz. *Geophys. Res. Lett.*, **10**, 91 – 92.
- 264 **Ueyama, K., G. E. Matsubayashi and T. Tanaka** (1984) Syntheses and electrical resistivities of TTF and TSF salts with tris(oxalato)silicate, -germanate, and -stannate. *Inorg. Chim. Acta.*, **87**, 143 – 146.
- 265 **Uno, H., T. Suzuki, Y. Goto, S. Itoh, T. Yasui and A. Yuchi** (2004) Performance of germanium(IV) complexes as anionophore. *Bunseki Kagaku*, **53**, 1035 – 1038.
- 266 **Vijayalakshmi, U., K. Prabakaran and S. Rajeswari** (2005) Fabrication, development and characterization of calcium phosphate based bioceramic coatings on 316L stainless steel for biomedical applications. *Surf. Eng.*, **21**, 225 – 228.
- 267 **Vittal, J. J., T. C. Deivaraj, J. H. Park and M. Afzaal** (2003) Novel bimetallic thiocarboxylate compounds as single-source precursors to binary and ternary metal sulfide materials. *Chem. Mater.*, **15**, 2383 – 2391.
- 268 **Van Soest, P. J.** (2006) Rice straw, the role of silica and treatments to improve quality. *Animal Feed Sci. Techn.*, **130**, 137 – 171.
- 269 **Vogel, A.I.** (1975) A textbook of practical organic chemistry, ELBS and Longman group Ltd., London.
- 270 **Watanabe, K., K. Rokugawa and M. Itagaki** (1995) Fluorometric determination of manganese(II) by the catalytic oxidation of 2,3 -dihydroxynaphthalene in the

- presence of ethylenediamine and hydrogen peroxide. *Bunseki Kagaku*, **44**, 933 – 938.
- 271 **Walawalkar, M. G.** (2005) Multiple bonds continue to fascinate chemists: discovery of stable Si=Si and B=O bonds. *Curr. Sci.*, **89**, 606 – 607.
- 272 **Weissenberg, M., J. Meisner, M. Klein, I. Schaeffler, M. Eliyahu, H. Schmutterer and K. R. Ascher** (1997), Effect of substituent and ring changes in naturally occurring naphthoquinones on the feeding response of larvae of the Mexican bean beetle, *Epilachna varivestis*. *J. Chem. Eco.*, **23**, 3 – 18.
- 273 **Wagler, J., U. Boehme, E. Brendler, S. Blaurock and G. Roewer** (2005a) Novel hexacoordinate diorganosilanes with salen-type ligands: molecular structure versus  $^{29}\text{Si}$  NMR chemical shifts. *Z. Anorg. Allg. Chem.*, **631**, 2907 – 2913.
- 274 **Wagler, J. and G. Roewer** (2005b) First X-ray structures of ethylene bridged neutral dimeric hexacoordinate silicon complexes with tetradentate Salen-type ligands. *Z. Natur., B: Chem. Sci.*, **60**, 709 – 714.
- 275 **Weiss, A. and D. R. Harrey** (1964) Water-soluble silicic acid esters. *Z. Anorg. Allg. Chem.*, **311**, 151 – 179.
- 276 **Whuler, A., C. Brouty, P. Spinat and P. Herpin** (1975) Etudes structurales des complexes racémiques hydratés  $(\pm)\text{-Co(en)}_3\text{Cl}_3$  et  $(\pm)\text{-Cr(en)}_3\text{Cl}_3$ . *Acta Cryst.*, **B31**, 2069 – 2076.
- 277 **Wijnen, P. W. J. G.** (1990) The structure directing effect of cations in aqueous silicate solutions - A  $^{29}\text{Si}$  NMR study. *Colloids Surf*, **45**, 255 – 268.
- 278 **Williams, E. A. and J. D. Cargioli** (1979) Silicon-29 NMR spectroscopy in Ann Reports NMR spectroscopy. pp 221.
- 279 **Winkelmann, G. and H. G. Huschka** (1987) Molecular recognition and transport of siderophores in fungi. In: Winkelmann G, van der Helm D, Neilands JB, eds. *Iron Transport in Microbes, Plants and Animals*. VCH Verlagsgesellschaft, 317 – 336,
- 280 **Winkler, A. and D. Hoebbel** (1988) Über ein Strontiumbromidsilicat und den molekularen Aufbau seines Silicatanions., *Z. Anorg. Allg. Chem.*, **562**, 170 – 174
- 281 **Wong, C. Y. and J. D. Wollins** (1994) Bidentate oxygen donor chelates of silicon, germanium and tin. *Coord. Chem. Rev.*, **130**, 175 – 241.
- 282 **Wronski, C. R.** (1988) Amorphous silicon and its applications. *Solid State Technology*, **31**, 113 – 117.

- 283 **Wanzlick, H.W., M. Lehmann-Horchler and S. Mohrmann** (1957) The blue coloration of  $\beta$ -tetralone. *Chem. Ber.*, **90**, 2521 – 2526.
- 284 **Xu, C., T. H. Baum and A. L. Rheingold** (2004) Synthesis and characterization of neutral cis-hexacoordinate bis( $\beta$ -diketonate)silicon(IV) complexes. *Inorg. Chem.*, **43**, 1568 – 1573.
- 285 **Yamaguchi, D. T., G. Y. Lin and C. A. Wilike** (1980) Electrochemistry of  $\text{Fe}(\text{CO})_2(\eta^5\text{-C}_5\text{H}_5)\text{X}$ -series. I. Detailed mechanism of reduction of  $[\text{Fe}(\text{CO})_2(\eta^5\text{-C}_5\text{H}_5)]_2$  and  $[\text{Fe}(\text{CO})_2(\eta^5\text{-C}_5\text{H}_5)]_2\text{Hg}$  *Inorg. Chim. Acta.*, **40**, 119 – 122.
- 286 **Yamazaki, S.** (2001) Chromium (VI) oxide-catalyzed oxidation of arenes with periodic acid. *Tetrahedron. Lett.*, **42**, 3355 – 3357.
- 287 **Yang, K., J. A. Martin, S. G. Bott and M. G. Richmond** (1997)  $\text{Cp}^*\text{Ru}(\text{NO})(\text{catechol})$  compounds. Synthesis, redox behavior, extended Huckel molecular orbital calculations, and X-ray diffraction structure of the pentamethylcyclopentadienylruthenium complex  $\text{Cp}^*\text{Ru}(\text{NO})(2,3\text{-naphthalenediolate})$   $\text{CH}_2\text{Cl}_2$ . *Inorg. Chim. Acta.*, **254**, 19 – 27.
- 288 **Yin, Y. and A. P. Alivisatos** (2005) Colloidal nanocrystal synthesis and the organic-inorganic interface. *Nature*, **437**, 664 – 670.
- 289 **Yoshida, H., T. Tanaka, M. Yamamoto, T. Funabiki and S. Yoshida** (1996) Photooxidation of propene by  $\text{O}^{\cdot -}$  over silica and Mg-loaded silica. *Chem Commun.* 2125 – 2126.
- 290 **Yoshida, S., Y. Magatani, S. Noda and T. Funabiki** (1981) Partial oxidation of propene over U.V.-irradiated vanadium oxide supported on silica. *J. Chem. Soc. Chem. Commun.*, **12**, 601 – 602.
- 291 **Yoshida, H. T., M. Yamamoto, T. Yoshida, T. Funabiki and S. Yoshida** (1997) Epoxidation of propene by gaseous oxygen over silica and Mg-loaded silica under photoirradiation. *J. Catal.*, **171**, 351 – 357.
- 292 **Yoshida, H., M. Chizu and H. Tadashi** (2000) Screening study of silica-supported catalysts for photoepoxidation of propene by molecular oxygen. *J. Catal.*, **194**, 364 – 372.
- 293 **Yu, S., Y. Wan and A. Zhou** (2005) Preparation organosilicon compounds from amorphous silica. *Shenqing Gongkai Shuomingshu*, pp 9.



- 294 **Zhang, X., D. O. Hayward and D. M. P. Muigos** (1999) Apparent equilibrium shifts and hot-spot formation for catalytic reactions induced by microwave dielectric heating. *Chem. Comm.*, **11**, 975 – 976.
- 295 **Zhang, Z. B., L. X. Zhou, M. Zhang, H. Wu and Z. J. Chen** (2001) One billionhertz microwave a thermal action on the synthesis of aromatic esters at normal pressure. *Synth. Commun.*, **31**, 2435 – 2439.
- 296 **Zheng, M. F., T. B Zhao, W. G Xu, F. Y. Li and Y. Yang** (2006) Preparation and characterization of CuO/SiO<sub>2</sub> and NiO/SiO<sub>2</sub> with bimodal pore structure by sol-gel method. *J. Sol-Gel Sci. Techn.*, **39**, 151 – 157.
- 297 **Zhao, Z. W., K. Konstantinov, L. Yuan, H. K. Liu and S. X. Dou** (2004) In-Situ fabrication of nanostructured cobalt oxide powders by spray pyrolysis technique. *J. Nanosci. Nanotechnol.*, **4**, 861 – 866.
- 298 **Zhou, Y.** (1996) Porous silicon and its applications. *Gongneng Cailiao*, **27**, 225 – 229.

## LIST OF PUBLICATIONS

### REFERRED JOURNALS

1. **A. Suvitha, Babu Varghese and M. N. Sudheendra Rao** (2006) “Bis(diisobutylammonium)tris(naphthalene-2,3-diolato)silicate acetonitrile trisolvate”. *Acta. Cryst. E62*, o344-o346.
2. **A. Suvitha, B. Varghese, M. N. Sudheendra Rao, G. Sundararajan, and B.Viswanathan** (2006) “Effective synthesis of hexacoordinate silicates of 2,3-dihydroxynaphthalene under microwave condition and X - ray crystal structure of bis (tri-*n*-butylammonium)tris(2,3-dihydroxynaphthalato) silicate” *Indian Journal of chemistry sec.A: Inorg. Phy. Theo.& anal.* **45A**, 2193-2198.
3. **A. Suvitha, G. Sundararajan and B. Viswanathan** “Synthesis of porous silica by pyrolysis and hydrolysis of bis(ammonium)tris(2,3-dihydroxynaphthalato)silicates” (to be communicated).
4. **A. Suvitha, G. Sundararajan and B. Viswanathan** “Cyclic Voltammetric and thermal studies of bis(ammonium)tris(2,3-dihydroxynaphthalene) – an counter cation effect” (to be communicated)

### POSTER PRESENTATION IN NATIONAL CONFERENCES:

1. **Suvitha, A., M.Hojo, T.Yonemura, T.Ueda and M.N.Sudheendra Rao** “Six coordinate silicate derivative of 2,3-dihydroxynaphthalene – Synthesis, structure and electrochemical studies in MTIC-X conference held at IITB, Mumbai, December 15-17 2003.
2. **Suvitha, A. and M.N.Sudheendra Rao** “Hyper coordinate silicates of 2,3-dihydroxynaphthalene- synthesis, mass spectral and thermal behaviour” in Chemists meet, IITM, Chennai, March 26-27.2004.
3. **Suvitha,A., B.Varghese, D., Aadi Narayana, Brindha and M. N. Sudheendra Rao**”New higher-coordinate silicate- synthesis and characterization and single Crystal X – ray structure of  $[\text{((C}_4\text{H}_9)_2\text{NH}_2)_2[\text{(C}_{10}\text{H}_6\text{O}_2)_3\text{Si}]] \cdot 2\text{CH}_3\text{CN}$  and  $[\text{((C}_4\text{H}_9)_3\text{NH})_2[\text{(C}_{10}\text{H}_6\text{O}_2)_3\text{Si}]]$  MTIC- XI, IITD, Delhi, December 8-10, 2005.